An Exploration of Solution-Based SERS with Gold Nanostars for Quality Control in the Cannabis Industry

by

Taylor Paige Lynk

A thesis submitted in partial fulfillment of the requirements for the degree of

Master of Science

Department of Chemistry
University of Alberta

Abstract

The recent legalization of cannabis and cannabis consumables in Canada presents a new analytical challenge for quality control of cannabis products. A high-performance analytical tool for such purposes would be crucial for the rapidly expanding Canadian and global cannabis markets. This project aims to explore the use of Raman spectroscopy and surface-enhanced Raman spectroscopy (SERS) for it's potential to be used as a rapid, sensitive, and cost-effective detection platform for quality control in the cannabis industry. The availability of portable Raman spectrometers also makes these methods ideal for in-process analysis. Both cannabinoids and terpenes will need to be monitored, due to their synergistic effects on the medicinal properties of cannabis. Growing hemp plants and dried hemp and cannabis plants were analyzed using a handheld Raman spectrometer. Solution-based SERS using gold nanostars (AuNSs) was also employed for the detection of cannabinoids and terpenes. The purpose of employing solution-based SERS was to develop a method that could easily be used for in-process analysis of cannabis infused beverages. This thesis work also focuses on method development for polymer-controlled aggregation of AuNSs for solution-based SERS, a concept that has not yet been used with AuNSs or for cannabinoid or terpene detection. This project highlights the potential of Raman and SERS to be used in the cannabis industry for rapid and affordable quality control for cannabis products.

Preface

The calculations for the theoretical Raman spectra presented in Chapter 2 were done by Arsh Hazrah from Dr. Jaeger Wolfgang's research group at the University of Alberta. The preparation and analysis of the data was done by me.

The data collected of living and dried hemp and cannabis plants presented in Chapter 2 was done in collaboration with Alberta Innovates, led by Dr. Sunil Rajput. I was responsible for data collection, analysis, and interpretation.

Acknowledgements

My degree would not have been possible without the help and encouragement that I have received along the way. I would like to thank my research supervisor, Dr. Mark T. McDermott for his knowledge and guidance throughout my time in graduate school, his support of my professional and personal development made my time in his group a pleasure. I would also like to thank current and past MTM group members: Nicole Jankovic, Dr. Kenny Xu, Akib Shahriar, Thuy Nguyen, Amy Mao, Abdelhaq Benkaddour, and especially Dr. Sunil Rajput, Dr. Ahmed Mahmoud, and Dr. Casey Rusin for being my Raman mentors. I would also like to especially thank Nicole Jankovic and Caley Craven for welcoming me to Edmonton and being amazing friends along my journey. I would also like to acknowledge the help of my committee throughout the process of my degree, as well as the support of the Department of Chemistry. I am also thankful to have had my degree funded by the University of Alberta Thesis-Based Master's Recruitment Scholarship, an NSERC CGS-M, and the NSERC CGS-M COVID-19 Extension. Finally, I would like to thank my friends, family, and boyfriend for their love and support.

Table of Contents

List of Figures

Abbreviations

AuNS	gold nanostar
AuNP	gold nanoparticle
AgNP	silver nanoparticle
SERS	surface-enhanced Raman spectroscopy
IR	infrared spectroscopy
PVP	polyvinylpyrrolidone
MBN	4-mercaptobenzonitrile
EtOH	ethanol
SEM	scanning electron microscopy
TEM	transmission electron microscopy
UV-Vis	ultraviolet-visible spectroscopy
THC	tetrahydrocannabinol
CBD	cannabidiol
CBN	cannabinol

Chapter 1: Introduction

1.1 Research Scope and Objectives

The goal of this thesis is focused on developing an analytical platform for in-process quality control for cannabis-based consumables and for growing cannabis plants. The recent legalization of cannabis and cannabis edibles in Canada presents an opportunity to develop methodology to be used for quality control for cannabis plants and consumable products due to the strict regulations in place in the cannabis industry.[1] With the rise in popularity of cannabis-based beverages that is expected,[2,3] a solution-based analytical platform will need to be established for quality control purposes. The ideal analytical platform would be able to characterize both cannabinoids and terpenes present in cannabis products, as they have synergistic effects.[4,5]

An ideal candidate for in-process monitoring of cannabis-based beverages and edibles is Raman spectroscopy due to its cost effective nature and ability for rapid and non-destructive analyte detection.[6] Raman spectroscopy was discovered in 1928 and is able to probe the molecular vibrations of a target analyte.[7] It is able to rapidly provide a chemical fingerprint for target molecules with a high degree of sensitivity and selectivity, in any optically accessible sample, including those in water.[8] Raman, however, is an inherently weak effect as a result of the low amount of Raman scattering that naturally occurs.[9,10] This weakness can be overcome by using Surface-enhanced Raman spectroscopy (SERS).[9,10] A SERS measurement involves locating the analyte molecules on the surface of a nanoscale noble metal substrate.[9,10] By using SERS, the intensity of the normal Raman spectra can be improved immensely through both the electromagnetic and chemical enhancement of the signal.[10] The use of portable handheld Raman

spectrometers is emerging for drug identification and can provide results in near-real time,[11] and would therefore be well-suited for this work.

While several studies have investigated SERS detection of natural and synthetic cannabinoids,[12-16] the current literature lacks studies investigating beverage matrices, which is what my project will focus on. Cannabinoids have shown to be an analytical challenge for Raman, with significant inconsistencies amongst the publications of SERS spectra of cannabinoids due to its low Raman cross section.[17] This thesis aims to investigate what role, if any, solution-based SERS can play in improving the SERS signal of cannabinoids. This thesis work also provides and important investigation of terpenes relevant to the cannabis industry using Raman and spectra calculated using density functional theorem (DFT). Controlled aggregation of gold nanostars is also investigated in order to address the lack of applicability of solution-based SERS with terpene analysis.

1.2 Raman and Surface-Enhanced Raman Spectroscopy Theory

1.2.1 Raman Spectroscopy

Spectroscopic techniques can offer valuable chemical and structural information about a sample through the study of the interaction between the sample and incident electromagnetic radiation. Raman spectroscopy is based on the inelastic scattering of monochromatic light and was first introduced by Raman and Krishnan in 1928.[7] Inelastic scattering occurs when light scatters at a different frequency than that of the incident light, however only a small proportion of light undergoes this type of scattering.[18] The majority of scattered light undergoes elastic scattering, also known as Rayleigh scattering, which occurs when the light scatters at the same frequency as that of the incident light.[18] Of the inelastically scattered light, the photons can either

have lower energy than the elastic Rayleigh line with Stokes scattering, or higher energy than the elastic Rayleigh line with anti-Stokes scattering.[19] Stokes lines are more intense, as this intensity is proportional to the number of molecules of analyte in the ground state, which is more populated than the excited states that are proportional to the anti-Stokes lines.[18] Figure 1-1 shows a schematic representation of the Rayleigh, Stokes, and anti-stokes scattering of light.

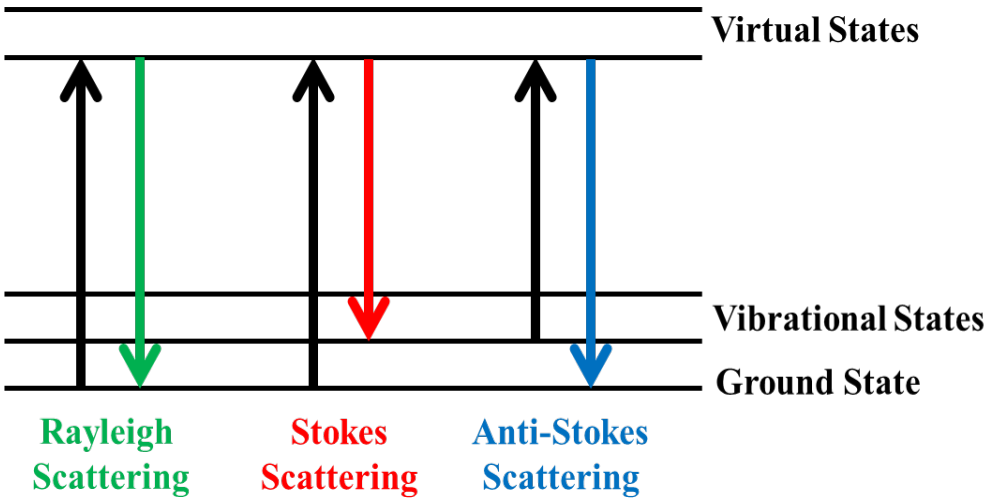

Figure 1-1. Schematic of the different light scattering modes: Rayleigh, Stokes, and anti-Stokes scattering.

Raman activity is based on a change in polarizability of a molecule during molecular vibration, which is probed by the incident radiation.[18] It is a complementary technique to infrared spectroscopy, which is based on a change in dipole moment and the absorption of light rather than scattering.[20] Raman spectroscopy is an extremely valuable technique, as it provides a molecular fingerprint for an analyte of interest.[21] Raman spectroscopy is widely applicable due to its non-destructive nature, and can support gold standard techniques to reduce the cost of

analysis.[20] The main disadvantage of Raman spectroscopy is the small amount of Raman scattering that occurs, causing this technique to be inherently weak.[20] This weakness of Raman can often mean that longer spectral acquisitions must be employed for sample collection, which can risk damaging the sample.[20]

1.2.2 Surface-Enhanced Raman Spectroscopy

While the technique of surface-enhanced Raman spectroscopy (SERS) is only about 40 years old, it is a field of research within itself. SERS was discovered accidently in 1974 by Fleischmann and coworkers while collecting Raman spectra of pyridine adsorbed on a silver electrode.[22] In 1977 the technique was identified by Jeanmarie and Van Duyne and by Albrecht and Creighton, where both studies discovered that the field of plasmonics could help to overcome the inherent weakness of Raman spectroscopy.[23,24] They showed that the intensity of Raman scattering could be increased significantly by locating the analyte of interest on or very near to a roughened noble metal substrate,[23,24] a technique now called surface-enhanced Raman spectroscopy or surface-enhanced Raman scattering (SERS). SERS has since been developed to the point of being sensitive enough for single molecule detection and has been used for a wide variety of sensing applications with tens of thousands of publications.[10]

The SERS enhancement has two mechanisms, electromagnetic and chemical. The overall enhancement factor of SERS has been reported to be between 10^4 to 10^{14} with high performing, optimized substrates.[25] Single molecule detection has been reported with enhancement factors of only 10^7 to 10^8.[25] The electromagnetic enhancement of SERS has theoretical enhancement factors of 10^{10}, therefore being the main contributor to the power of SERS.[25] The electromagnetic enhancement factor of SERS makes use of the localized surface plasmon

resonance (LSPR) of nanoscale metals.[26] The LSPR of nanoscale noble metal substrates can be excited by incident radiation,[10] which generates strong electromagnetic fields and causes and increase in the induced dipole of the analyte molecules.[10] This effect results in more inelastic scattering, and a stronger Raman signal.[10] The other contributor to the total SERS enhancement is the chemical enhancement, for which enhancement factors of up to 10^3 have been reported.[27] The chemical enhancement of SERS is probe dependent, and can be a result of electron transfers in the ground and excited states of the molecule-metal system.[10,25]

SERS substrates typically make use of gold, silver, and copper.[27] While copper is the most earth abundant of the three metals, and therefore the most environmentally friendly and cost effective choice, it is prone to oxidization in air and is not often employed for SERS due to its lack of stability.[27] The ability of a metal to be plasmonic and support an LSPR is based on Mie theory and the extinction cross section equation, where the value for the extinction cross section can be maximized by using a plasmonic metal that supports the electromagnetic enhancement of SERS by having a complex dielectric function (ε) with a negative real component (ε_r) and a small, positive imaginary component (ε_i).[27]

When comparing normal Raman and SERS spectra of molecules, these spectra can differ in terms of both peak location and peak intensity. In normal Raman, the analyte molecules are randomly oriented in respect to the optical field, and the spectrum obtained is therefore an average of all possible orientations.[28] In SERS, the analyte molecule forms a weak covalent bond with the surface of the metal which directs the molecule's orientation.[28] With the majority of the molecules in the most favourable orientation to the surface, this can cause some vibrational lines to be enhanced, and others reduced.[28] New peaks can also appear in the SERS spectrum as a result of the bonds formed between the metal surface and the analyte, as this bonding lowers the

symmetry of the molecule which could allow for peaks that were previously forbidden to appear in the SERS spectrum.[28,29] The Raman and SERS peak intensities can also differ due to the changes in selection rules as a result of surface effects from the metal, including the introduction of charge transfer states which do not play a role in Raman.[28-30]

1.3 Instrumentation and Substrates

1.3.1 Handheld Raman Spectrometers

While Raman spectrometers used to be primarily benchtop instruments confined to laboratory use, portable handheld Raman spectrometers are now commercially available and are allowing Raman and SERS to push the boundaries of point-of-need chemical analysis. Portable handheld Raman spectrometers are more cost effective than benchtop instruments, and they can reduce analysis time by providing a method for preliminary screening, or even prevent samples from having to be sent to a laboratory for analysis.[31] One potential application of portable Raman spectrometers is in art analysis, where many objects of great cultural heritage consist of immovable objects or objects that may be difficult and expensive to move.[32] In one study, a portable Raman spectrometer was used for art analysis using the BRAVO spectrometer by Bruker.[32] This spectrometer has the advantage of using Sequentially Shifted Excitation (SSE) to overcome the fluorescence which can limit the use of handheld Raman spectrometers for artwork analysis.[32] A portable Raman spectrometer was also used in the art community for pigment identification for a mediaeval wall painting.[33] These studies show the applicability of portable Raman spectrometers in the art community, which is largely due to its non-destructive and portable nature.[32]

Several studies have compared handheld spectrometers to benchtop spectrometers, where one study by Dégardin and coworkers used a portable Raman spectrometer for drug identification.[31] The handheld spectrometer proved to be just as powerful as the laboratory spectrometer, however the handheld instrument did produce spectra with more noise.[31] Another study compared the performance of a portable Raman spectrometer to a benchtop spectrometer for pesticide detection.[34] This study found that the handheld spectrometer had better data consistency and more accurate quantification capacity, while the benchtop spectrometer was found to be more sensitive and more tunable in terms of different acquisition parameters.[34] While portable Raman spectrometers are a major advance for point-of-need screening, they do not come without their disadvantages compared to their benchtop counterparts.

A study by Izake outlines the valuable contribution handheld spectrometers can provide for forensic and homeland security applications, where the user can be at a safe distance from the analyte for the analysis of hazardous goods.[8] THC has also been analyzed using a handheld Raman spectrometer,[16] and the differentiation between cannabis and hemp plants was also successfully completed using a portable instrument.[6] Overall, portable spectrometers offer the advantage of being cost effective, fast and easy to use, and field applicability. Two different Raman spectrometers, the B&W Tek TacticID® -GP Plus spectrometer and the B&W Tek NanoRam® spectrometer were both employed for various studies throughout this thesis work.

1.3.2 SERS Substrates

The substrates used when SERS was first observed were electrochemically roughened electrodes,[22-24] although the use of metallic nanoparticles was discovered soon after and they are frequently used today.[35] The development of reproducible, reliable, and stable substrates is still of great interest in the SERS field.[10] The substrate used in SERS plays the most important role in the enhancement factor through both the electromagnetic and chemical enhancement mechanisms, and is also responsible for the reproducibility of the SERS signal obtained. There are three main types of SERS substrates that have been explored; (1) metal nanoparticles on a surface, (2) colloidal dispersions of metal nanoparticles, and (3) solid substrates fabricated using nanolithography or template synthesis.[35] While all types of substrates come with their own challenges, they all offer unique benefits and have been used for the sensing of a wide variety of analytes.

The first type of SERS substrate that is often explored involves metal nanoparticles on a surface, for which the surface can be a variety of things such as filter paper, glass slides, electrodes, etc. One major challenge with solid surface decorated with nanoparticles is getting the nanoparticles onto the surface, as is especially true with filter paper-based substrates.[36] A surface treatment to change the hydrophobicity of the substrate can often aid in getting the nanoparticles onto the surface of filter paper substrates.[36] With solid substrates, sometimes lithography or electrochemical methods need to be employed in order to achieve the production of reproducible substrates on solid surfaces like glass.[37] Self-assembled monolayers are also used frequently to achieve well-ordered SERS substrates, these methods can range from simple self-assembly protocols to more complicated methods such as the Langmuir-Blodgett technique, spin-casting, and solvent evaporation.[38,39] One of the more simple ways to fashion a solid

substrate is to drop-cast a nanoparticle suspension or paste onto the substrate being used, which typically requires several layers to combat the coffee-ring formation that occurs when the nanoparticles congregate around the edges of the surface rather than covering the surface uniformly.[40]

Another type of SERS analysis is done using solution-based substrates, where a colloidal dispersion of nanoparticles is used. Solution substrates can offer improved reproducibly, cost-efficiency, simplicity, and can allow for more tailored optical properties.[10] Since solution-based substrates involve the collection of a spectrum directly from the nanoparticle solution that contains the analyte, it is considered to be a 3D distribution of hotspots, which can account for some of the success of solution-based substrates.[10] One downside to solution-based substrates is that they do require aggregation, which is a dynamic event, therefore leaving a finite time window in which the substrate can be used.[10] Solution substrates can be stored for some amount of time before sedimentation, and are actually considered to be metastable due to the frequent collisions of nanoparticles as a result of colloidal dynamics.[10] Solution-based substrates have recently attracted much attention in the SERS community and many types of nanomaterials have been explored for solution-based SERS. Silver and gold colloidal suspensions, nanosphere oligomers, gold nanostars, gold nanorods, and even plasmonic cellulose nanofibers have been used for solution-based SERS of a variety of analytical targets, showing the diversity and promise of solution-based SERS techniques.[41-47]

The last type of SERS substrates that have been explored are those made using more advanced fabrication techniques such as lithography. These techniques are often considered to be "top down" approaches, as opposed to the techniques previously discussed that would be "bottom up" approaches. Nanolithography techniques involve the etching of a SiO_x/Si surface

with an electron beam to achieve nanoscale roughness.[35] Advanced fabrication techniques can also include nanoparticle arrays, which are promising for microfluidics, and template techniques such as electrochemical and vapour deposition.[35] One study made use of nanoimprint lithography to produce flexible plasmonic sensors fashioned with nanocones on polycarbonate sheets, which offer the benefit of being applicable for environmental monitoring when rigid substrates would be less appropriate.[48] Template-based synthetic approaches offer the advantage of being used to create unusual structural properties that would be otherwise impossible to synthesize.[49] Of course, one major downfall of these SERS substrate production techniques is that they are more laborious, time consuming, and require expensive instrumentation, although these substrates are moving towards being more cost-effective to produce.[49]

1.3.3 Gold Nanostars

One class of metal nanostructures that have shown remarkable SERS performance is anisotropic nanostructures.[45,50] Mie theory explains the scattering of electromagnetic radiation on isotropic nanoparticles, where the surface charge density changes with change in the nanoparticle diameter.[50] When the nanoparticle diameter increases, the plasmon absorption band occurs at a higher wavelength.[50] When anisotropic nanoparticles are used, this means there is a change in geometry rather than size (although the size can also vary), and this change in geometry affects the surface plasmon absorption band.[50] Often times with anisotropic nanoparticles we see multiple bands, and there is typically a stronger electromagnetic field at the tips or protrusions of these particles.[50] Anisotropic nanoparticles have applications in SERS,[51] catalysis,[52] biomedical sensing,[53] and cancer drug delivery.[54]

The interest of this thesis is to use anisotropic nanoparticles, specifically gold nanostars (AuNSs), for SERS. AuNSs have been explored for their use in SERS substrates, and have demonstrated the ability to be capable of providing extraordinary SERS enhacement.[44,45,51] Saverot and coworkers synthesized AuNSs using a two-step seed-mediated method with HEPES buffer, which is a commonly used zwitterionic organic buffer agent used in AuNS synthesis.[55] They used the AuNSs for SERS to detect 4-mercaptobenzoic acid.[55] Another study by Song and coworkers investigated the design of multifunctional AuNSs that could be labeled with a Raman reporter for cancer cell targeted SERS imagining with human lung adenocarcinoma cells.[56] This study found that AuNSs can be used for optical imagining and image guided phototherapy.[56] The morphology of AuNSs has also been shown to be controllable using 4-mercaptobenzoic acid in a study by Meng et al.[57] The same study found that AuNSs with sharp branches are better for SERS than AuNSs with rough surfaces.[57] Yolk-shell AuNSs have also been synthesized and explored, where it was found that monomers of these AuNSs can have plasmonic properties of a dimer to contribute to a large increase in the electromagnetic field.[58]

The AuNSs used in this work were made in a simple, one-pot synthesis by mixing gold salt and a Good's buffer to alter the R value, which is the gold to buffer ratio.[44] In this synthesis, the R value is used to tune the length of the branches on the AuNS, where a larger R value results in the formation of longer branches.[44] During AuNS synthesis, the Au^{3+} ions are reduced to Au by the radicals formed from the tertiary amines from the piperazine group.[44] The shape formation is dictated by the terminal alkanesulfonate, and the colloidal and shape stability is stabilized through hydrogen bonding.[44] Figure 1-2 shows the characterization of the AuNSs used in this work from a previous publication from our research group. The higher R value is shown

to be associated with AuNSs with longer branches and a longer wavelength of the absorption band.

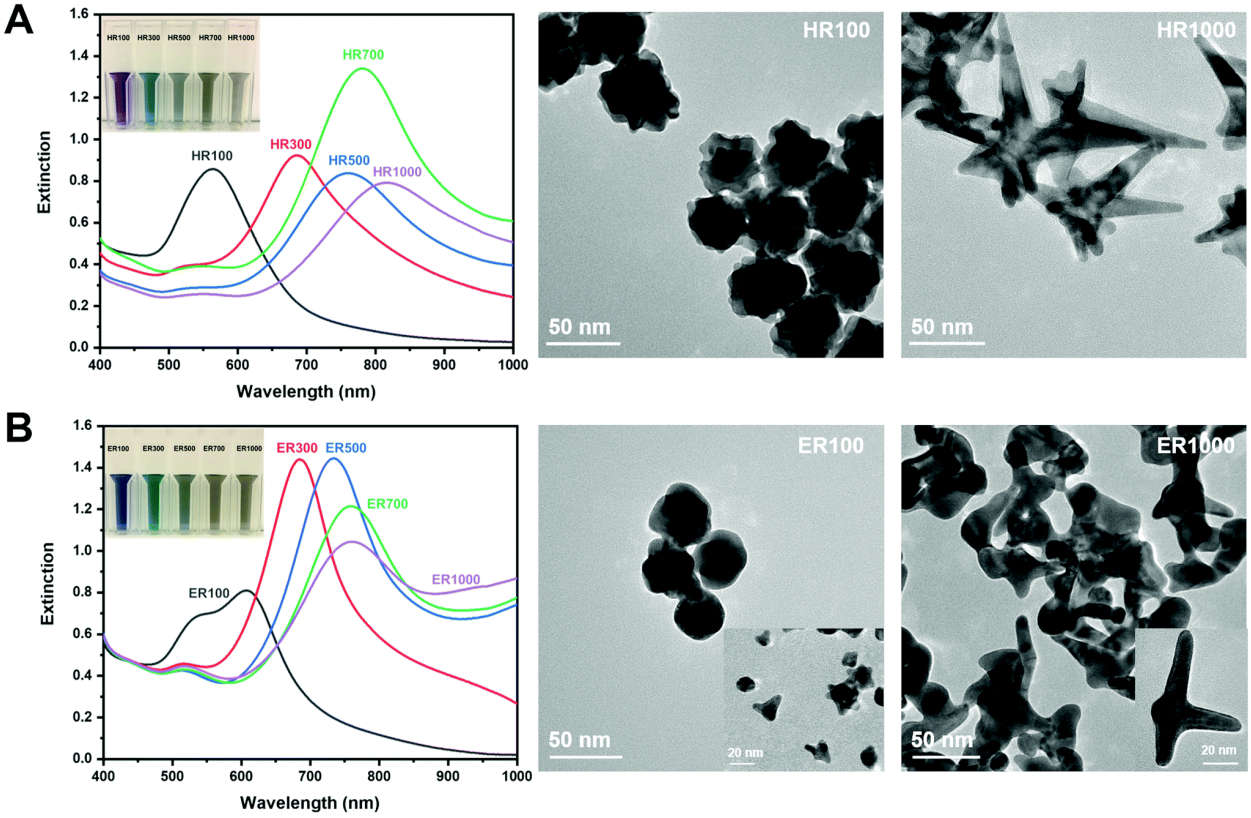

Figure 1-2. Extinction spectra of (A) HEPES (code HR) and (B) EPPS (code ER) buffers. The inset images show the colour of the AuNS solutions at the given ratios. TEM images correspond to AuNS at *R* 100 and 1000. Reprinted from Mahmoud, E. Y. F.; Rusin, C. J.; McDermott, M. T., Gold nanostars as a colloidal substrate for in-solution SERS measurements using a handheld Raman spectrometer. *Analyst* **2020**, 145, 1396-1407.[44] Copyright 2020, with permission from the Royal Society of Chemistry.

1.4 Cannabis

1.4.1 Cannabis Plants, Terpenes, and Cannabinoids

Cannabis is the most widely cultivated drug in the world, it is used recreationally and medicinally by over 183 million users every year.[6,17] Although cannabis is a commonly used drug, the legality of its use varies between and within countries.[6] Cannabis is cultivated from the flowering plant *cannabaceae* and the most popular of its species are *Cannabis sativa* and *Cannabis indica*.[17] Hemp is also derived from the same plant, although legally hemp can only contain up to 0.3% THC.[6] Cannabinoids and terpenoids are the major components of interest in cannabis for their medicinal properties, and they are synthesized by cannabis plans in the glandular trichomes.[5] Cannabis plants produce over 500 cannabinoids, although only over 100 have been identified.[17] Tetrahydrocannabinol (THC) is the most well studied psychoactive cannabinoid in cannabis, and has been the primary research focus for cannabis related research since 1964.[5,17] Cannabidiol (CBD) is another important cannabinoid due to its range of medicinal effects,[5] although pharmacological effects have been reported for cannabidiolic acid (CBDA), cannabigerol (CBG), cannabigerolic acid (CBGA), Δ9 -tetrahydrocannabivarin (THCV), Δ9 -tetrahydrocannabivarinic acid (THCVA), cannabidivarin (CBDV), and cannabidivarinic acid (CBDVA; 3) as well.[59]

The other therapeutic agents to consider with cannabis are terpenoids, as they contribute to the flavour and fragrance of the plant, and can have synergistic effects with cannabinoids, which is termed the entourage effect.[4,5] Over 130 terpenoids have been identified in cannabis, and the terpene profile of different cultivars of cannabis is often reported, although only approximately 17 terpenes are the most common.[59] Terpenes are also a major component of the essential oil extracted from hemp leaves, and are typically responsible for the characteristic smell

of essential oils.[60] Some of the major terpenes found in cannabis to note are myrcene, α and β-pinene, linalool, and limonene.[61-63] Cannabinoids typically contribute 0.1% to 40% of the dry weight of cannabis, where terpenoids range from 0.01% to 1.5% of dry weight. While other metabolites exist in cannabis, it is cannabinoids and terpenoids that are considered the most important to identify during analytical testing.[59]

1.4.2 Canadian Cannabis Beverage Market

Cannabis was legalized in Canada in 2018, and cannabis edibles in 2019.[1] Bill C-45 (Cannabis Act) outlines the regulations pertaining to the cannabis industry, including the requirements to regulate the characteristics, composition, strength, concentration, potency, purity, quality, and other properties of cannabis and cannabis products.[1] Because of the strict quality control regulations in place, there is a new analytical opportunity to meet the needs of the cannabis industry. With the legalization of cannabis edibles in Canada and other places around the world comes the introduction of new cannabis-infused products, such as beverages. This new class of beverage products will present additional challenges for quality control, with a need to quickly and cost effectively monitor the cannabinoid and terpene content of beverages during and after production. The vast interest and large market potential for the cannabis beverage market and the need for new analytical tools motivated this thesis work.

The cannabis beverage market presents many possibilities for cannabis infused beverages including beer, wine, sparkling water, kombucha, and soft drinks. This market has the potential to be worth millions of dollars. For example, with beer sales accounting for approximately 40% of total alcoholic beverage sales in Canada,[64] there is an opportunity for non-alcoholic, cannabis beer alone to drive high sales. It has been speculated that the market for cannabis beverages

could be worth about $1.5 billion, based on the total cannabis market being worth between $7 billion and $10 billion, and about 20-30% of that having the potential to come from non-alcoholic, cannabis beverages.[2] Deloitte's estimate of the worth of the cannabis beverage market in Canada is more conservative at $529 million.[3]

Many North American companies have or are preparing to add cannabis beverages to their product roster. Cannabis-infused beverages cannot contain alcohol, and in fact they are an attractive alternative to alcoholic beverages due to their ability to eliminate the calories attributed to alcohol, they come without the price tag of a hangover, and can even have therapeutic effects depending on their cannabinoid profile. Rebel Coast Winery will be producing a Sauvignon Blanc with 20 mg of THC in the bottle, with one glass containing only 35 calories in comparison to the 150 calories in regular, alcoholic wine.[65] Molson Coors is considering selling marijuana-infused beers in hopes to help combat declining sales by entering the cannabis beverage market.[66] There were rumors of Coca Cola and Aurora considering striking a deal for producing cannabis infused beverages,[67] however when nothing materialized of this and Aurora stated there would not be a market for cannabis beverages,[2] it was speculated to be a poor business decision for Aurora due to the loss in potential sales.[67] Canopy Growth has partnered with Constellation Brands (producer of Corona), while Hexo Corp has a deal with Molson Coors Canada to produce cannabis beverages.[68] Toronto based startup Province Brands is developing cannabis beer with $300,000 in funding from the Ontario government.[69,70] Cannabis producer Zenabis signed an agreement with HYTN Beverages to produce various flavours of cannabis infused sparkling water.[71] Clearly, the cannabis beverage industry is one that is quickly growing and presents new analytical challenges.

1.4.3 Detection of Cannabis, Terpenes, and Cannabinoids

Typical methods for cannabinoid and terpene detection are GC-MS, GC-MS/MS, GC-FID, HPLC-DAD, and LC-MS/MS, which are able to quantitatively and reliable detect low levels of cannabinoids and terpenes.[17,59,61] While these gold standard techniques exist for cannabinoid and terpene detection, it is still of great interest to develop methodology that is more suited for rapid, in-field detection of these analytes at a lower cost, which is why Raman and SERS have begun to be explored for such applications.[17] SERS detection of cannabis mainly focuses on the cannabinoids, although the Raman spectra of cannabinoids is very weak, and often differs between publications.[17] SERS has been conducted of synthetic cannabinoids in artificial urine using a solution-based method.[12] THC, along with heroin, cocaine, and oxycodone were detected in saliva using a microchip SERS substrate.[13] They found that there are not distinct peaks for THC, and it cannot be easily identified using a database.[13] Contrary to this, another SERS study looking at THC in silver coated capillaries reported a spectrum for THC with strong peaks.[14] The first reported detection of cannabinol (a metabolite of THC) also showed a weak signal on a nanorod array substrate.[15] Synthetic cannabinoids have also been a somewhat popular analyte due to their extreme psychoactive effects and have been detected using SERS.[72] Overall the spectra found in literature for cannabinoids are often weak and irreproducible, although one study showed that electrochemical SERS could help to enhance the signal of THC.[17] Hemp and cannabis plants have also been shown to be differentiable using Raman spectroscopy,[6] and glandular trichomes of cannabis plants have also been studied using anti-Stokes Raman spectroscopy.[73]

Terpenes have been detected in essential oils in the past using Raman spectroscopy, however not many studies have employed SERS to study essential oils. There is also a lack of

literature looking at terpenes from cannabis samples or for application in the cannabis industry. One study reported the detection of terpenes in citrus oil using Raman spectroscopy as well as IR spectroscopy.[74] Another study used Raman to analyze isoprene and pinenes for applications in the detection of aerosols in pollution.[75] This study found that the experimental results for β-pinene matched the theoretical results for dimers the best.[75] Hanif and coworkers also looked at terpenes from hemp oil using Raman and principal component analysis.[60] Raman has also been used in several other studies for the detection of terpenes for applications in herbal medicine and essential oils.[76,77] One recent study did employ SERS for terpene detection from live cotton plants and dried teas,[78] which could serve as a proof of concept that SERS has potential to be used for headspace terpene detection for cannabis plants and dried cannabis as well.

1.5 Thesis Outline

The first research chapter of this thesis, Chapter 2, will explore the use of Raman spectroscopy for its potential role in quality control in the cannabis industry. Both live and dried hemp plants will be exa using a handheld Raman spectrometer. The characterization of major terpenes found in cannabis is also explored using DFT, Raman, and SERS to provide an important reference for future SERS studies of cannabis and cannabis products. A solution-based SERS substrate for cannabinoid and terpene detection using anisotropic AuNSs will also be explored with the goal of analyzing cannabis beverages using SERS.

The second research chapter of this thesis, Chapter 3, will explore the use for AuNSs for solution-based SERS with PVP-mediated aggregation control. While the AuNS substrate is explored in Chapter 2, the method does suffer from a lack of applicability to a wide range of probes due to the lack of control of the aggregation mechanism. PVP addition will be explored in

order to have more consistent aggregation and have the aggregation occur before the addition of the probe molecule with the goal of making solution-based SERS with AuNSs more applicable for terpene analysis. This chapter presents the method development, optimization, and validation for PVP addition to AuNSs for SERS, as well as some preliminary terpene analysis using this method.

1.6 References

1. Bill C-45, *An Act Respecting Cannabis and to Amend the Controlled Drugs and Substances Act, the Criminal Code and Other Acts*, 1st Sess, 42nd Parl, Canada, 2018 (assented to June 21, 2018).
2. Lagerquist, J. Aurora CEO Says 'The Market is Just Not There' for Cannabis Drinks. *Yahoo Finance Canada* [Online], May 15, 2019 https://ca.finance.yahoo.com/news/aurora-ceo-says-the-market-is-just-not-there-for-cannabis-drinks-190208438.html (accessed Apr 3, 2020).
3. Nurturing New Growth: Canada Gets Ready for Cannabis 2.0. *Deloitte*. https://www2.deloitte.com/content/dam/Deloitte/ca/Documents/c-and-ip/ca-en-consumer-nurturing-new-growth-en-aoda-may31.pdf (accessed Apr 6, 2020).
4. Russo, E. B. The Case for the Entourage Effect and Conventional Breeding of Clinical Cannabis: No "Strain," No Gain. *Front Plant Sci.,* **2018**, 9, 1969.
5. Russo, E. B. Taming THC: Potential Cannabis Synergy and Phytocannabinoid-Terpenoid Entourage Effects. *Br J Pharmacol.*, **2011**, 163, 1344–1364.
6. Sanchez, L.; Filter, C.; Dalensperger, D.; Kurouski, D. Confirmatory Non-Invasive and Non-Destructive Differentiation between Hemp and Cannabis using a Hand-Held Raman Spectrometer. *RSC Adv.* **2020**, 10, 3212-3216.
7. Raman, C. V.; Krishnan, K. S. A New Type of Secondary Radiation. *Nature* **1928**, *121*, 501.
8. Izake, E. L. Forensic and Homeland Security Applications of Modern Portable Raman Spectroscopy. *Forensic Sci. Int.* **2010**, 202, 1-8.

9. Haynes, C. L.; McFarland, A. D.; Van Duyne, R. P. Surface-Enhanced Raman Spectroscopy. *Anal. Chem*. **2005**, 77, 338A-346A.

10. Langer, J.; de Aberaturi, D. J.; Aizpurua, J.; Alvarez-Puebla, R. A.; Auguié, B.; Baumberg, J. J.; Bazan, G. C.; Bell, S. E. J.; Boisen, A.; Brolo, A. G.; Choo, J.; Cialla-May, D.; Deckert, V.; Fabris, L.; Faulds, K.; de Abajo, F. J. G.; Goodacre, R.; Graham, D.; Haes, A. J.; Haynes, C. L.; Huck, C.; Itoh, T.; Käll, M.; Kneipp, J.; Kotov, N. A.; Kuang, H.; Ru, E. C. L.; Lee, H. K.; Li, J. -F.; Ling, X. Y.; Maier, S. A.; Mayerhöfer, T.; Moskovits, M.; Murakoshi, K.; Nam, J. -M.; Nie, S.; Ozaki, Y.; Pastoriza-Santos, I.; Perez-Juste, J.; Popp, J.; Pucci, A.; Reich, S.; Ren, R.; Schatz, G. C.; Shegai, T.; Schlücker, S.; Tay, L. -L.; Thomas, K. G.; Tian, Z. -Q.; Van Duyne, R. P.; Vo-Dinh, T.; Wang, Y.; Willets, K. A.; Xu, C.; Xu, H.; Xu, Y.; Yamamoto, Y. S.; Zhao, B.; Liz-Marzán, L. M. Present and Future of Surface-Enhanced Raman Scattering. *ACS Nano* **2020**, 14, 28-117.

11. Visser, B. J.; de Vreies, S. G.; Bache, E. B.; Meerveld-Gerrits, J.; Kroon, D.; Boersma, J.; Agnandji, S. T.; van Vugt, M.; Grobusch, M. P. *Malar. J.* **2016**, 15.

12. Mostowtt, T.; McCord, B. Surface Enhanced Raman Spectroscopy (SERS) as a Method for the Toxicological Analysis of Synthetic Cannabinoids. *Talanta* **2017**, *164*, 396.

13. Dies, H.; Raveendran, J.; Escobedo, C.; Docoslis. Rapid Identification and Quantification of Illicit Drugs on Nanodendritic Surface-Enhanced Raman Scattering Substrates. *Sens. Actuators B Chem.* **2018**, *257*, 382.

14. Yüksel, S.; Schwenke, A. M.; Soliveri, G.; Arsizzone, S.; Weber, K.; Cialla-May, D.; Hoeppener, S.; Schubert, U. S.; Popp, J. Trace Detection of Tetrahydrocannabinol (THC) with a SERS-Based Capillary Platform Prepared by The In Situ Microwave Synthesis of AgNPs. *Anal. Chim. Acta* **2016**, *939*, 93.

15. Milliken, S.; Fraser, J.; Poirier, S.; Hulse, J.; Tay, L. L. Self-Assembled Vertically Aligned Au Nanorod Arrays for Surface-Enhanced Raman Scattering (SERS) Detection of Cannabinol. *Spectrochim. Acta A* **2018**, *196*, 222.

16. Sivashanmugan, K.; Zhao, Y.; Wang, A. X. Tetrahydrocannabinol Sensing in Complex Biofluid with Portable Raman Spectrometer Using Diatomaceous SERS Substrates. *Biosensors* **2019**, 9, 125.

17. Bindesri, S. D.; Jebailey, R.; Albarghouthi, N.; Pye, C. C.; Brosseau, C. L. Spectroelectrochemical and Computational Studies of Tetrahydrocannabinol (THC) and Carboxy-Tetrahydrocannabinol (THC-COOH). *Analyst* **2020**, 145, 1849-1857.

18. Bumbrah, G. S.; Sharma, R. M. Raman Spectroscopy – Basic Principle, Instrumentation and Selected Applications for the Characterization of Drugs and Abuse. *Egypt. J. Forensic Sci.* **2016**, 6, 209-215.

19. Kauffman, T. H.; Kokanyan, N.; Fontana, M. D. Use of Stokes and Anti-Stokes Raman Scattering for New Applications. *J. Raman Spectrosc.* **2019**, 50, 418-424.

20. Eberhardt, K.; Stiebing, C.; Matthaus, C.; Schmitt, M.; Popp, J. Advantages and Limitations of Raman Spectroscopy for Molecular Diagnostics: An Update. *Expert Rev. Mol. Diagn.* **2015**, 15, 773-787.

21. Kudelski, A. Analytical Applications of Raman Spectroscopy. Talanta **2008**, 76, 1-8.

22. Fleischmann, M.; Hendra, P. J.; McQuillan, A. J. Raman Spectra of Pyridine Adsorbed at a Silver Electrode. *Chem. Phys. Lett.* **1974**, 26, 163-166.

23. Jeanmarie, D. L.; Van Duyne, R. P. Surface Raman Spectroelectrochemistry: Part I. Heterocyclic, Aromatic, And Aliphatic Amines Adsorbed on the Anodized Silver Electrode. *J. Electroanal. Chem. Interfacial Electrochem.* **1977**, 84, 1-20.

24. Albrecht, M. G.; Creighton, J. A. Anomalously Intense Raman Spectra of Pyridine at a Silver Electrode. *J. Am. Chem. Soc.* **1977**, 99, 5215-5217.

25. Le Ru, E. C.; Blackie, E.; Meyer, M.; Etchegoin, P. G. Surface Enhanced Raman Scattering Enhancement Factors: A Comprehensive Study. *J. Phys. Chem. C* **2007**, 111, 13794-13803.

26. Rycenga, M.; Cobley, C. M.; Zeng, J.; Li, W.; Moran, C. H.; Zhang, Q.; Qin, D.; Xia, Y. Controlling the Synthesis and Assembly of Silver Nanostructures for Plasmonic Applications. *Chem. Rev*. **2011**, 111, 3669-3712.

27. Sharma, B.; Frontiera, R. R.; Henry, A. I.; Ringe, E.; Van Duyne, R. P. SERS: Materials, Applications, and the Future. *Mater. Today* **2012**, 15, 16-25.

28. Lombardi, J. R.; Birke, R. L. A Unified Approach to Surface-Enhanced Raman Spectroscopy. *J. Phys. Chem. C* **2008**, 112, 5605-5617.

29. Lombardi, J. R.; Birke, R. L.; Lu, T.; Xu, J. Charge-Transfer Theory of Surface Enhanced Raman Spectroscopy: Herzberg-Teller Contributions *J. Chem. Phys.* **1986**, 84, 4174-4180.
30. Leonard, J.; Haddad, A.; Green, O.; Birke, R.; Kubic, T.; Lombardi, J. R. SERS, Raman and DFT Analyses of Fentanyl and Carfentanil: Toward Detection of Trace Samples. *J. Raman Spectrosc*. **2017**, 48, 1323-1329.
31. Dégardin, K.; Guillemain, A.; Roggo, Y. Comprehensive Study of a Handheld Raman Spectrometer for the Analysis of Counterfeits of Solid-Dosage Form Medicines. *J. Spectrosc.* **2017**, 2017.
32. Vagnini, M.; Gabrieli, F.; Daverni, A.; Saili, D. Handheld New Technology Raman and Portable FT-IR Spectrometers as Complementary Tools for the In Situ Identification of Organic Materials in Modern Art. *Spectrochim. Acta A* **2017**, 176, 174-182.
33. Lauwers, D.; Hutado, A. G.; Tanevska, V.; Moens, L; Bersani, S.; Vandenabeele, P. Characterization of a Portable Raman Spectrometer for *In Situ* Analysis of Art Objects. *Spectrochm. Acta A* **2014**, 118, 294-301.
34. Zheng, J.; Pang, S.; Labuza, T. P.; He, L. Evaluation of Surface-Enhanced Raman Scattering Detection Using a Handheld and a Bench-Top Raman Spectrometer: A Comparative Study. *Tantala* **2014**, 129, 79-85.
35. Fan, M.; Andrade, G. F. S.; Brolo, A. G. A Review on the Fabrication of Substrates for Surface Enhanced Raman Spectroscopy and Their Applications in Analytical Chemistry. *Anal. Chim. Acta* **2011**, 693, 7-25.
36. Lee, M.; Oh, K.; Choi, H. -K.; Lee, S. G.; Youn, H. J.; Le, H. L.; Jeong, D. H. Subnanomolar Sensitivity of Filter Paper-Based SERS Sensor for Pesticide Detection by Hydrophobicity Change of Paper Substrate. *ACS Sens.* **2018**, 3, 151-159.
37. Su, Q.; Ma, X.; Dong, J.; Jiang, X.; Qian, W. A Reproducible SERS Substrate Based on Electrostatically Assisted APTES-Functionalized Surface-Assembly of Gold Nanostars. *ACS. Appl. Mater. Interfaces* **2011**, 3, 1873-1879.
38. Li, Z. Self-Assembly Ag Nanoparticle Monolayer Film as SERS Substrate for Pesticide Detection. *Appl. Surf. Sci.* **2013**, 270, 292-294.

39. Chen, W. -L.; Huang, Y. -H. Cheng, H. -Y. Kuo, T. -R. Chang, Y. -M. Statistical Analysis of Cuboctahedral Silver Nanocrystals Langmuir–Blodgett Film SERS Substrate. *J. Raman Spectrosc.* **2018**, 49, 792-799.
40. Lynk, T. P.; Clarke, O. J. R.; Kesavan, N.; Brosseau, C. L. Development of a Sustainable Plasmon-Enhanced Spectroelectrochemical Sensor Using Avocado Pit (*Persea Americana*) Extract. *Sens. Actuators, B*. **2018**, 257, 270-277.
41. Rusin, C. J.; El Bakkari, M.; Du, R.; Boluk, Y.; McDermott, M. T. Plasmonic Cellulose Nanofibres as Water-Dispersible Surface-Enhanced Raman Scattering Substrates. *ACS Appl. Nano Mater.* **2020**, 3, 6584-6597.
42. Faulds, K.; Smith, W. E.; Graham, D.; Lacey, R. J. Assessment of Silver and Gold Substrates for the Detection of Amphetamine Sulfate by Surface Enhanced Raman Scattering (SERS). *Analyst* **2002**, 127, 282-286.
43. Saute, B. Premasiri, R.; Ziegler, L.; Narayanan, R. Gold Nanorods as Surface Enhanced Raman Spectroscopy Substrates for Sensitive and Selective Detection of Ultra-Low Levels of Dithiocarbamate Pesticides. *Analyst* **2012**, 137, 5082-5087.
44. Mahmoud, E. Y. F.; Rusin, C. J.; McDermott, M. T., Gold Nanostars as a Colloidal Substrate for In-Solution SERS Measurements Using a Handheld Raman Spectrometer. *Analyst* **2020**, 145, 1396-1407.
45. Harder, R. A.; Wijenayaka, L. A.; Phan, H. T.; Haes, A. J. Tuning Gold Nanostar Morphology for the SERS Detection of Uranyl. *J. Raman Spectrosc.* **2020**, 1-9.
46. Van der Ende, E.; Bourgeois, M. R.; Henry, A.- I.; Chavez, J. L.; Krabacher, R.; Schatz, G. C.; Van Duyne, R. P., Physicochemical Trapping of Neurotransmitters in Polymer Mediated Gold Nanoparticle Aggregates for Surface-Enhanced Raman Spectroscopy. *Anal. Chem.* **2019**, 91, 9554-9562.
47. Negru, B.; McAnally, M. O.; Mayhew, H. E.; Ueltschi, T. W.; Peng, L.; Sprague-Klein, E. A.; Schatz, G. C.; Van Duyne, R. P. Fabrication of Gold Nanosphere Oligomers for Surface-Enhanced Femtosecond Stimulated Raman Spectroscopy. *J. Phys. Chem. C.* **2017**, 121, 27004-27008.
48. Suresh, V.; Ding, L.; Chew, A. B.; Yap, F. L. Fabrication of Large-Area Flexible SERS Substrates by Nanoimprint Lithography. *ACS Appl. Nano Mater.* **2018**, 1, 886-893.

49. Pazos-Perez, N.; Guerrini, L.; Alvarez-Puebla, R. A. Fabrication of Hybrid Silver Microstructures from Vermiculite Templates as SERS Substrates. *Nanomaterials* **2020**, 10, 481.
50. Ortiz-Castillo, J. E.; Gallo-Villanueava, R. C.; Madou, M. J.; Perez-Gonzalez, V. H. Anisotropic Gold Nanoparticles: A Survey of Recent Synthetic Methodologies. *Coord. Chem. Rev.* **2020**, 425, 213489.
51. Khoury, C. G.; Vo-Dinh, T. Gold Nanostars for Surface-Enhanced Raman Scattering: Synthesis, Characterization and Optimization. *J. Phys. Chem. C.* **2008**, 112, 18849-18859.
52. Liu, G.; Young, K. L.; Liao, X.; Personick, M. L.; Mirkin, C. A. Anisotropic Nanoparticles as Shape Directing Catalysis for the Chemical Etching of Silicon. *J. Am. Chem. Soc.* **2013**, 135, 12196-12199.
53. Kohout, C.; Santi, C.; Polito, L. Anisotropic Gold Nanoparticles in Biomedical Applications. *Int. J. Mol. Sci.* **2018**, 19, 3385.
54. Dreaden, E. C.; Austin, L. A.; Mackey, M. A.; El-Sayed, M. A. Size Matters: Gold Nanoparticles in Targeted Cancer Drug Delivery. *Ther. Deliv.* **2012**, 3, 457-478.
55. Saverot, S.; Geng, X.; Leng, W.; Vikesland, P. J.; Grove, T. Z.; Bickford, L. R. Facile, Tunable, and SERS-Enhanced HEPES Gold Nanostars. *RSC Adv.* **2016**, 6, 29669-29673.
56. Song, C.; Li, F.; Guo, X.; Chen, W.; Dong, C.; Zhang, J.; Zhang, J.; Wang, L. Gold Nanostars for Cancer Cell-Targeted SERS-Imaging and NIR Light-Triggered Plasmonic Photothermal Therapy (PPTT) in the First and Second Biological Windows. *J. Mater. Chem. B* **2019**, 7, 2001-2008.
57. Meng, X. Dyer, J.; Huo, Y.; Jiang, X. Greater SERS Activity of Ligand-Stabilized Gold Nanostars with Sharp Branches. *Langmuir* **2020**, 36, 3558-3564.
58. Li, Y.; Zhu, J.; Weng, G.; Li, J.; Xiang, T. Zhao, J. "Magic mitt": Morphologically Controllable AuAg@AuAg Yolk-Shell Nanostars with Better Plasmonic Optical Properties. *J. Alloys Compd.* **2020**, 844, 156134.
59. Giese, M. W.; Lewis, M. A.; Giese, L.; Smith, K. M. Development and Validation of a Reliable and Robust Method for the Analysis of Cannabinoids and Terpenes in Cannabis. *J. AOAC Int.* **2015**, 98, 1503-1522.

60. Hanif, M. S.; Nawaz, H.; Naz, S.; Mukhtar, R.; Rashid, N.; Bhatti, I. A.; Saleem, M. Raman Spectroscopy for the Characterization of Different Fractions of Hemp Essential Oil Extracted at 130 °C Using Steam Distillation Method. *Spectrochim. Acta A* **2017**, 182, 168-174.
61. Novak, J.; Zitterl-Eglsser, K.; Deans, S. G.; Franz, C. M. Essential Oils of Different Cultivars of *Cannabis sativa* L. and Their Antimicrobial Activity. *Flavour Fragr. J.* **2001**, 16, 259-262.
62. Salehi, B.; Upadhyay, S.; Orhan, I. E.; Jugran, A. K.; Jayaweera, S. L. D.; Dias, D. A.; Sharopov, F.; Teheri, Y.; Martins, N.; Baghalpour, N.; Cho, W. C.; Sharifi-Rad, J. Therapertic Potential of α- and β-Pinene: A Miracle Gift of Nature. *Biomolecules*, **2019**, 9, 738.
63. Jardine, J. The Four Terpenes Every Stoner Should Know. *The Stranger* [Online], Nov 8, 2018, https://www.thestranger.com/weed/2018/11/08/35236014/the-four-terpenes-every-stoner-should-know (accessed Jan 2, 2021).
64. Wu, L. New Beer Standards in Canada Could Lead To Big Profit With Marijuana-Infused Brews. *Forbes* [Online], Jun 28, 2018 https://www.forbes.com/sites/lesliewu/2018/06/28/new-beer-standards-in-canada-could-lead-to-big-profit-with-marijuana-infused-brews/#49e1197a7d1d (accessed Mar 30, 2020).
65. Moye, D. This Non-Alcoholic, Cannabis-Infused White Wine Might Be A Harbinger. *Huffington Post* [Online], July 24, 2018 https://www.huffingtonpost.ca/entry/molson-coors-marijuana-beer_n_5b3145e8e4b0b745f176fab1 (accessed Apr 1, 2020).
66. Moye, D. Molson Coors Considering Selling Marijuana-Infused Beers in Canada. *Huffington Post* [Online], July 24, 2018 https://www.huffingtonpost.ca/entry/molson-coors-marijuana-beer_n_5b3145e8e4b0b745f176fab1 (accessed Apr 1 2020).
67. Reuters, T. Coca-Cola, Aurora Exploring Potential for Cannabis-Infused Drinks. *CBC News* [Online], Sept 17, 2018 https://www.cbc.ca/news/business/coke-aurora-cannabis-drinks-1.4826474 (accessed Apr 1, 2020).
68. Jagielski, D. Why Aurora Cannabis May Have Made a Big Mistake by Not Partnering With a Beverage Company. *The Motley Fool* [Online], Aug 22, 2019

https://www.fool.com/investing/2019/08/22/why-aurora-cannabis-may-have-made-a-big-mistake-by.aspx (accessed Apr 3, 2020).

69. Toronto-Based Startup in Race to Develop Cannabis 'Beer'. *CityNews Toronto* [Online], June 26, 2018 https://toronto.citynews.ca/video/2018/06/26/toronto-based-startup-in-race-to-develop-cannabis-beer/ (accessed Mar 30, 2020).
70. Mazur, A. Ontario Government Gives $300,000 to Fund Research for World's First Cannabis Beer. *Global News* [Online], May 4, 2018 https://globalnews.ca/news/4187677/ontario-government-gives-300000-to-fund-research-for-worlds-first-cannabis-beer/ (accessed Mar 30, 2020).
71. Zenabis Provides Cannabis 2.0 Product and Strategy Update. Feb 19, 2020 https://www.zenabis.com/zenabis-provides-cannabis-2-0-product-and-strategy-update/ (accessed Apr 2, 2020).
72. Islam, S. K.; Cheng, Y. P.; Birke, R. L.; Green, O.; Kubic, T.; Lombardi, J. R. Rapid and Sensitive Detection of Synthetic Cannabinoids AMB-FUBINACA and α-PVP Using Surface Enhanced Raman Scattering (SERS). *Chem. Phys.* **2018**, 506, 31.
73. Ebersbach, P.; Stehle, F.; Kayser, O.; Freier, E. Chemical Fingerprinting of Single Glandular Trichomes of Cannabis Sativa by Coherent Anti-Stokes Raman Scattering (CARS) Microscopy. *BMC Plant Biol.* **2018**, 18, 275.
74. Schulz, H.; Schrader, B.; Quilitzsch, R.; Steuer, B. Quantitative Analysis of Various Citrus Oils by ATR/FT-IR -and NIR-FT Raman Spectroscopy. *Appl. Spectrosc.* **2002**, 56, 117-124.
75. An, P.; Yuan, C. -Q.; Liu, X. -H.; Xiao, D. -B.; Luo, Z. -X. Vibrational Spectroscopic Identification of Isoprene, Pinenes and Their Mixture. *Chin. Chem. Lett.* **2016**, 27, 527-534.
76. Huang, C. -C. Applications of Raman Spectroscopy in Herbal Medicine. *Appl. Spectrosc. Rev.* **2016**, 51, 1-11.
77. Schulz, H.; Baranska, M.; Belz, H. -H.; Rösch, P.; Strehle, M. A.; Popp, J. Chemotaxonomic Characterization of Essential Oil Plants by Vibrational Spectroscopy Measurements. *Vib. Spectrosc.* **2004**, 35, 81-86.

78. Park, J.; Thomasson, J. A.; Gale, C. C.; Sword, G. A.; Lee, K. -M.; Herrman, T. J.; Suh, C. P. -C. Adsorbent-SERS Technique for Determination of Plant VOCs from Live Cotton Plants and Dried Teas. *ACS Omega* **2020**, 5, 2779-2790.

Chapter 2: Exploration of Raman Spectroscopy and Surface-Enhanced Raman Spectroscopy for Terpene and Cannabinoid Detection

2.1 Introduction

This chapter aims to assess Raman and surface-enhanced Raman spectroscopy (SERS) for its applicability for quality control of cannabis-infused beverages in the cannabis industry. Due to the recent legalization of cannabis in Canada and the expected rise in popularity of cannabis-based beverages, cost effective and rapid analytical methods will need to be established for quality control purposes. The ideal analytical platform would be able to characterize both cannabinoids and terpenes present in cannabis products due to their synergistic effects.[1,2] In this chapter, SERS is assessed as a candidate for rapid cannabinoid and terpene measurement.

Cannabis is a plant that is used recreationally and medically and is used in many countries across the world. Given the regulations in Canada outlined by Bill C-45 (Cannabis Act, section 139), there is a need to regulate the characteristics, composition, strength, concentration, potency, purity, quality, and other properties of cannabis and cannabis products.[3] Raman spectroscopy has been used for the detection of cannabinol, synthetic cannabinoids, cannabis plants, and THC in the past due to its ability to rapidly provide a molecular fingerprint for the target molecule.[3-10] Raman spectroscopy is also able to be used to detect ethanol content in alcohol,[11] making it an ideal candidate for cannabis-infused beverage analysis.

Solution-based SERS with is a powerful emerging technique in the field of SERS due to its advantage of having a shorter preparation time.[12-18] Anisotropic metal nanostructures, such as

gold nanostars (AuNSs), have also been identified as being able to provide remarkable SERS enhancements over isotropic nanoparticles.[17-20] This work aims to benefit from the use of solution-based SERS and the use of anisotropic nanoparticles by developing a method for terpene and cannabinoid detection in cannabis-infused beverages using solution-based SERS with AuNSs. This work also uses a handheld Raman spectrometer for cannabis and hemp plant analysis. The comparison and characterization of the Raman and DFT spectra for all terpenes used is also presented.

2.2 Experimental

2.2.1 Materials

Gold (III) chloride trihydrate (99.995%, HAuCl4), 4-(2-hydroxyethyl)-1-piperazineethanesulfonic acid buffer solution (1 M in H2O, HEPES), 4-(2-Hydroxyethyl)-1-piperazinepropanesulfonic acid (99.5%, EPPS), N-(2-Hydroxyethyl)piperazine-N′-(4-butanesulfonic acid) (≥ 99%, HEPBS), sodium chloride (≥ 99.5%, NaCl), (-)-β-pinene (99%), (R)-(+)-limonene (97%), linalool (97%), α-pinene (98%), and myrcene (technical grade) were purchased from Sigma-Aldrich Canada (Oakville, Ontario). 4-mercaptobenzonitrile (MBN) was purchased from Combi-Blocks, Inc. (San Diego, California, USA). Sodium hydroxide (NaOH) was purchased from Fisher Scientific Canada. 1-dram clear threaded vials, 4-dram glass vials, and 1 mL clear shell glass vials were purchased from Fisher Scientific Canada. Commercial gold nanoparticles (AuNPs) were purchased from Ted Pella, Inc (Redding, CA). Hemp and cannabis samples were supplied by Innotech Alberta (Vegreville, AB). Scona Gold Kolsch beer was provided by Alley Kat Brewing (Edmonton, AB). Cannabinoid standards were purchased from

Cerilliant Corporation (Round Rock, TX). Deionized (DI) water (18.2 MΩ·cm) was used for all syntheses and measurements in this work.

2.2.2 Gold Nanostar Synthesis

The pH of 1 M HEPES buffer solution was adjusted to the specified pH (7.20 ± 0.01 was used for the majority of experiements) using a solution of 1 M NaOH and a Fisher Scientific accumet research AR15 pH meter. A solution of both 0.5 M EPPS buffer and a 0.5 M HEPBS buffer solution were prepared in DI water and the pH was also adjusted to the indicated value. A stock solution of $HAuCl_4$ (29.14 mM) was prepared in DI water. The ratio of buffer concentration to gold salt concentration, or the "R" value was investigated for this work with values ranging from R = 100 to R = 1000. For the various ratios investigated, the concentration of gold salt was held constant. Most of this work was done using AuNSs with an R value equal to 100, where the concentration of AuNSs is estimated to be ~2.2 nM.[17] 20 mL of AuNSs were synthesized by adding DI water, HEPES buffer, and a small stir bar to a 4-dram glass vial. The gold salt was added to the solution which was then stirred at a rate of 400 rpm for 5 minutes. After stirring, the stir bar was removed, and the solution left at room temperature overnight. Afterwards the AuNS solution was stored at 4°C for no more than one week before use. Detailed synthetic details and characterization of these AuNSs can be found in a paper published by previous members of our research group.[17]

2.2.3 Characterization

UV-Vis spectroscopy experiments were done using a PerkinElmer Lambda 35 spectrometer. All experiments used a slit width of 1 nm and a scan rate of 960 nm/min. The

samples were analyzed in 1.5 mL BRAND® polystyrene disposable cuvettes and scanned from 400 to 1100 nm.

Scanning electron microscopy (SEM) imaging was performed using a Hitachi S-4800 field emission SEM. Samples were prepared on Si wafers by drop-casting 10 µL of sample onto the wafer. Images were taken at 30 keV and 20 µA (SEM).

Transmission electron microscopy (TEM) imaging was performed using a JEOL JEM-ARM200CF S/TEM. Samples underwent a washing step to remove excess buffer by centrifuging three times: 12000 rpm for 10 minutes, 9000 rpm for 10 minutes and 6000 rpm for 10 minutes (Eppendorf Centrifuge 5417 R). The samples were re-dispersed in water and sonicated for 2 minutes between centrifugation steps. After the final centrifugation step the sample was concentrated by a factor of 10 for imaging. The sample (10 µL) was drop-casted onto a TEM grid for 10 minutes and the excess solution was wicked away. Samples were imaged at 200 kV.

2.2.4 Raman Instrumentation

Three different Raman spectrometers were used for this work, the instrument used is indicated in the figure caption. The first instrument used was a B&W Tek TacticID® -GP Plus handheld Raman spectrometer with a 785 nm laser. This instrument was standardized using a polystyrene standard and all samples were analyzed using a liquid cell adapter at 100% laser power (~330 mW). Acquisition time is not user controlled for this instrument, so it varied from sample to sample.

The second instrument used was a B&W Tek NanoRam® handheld Raman spectrometer with a 785 nm laser. This instrument was standardized using a polystyrene standard and all

samples were analyzed sing a liquid cell adapter at 100% laser power (~298 mW). Acquisition time is not user controlled for this instrument, so it varied from sample to sample.

The last instrument used was a Renishaw inVia confocal Raman microscope with a 785 nm laser. Samples were analyzed using a liquid cell adapter at 100% (~294 mW) for 10 seconds with 3 accumulations in extended mode. Data were acquired using Wire 3.4 software.

All spectra shown are corrected for power and time and are without baseline correction. All spectra shown are an average of 3 spectra to ensure accurate representation of results, unless indicated to be individual samples. All spectra were analyzed and prepared using Origin 2019 software (OriginLab Corporation, Northampton, MA, USA).

2.2.5 Solution-Based SERS Analysis

To a microcentrifuge tube containing an 895 µL aliquot of colloidal AuNS, 5 uL of probe solution was added and vortex mixed for two minutes, followed by the addition of 100 µL of 2 M NaCl. The resulting solution was vortex mixed for another one minute before being transferred to a glass vial for a SERS measurement to be obtained a total of 2 minutes after salt addition, or 4 minutes after the addition of the probe molecule. All samples contained the same concentration of AuNSs and a total sample volume of 1 mL.

2.2.6 Filter Paper SERS Substrates

10 mL of colloidal AuNS solution was divided into 1 mL aliquots and centrifuged for 15 minutes at 14,000 rpm at room temperature (Eppendorf Centrifuge 5417 R). The supernatant was removed from the resulting solution, all aliquots were then combined into one tube and centrifuged again under the same conditions. The supernatant was removed once more, and the

resulting AuNS paste was combined with 15 μL of water. Whatman #1 filter paper cut into 5 mm x 5 mm squares was used for the substrates. The substrates were prepared by drop coating 5 μL of the final AuNS paste. For cases when more than one layer was used, the substrate was completely dried between layers. All solid substrate SERS analysis was carried out with an excitation wavelength of 785 nm using the TacticID® - GP Plus spectrometer.

2.3 Results and Discussion

2.3.1 Raman Spectroscopy and SERS for Hemp and Cannabis Plant Analysis

Before SERS was used, a preliminary assessment of the effectiveness of Raman spectroscopy for live hemp plant analysis was carried out to assess its ability to be used for quality control for hemp or cannabis plants during growth. Raman spectroscopy has recently been used for the differentiation between hemp and cannabis plants.[9] For this work, a handheld Raman spectrometer was used to collect spectra from growing hemp plants using a point and shoot method at 100% power in the field in which plants were grown. Many plants produced only background fluorescence, although some plants produced Raman bands. Examples of Raman spectra produced by some hemp plants are shown in Figure 2-1A. The cultivars Silesia, Grandi, and CFX-2 were used as they were the plants with the greenest leaves remaining, as this study was done near the end of the growing season for hemp. It was observed that plants with a strong smell and those with the greenest leaves produced the strongest Raman signals, an example of a section of green leaves that were analyzed is shown as an inset in Figure 2-1A. Some of the same bands produced from this hemp were also observed in the published study of Raman analysis of hemp plants. The band at 1000 cm^{-1} is from v_3(C-CH_3 stretching) from carotenoids and proteins.[9] The paper reports a band at 1376 cm^{-1} from CH_2 aliphatic bending,[9]

where as the spectra in 2-1A has a band at 1382 cm^{-1} which is close enough given the 9 cm^{-1} resolution of the spectrometer to have the same origin. The other study also reports a band at 1610 cm^{-1} from v(C-C) in the aromatic ring of lignin,[9] where the possible corresponding band in Figure 2-1A is at 1614 cm^{-1}.

Figure 2-1B shows the data obtained from using the point and shoot method at 10% power to collect Raman spectra of dried hemp plant samples. 10% power was used as opposed to 100% as the dried samples were showing evidence of being burned when 100% power was used. The cultivars Grandi and CFX-2 were used for this study to provide a similar comparison to the study of living plants in Figure 2-1A. No spectral features were observed from these samples, indicating that Raman is potentially more useful for live plant analysis rather than dried plant analysis. This data can prove useful as a background signal for cannabis plants or dried plant material, as cannabis would have the same components as hemp but with higher cannabinoid concentrations. This data also demonstrates the versatility of handheld Raman spectrometers, as they can be used both in a lab setting or for field work.

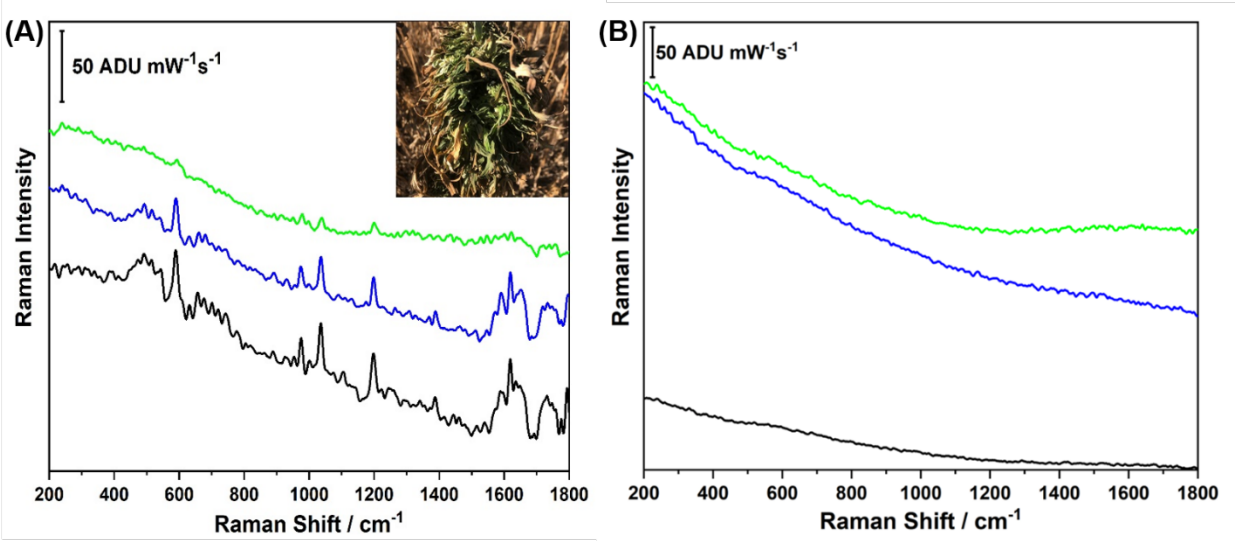

Figure 2-1. (A) Raman spectra of various cultivars of hemp; Silesia (black), Grandi (blue), and CFX-2 (green) with inset photo of typical hemp plant measured, and (B) Raman spectra of various cultivars of dried hemp samples; Grandi (blue), and two different CFX-2 plants (green and black). Raman spectra were collected with an excitation wavelength of 785 nm using the TacticID® - GP Plus spectrometer.

As Raman analysis of dried plant material was shown to be ineffective, a method was established to benefit from SERS by using a nanoparticle substrate with dried plant analysis. Dried cannabis was added to a colloidal dispersion of 30 nm AuNPs and the spectra were collected immediately. These results are shown in Figure 2-2 for three different strains of cannabis with an inset photo of the corresponding samples. The SERS signal observed decreased after 2.5 hours of initial hydration. Plant sugars and proteins are the main contributors to the broad bands that are visible in Figure 2-2. The data presented in Figures 2-1 and 2-2 suggest that Raman spectroscopy or SERS of living plants or hydrated plants may prove more useful than the analysis of dried plants.

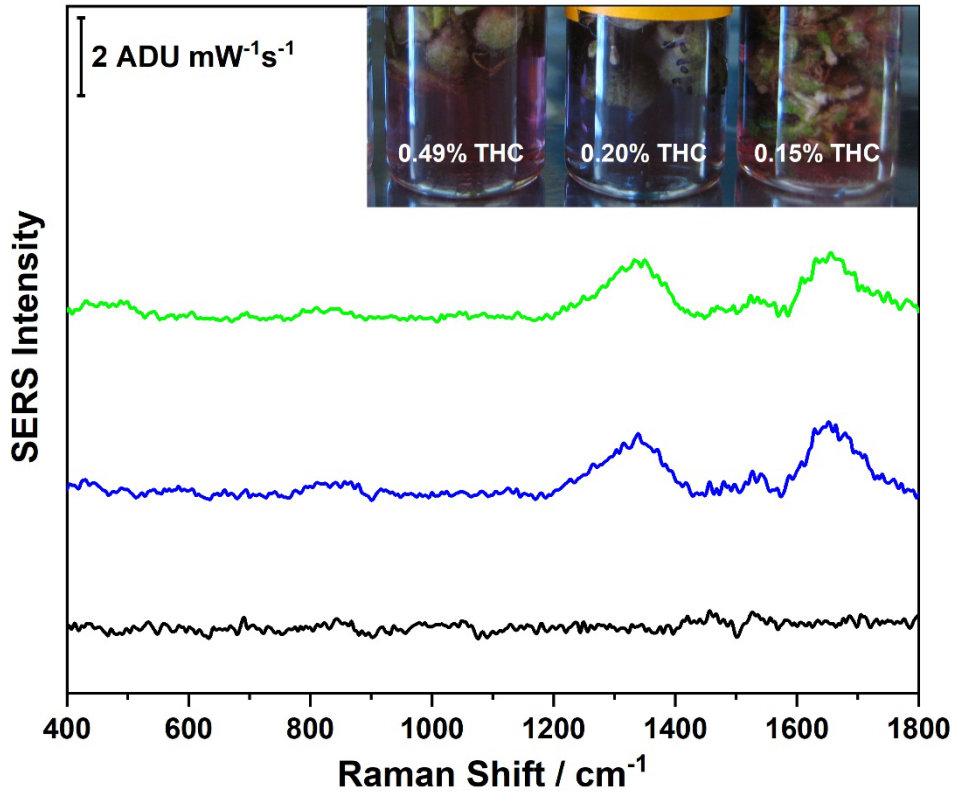

Figure 2-2. SERS spectra of various strains of dried cannabis hydrated with 30 nm AuNPs; Lemon Skunk (green), Banana Split (blue), and Zen Berry (black) containing 0.49%, 0.20%, and 0.15% THC respectively. Inset photo of corresponding hydrated plant samples. SERS spectra were collected with an excitation wavelength of 785 nm using the NanoRam® spectrometer.

2.3.2 Terpene Characterization with Raman Spectroscopy

In order to have reference spectra for some of the main terpenes found in cannabis (α- and β- pinene, linalool, limonene, and myrcene) a normal Raman spectrum was collected for each molecule to be compared to the theoretical spectrum generated using density functional

theorem (DFT). Figure 2-3 shows the experimental Raman (black) and DFT (red) spectra of five terpenes (A) α-pinene, (B) β-pinene, (C) linalool, (D) limonene, and (E) myrcene.

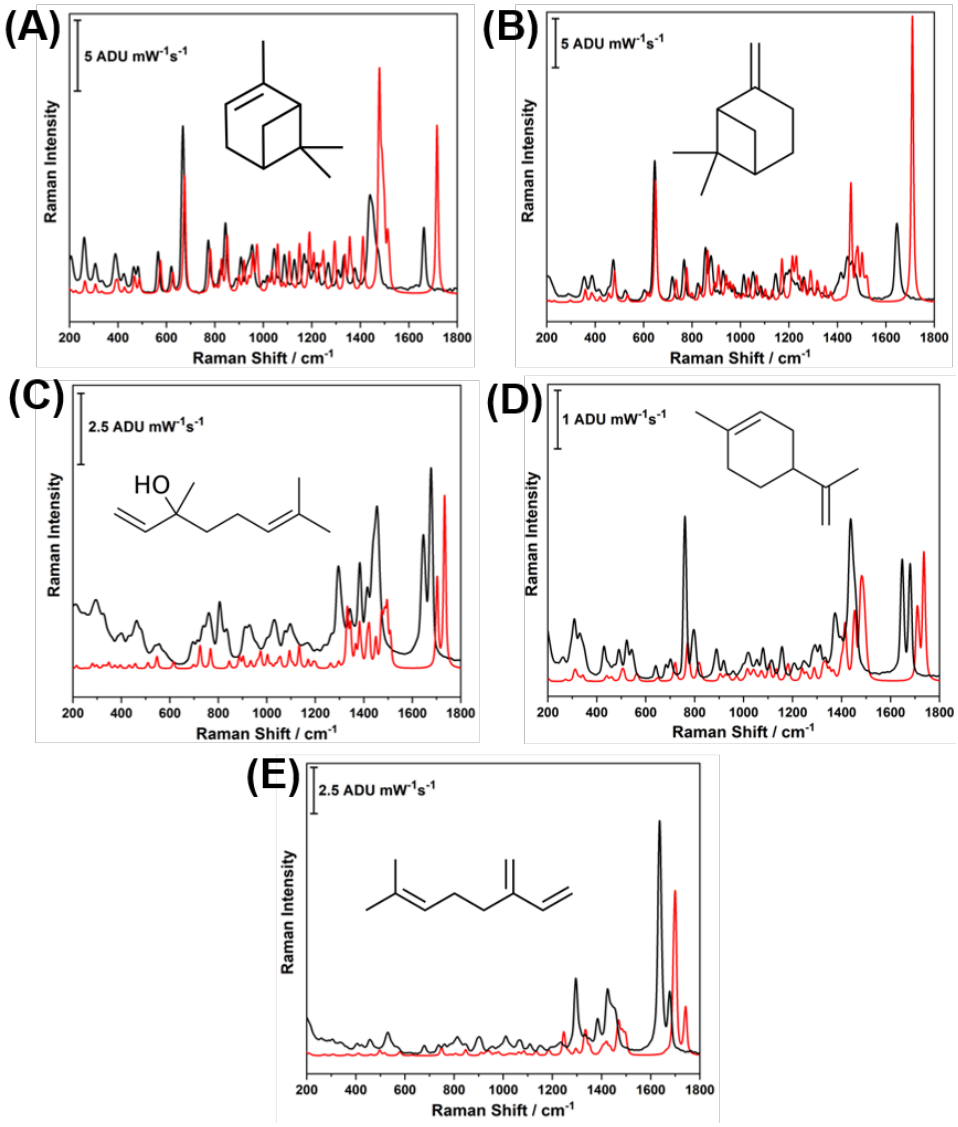

Figure 2-3. Experimental (black) and theoretical (red) Raman spectra for (A) α-pinene, (B) β-pinene, (C) linalool, (D) limonene, and (E) myrcene. Theoretical spectra calculated using DFT at the B3LYP-D3(BJ)/def2-TZVPD level of theory. Raman spectra were collected with an excitation wavelength of 785 nm using the TacticID® - GP Plus spectrometer.

The band observed in the Raman spectrum for β-pinene at 646 cm^{-1} can be attributed to ring, this band was also observed in the DFT spectrum.[22] The 1440 cm^{-1} band in the Raman spectrum can be attributed to CH_2/CH_3 bending, and the 1644 cm^{-1} band in the Raman spectrum is from C=C stretching.[22] In the Raman and DFT spectra for α-pinene, a band at 666 cm^{-1} is observed as a result of ring deformations, and the Raman spectrum has a band at 1440 cm^{-1} from CH_2/CH_3 bending.[22] The Raman spectrum for linalool contains weak bands at 1097 cm^{-1}, and 1027 cm^{-1}, where the DFT spectrum has weak bands at 1097 cm^{-1} and 932 cm^{-1}.[22] The Raman spectrum for linalool also contains band at 1675 cm^{-1}, 1642 cm^{-1}, and 1292 cm^{-1} that can be attributed to C=C stretching, C=C stretching, and $(CH_2)_2$ respectively.[22] The Raman spectrum for limonene contains bands at 1678 cm^{-1}, 1645 cm^{-1}, 1435 cm^{-1}, and 760 cm^{-1} from cyclohexane, the C=C in ethylene, CH_2CH_3 bending, and ring vibrations respectively.[22] The spectrum also contains weak bands at 1376 cm^{-1}, 1291 cm^{-1}, 1018 cm^{-1}, and 888 cm^{-1}, where the 1291 cm^{-1} and 1018 cm^{-1} bands are also observed in the DFT spectrum.[22] Lastly, the Raman spectrum for myrcene contains bands at 1677 cm^{-1}, 1639 cm^{-1}, and 1295 cm^{-1} from C=C stretching, C=C stretching, and $–(CH_2)_2$ bending respectively, and a band from cyclohexane is observed at 805 cm^{-1} in the DFT spectrum.[22] Overall, the majority of the bands in the DFT spectrum were similar to the Raman spectra, however they are shifted approximately 50 cm^{-1} towards higher wavenumbers.

As Raman spectroscopy had previously proven to not be adequately powerful to detect terpenes in hemp or cannabis samples, standard solutions were used to determine the concentration of these molecules that could be detected using Raman spectroscopy without employing surface-enhancement. Figure 2-4 shows the Raman spectra of various concentration of the terpene solutions prepared in ethanol collected directly from glass vials. Figure 2-4A

shows the spectra for α-pinene, 2-4B for β-pinene, and 2-4C for linalool. It is important to note that the bands at 435 cm^{-1}, 882 cm^{-1}, 1048 cm^{-1}, 1086 cm^{-1}, 1276 cm^{-1}, 1456 cm^{-1}, and the shoulder at 1485 cm^{-1} are due to the ethanol solvent. This experiment made it clear that SERS would be required to detect lower terpene concentrations, as discernible terpene bands were not present until concentrations of 1 M were used for normal Raman spectroscopy.

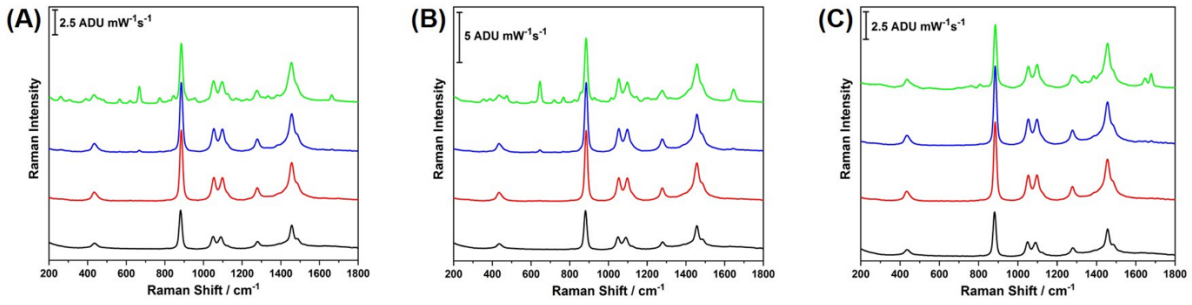

Figure 2-4. Raman spectra of 50% EtOH (black), 0.01 M terpene solution (red), 0.1 M terpene solution (blue), and 1 M terpene solution (green) for (A) α-pinene, (B) β-pinene, and (C) linalool. All solutions were measured in EtOH, and Raman spectra were collected with an excitation wavelength of 785 nm using the TacticID® - GP Plus spectrometer.

2.3.3 Gold Nanostar Optimization

As the previous results showed, SERS would need to be employed to obtain spectra from terpenes, as normal Raman was not sufficient at low concentrations. Gold nanostars (AuNSs) were selected as the substrate for solution-based SERS, given the convenience it would provide for analyzing beverage samples using a handheld Raman spectrometer. Our group has recently published a manuscript describing the optimization of AuNS synthesis for in-solution SERS measurements.[17] AuNSs are synthesized by mixing gold salt and a Good's buffer to obtain the

desired gold to buffer ratio (R value). The R value can be used to tune the shape configuration of the nanostars. The tertiary amines from the piperazine group are able to form free radicals to reduce the Au^{3+} ions to Au.[17] The terminal alkanesulfonate can direct the shape of the AuNSs.[17] The formation of the bilayer is promoted by the terminal alkanesulfonate and the terminal hydroxyl groups, which also contributes to the colloidal and shape stability through hydrogen bonding.[17] Figure 2-5 shows some characterization of the AuNSs, where 2-5A displays an overlay of the extinction spectra for AuNS of various R values with an inset photo of the corresponding colloidal solution. Figure 2-5B is an SEM image of gold nanostars with an R value of 100, and 2-5C is a TEM image of gold nanostars with an R value of 700. This figure demonstrates that the higher the R value, the longer the branches produced on the nanostars and the more red-shifted the extinction will be.

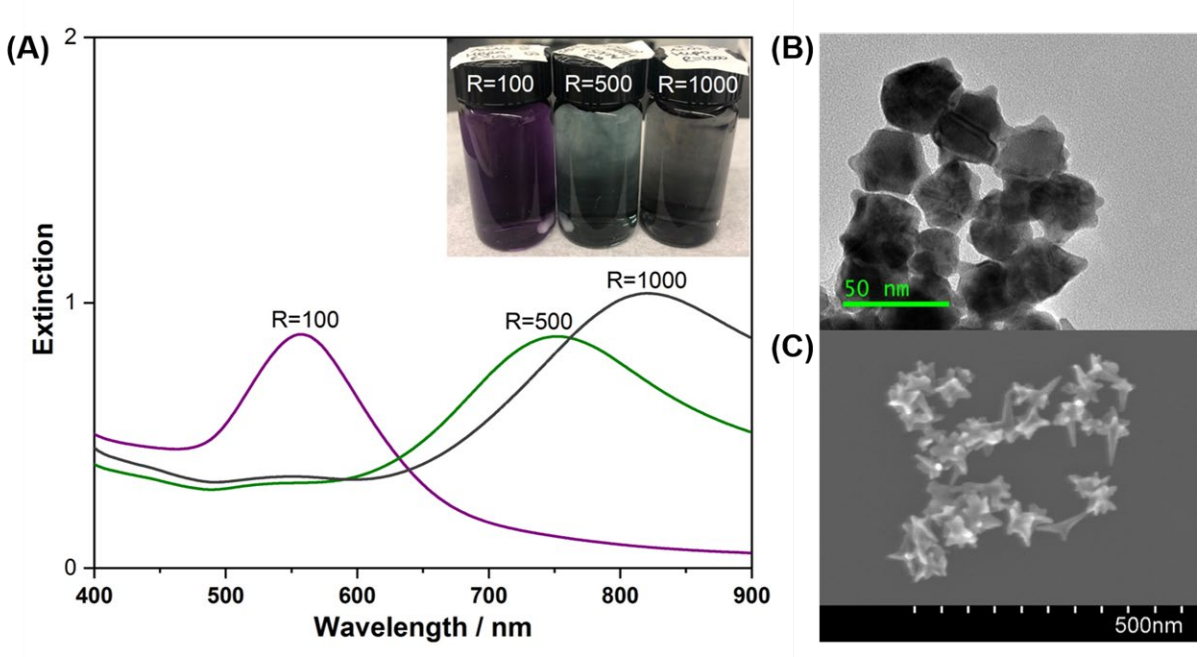

Figure 2-5. (A) Extinction spectra for gold nanostars of various R values with inset photo of corresponding colloidal solutions, (B) SEM image of gold nanostars with an R value of 100, and (C) TEM image of gold nanostars with an R value of 700.

SERS optimization using AuNSs was carried out using 4-mercaptobenzonitrile (MBN), as it is a strong SERS reporter. The results of this study are shown in Figure 6A, where the first number of the code indicates the R values (where 1 is for R=100, and 5 is for R=500), and the last two numbers indicate the pH (where 80 is a pH of 8.0, 72 is a pH of 7.2, and 76 is a pH of 7.6), and the letter indicates the Good's buffer used (where B indicates HEPBS, E indicates EPPS, and H indicates HEPES). This study found that HEPES buffer at a pH of 7.2 with and R value of 100 was the best candidate for solution-based SERS, and thus is the substrate used going forward. Figure 6B shows the corresponding extinction spectra for each AuNS solution that was analyzed, where the top performing substrate has a λmax at 580 nm.

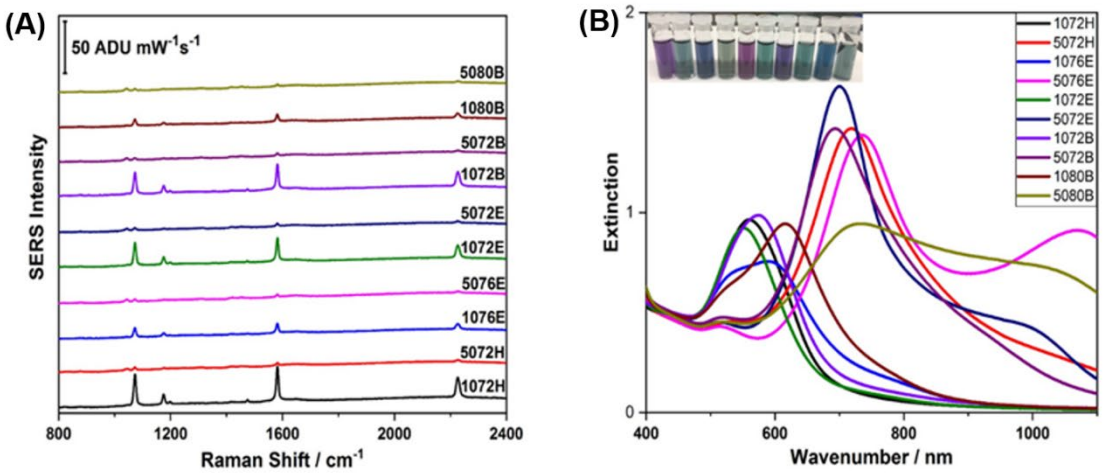

Figure 2-6. (A) SERS spectra of 1 μM 4-MBN using AuNSs made with various buffers, pHs, and R values collected using the InVia spectrometer, and (B) the extinction spectra of each AuNS solution with inset of photo showing LSPR (in order as listed in the legend).

The results of this study are particularly interesting, as the results are contradictory to what is typically observed for these types of nanoparticles. It is likely that the reasoning for the increased SERS performance of the shorter branched stars is a result of the ability of the reporter molecule to access the surface of the nanostars. An important consideration is that the surface of these nanostructures is populated with buffer molecules, which act as a capping agent to prevent aggregation of the AuNS. With the longer branches, it is possible that the buffer is preventing the reporter molecule from accessing the surface of the branches.

Figure 12A shows the SERS spectra of various concentrations of MBN, where the signal intensity is found to increase going from low to high concentration. Figure 12B shows the corresponding calibration curve, constructed using the intensity of the 1076 cm^{-1} band of MBN.

This calibration curve produces a linear fit, with an R^2 value of 0.97. This supports that this method can be used for quantitative detection.

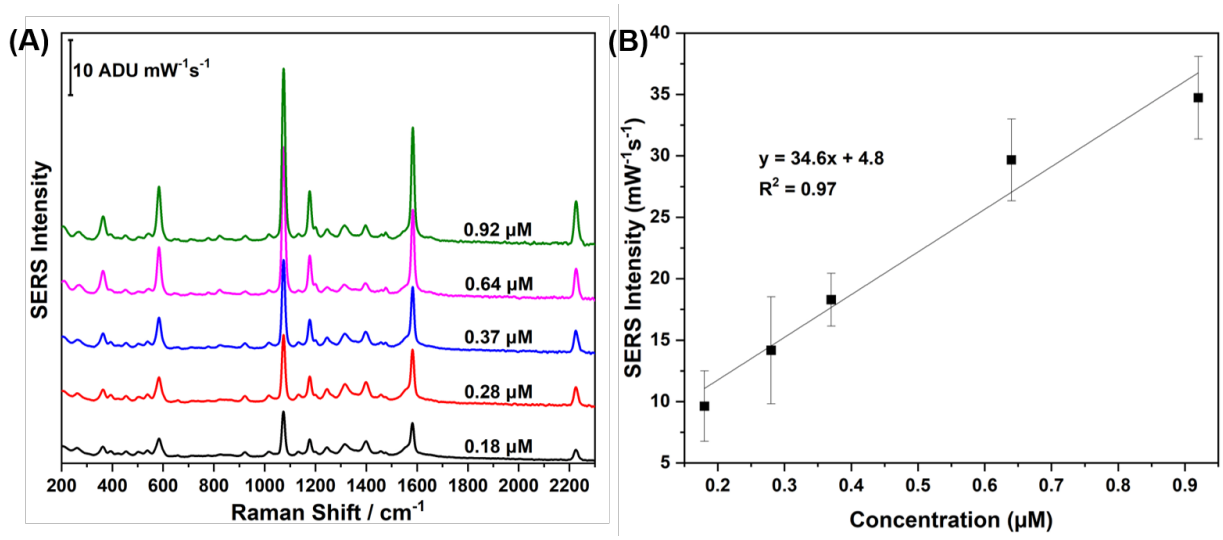

Figure 2-7. (A) Overlay of SERS spectra of various concentrations of MBN (indicated) using solution-based SERS with AuNSs, and (B) calibration curve of intensity of 1076 cm^{-1} band, where the points represent the mean of three measurements and the error bars represent the standard deviation. SERS spectra were collected with an excitation wavelength of 785 nm using the NanoRam® spectrometer.

2.3.4 Terpene and Cannabinoid Analysis using Solution-Based SERS with AuNSs

The method for solution-based SERS optimized in the above section was evaluated for its applicability for terpenes, as terpenes are an important compound of cannabis and can have synergistic effects with cannabinoids.[1,2] Myrcene, β-pinene, α-pinene, linalool, and limonene were all analyzed using this method, as is shown in Figure 2-8. These terpenes were chosen as they are either found in many cultivars of cannabis or have medicinal properties of their own.[21-23] For this analysis, 5 µL of neat liquid of each terpene was spiked into the AuNS solution for

SERS analysis. The approximate final concentration of myrcene was 0.02 M, and the final concentration of the other terpenes was 0.03 M. Myrcene produced a strong signal, however all the bands can be attributed to ethanol (shown in Figure 2-8 as well), as the myrcene used was technical grade, it likely contained ethanol. β-pinene was also able to be detected, with the most prominent band present at 844 cm^{-1}, which is likely from deformations of the C skeleton.[24] Linalool also has well defined bands at 1545 cm^{-1} and 1672 cm^{-1}, where the 1672 cm^{-1} band is likely from C=C stretching.[22] α-pinene and limonene produced similar spectra, with the band present in their spectra being from the substrate itself or ethanol impurities. The spectra in Figure 2-8 demonstrate that AuNS for in solution-SERS can be used to detect two out of five of the terpenes investigated.

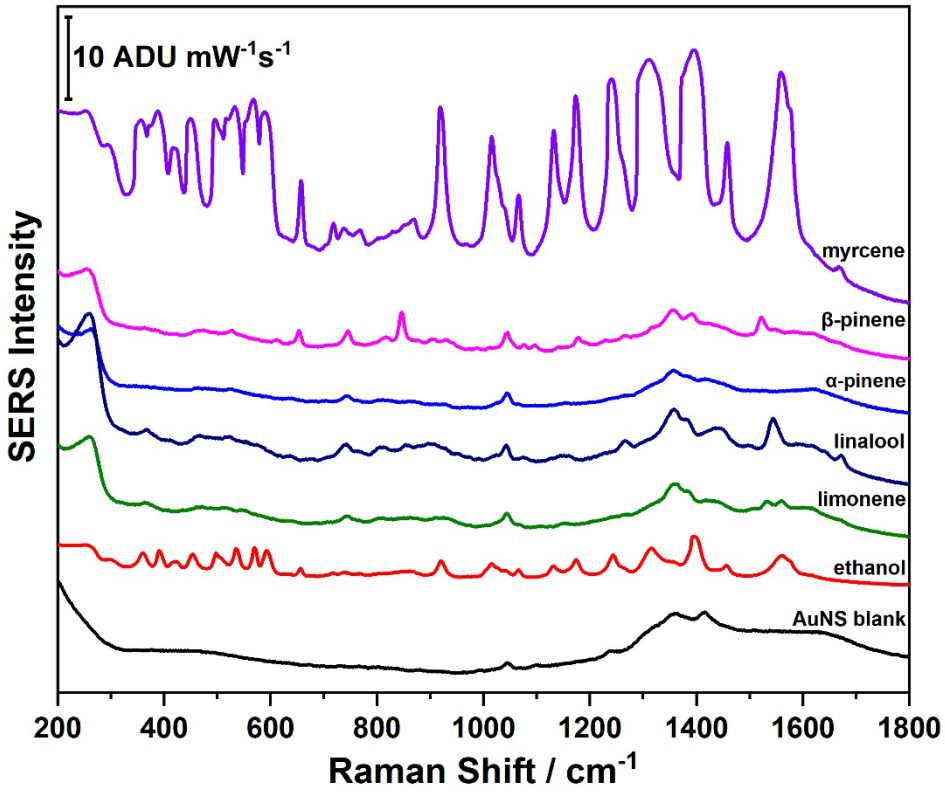

Figure 2-8. Overlay of SERS spectra of various terpenes (indicated) with ethanol spectrum and AuNS blank spectrum obtained using solution-based SERS with AuNSs. SERS spectra were collected with an excitation wavelength of 785 nm using the InVia spectrometer.

The optimized AuNS for solution-based SERS method was also applied to the detection of cannabinoids, which is typically a challenging target. There is a lack of agreement about the observed SERS signals for cannabinoids across the published work, as cannabinoids are a difficult target due to their low affinity for metal surfaces in SERS as well as their low Raman cross-section.[10] CBD, (-)-delta9-THC, and (-)-delta8-THC were all spiked directly into the AuNSs from the 1 mg/mL solution in ethanol for a final concentration of 0.005 mg/mL. Figure 2-9A shows the structures of the three cannabinoids used in this study, and the SERS spectra

obtained are shown in Figure 2-9B. The majority of the bands in the observed spectra, such as the band at 1042 cm^{-1}, are from either the substrate itself or ethanol. However, there is a band at 637 cm^{-1} and at 740 cm^{-1} in all the spectra that does not appear to be from either ethanol or the substrate. While this does show some promise for the detection of cannabinoids with solution-based SERS with AuNS, SERS detection of cannabinoids remains a challenge.

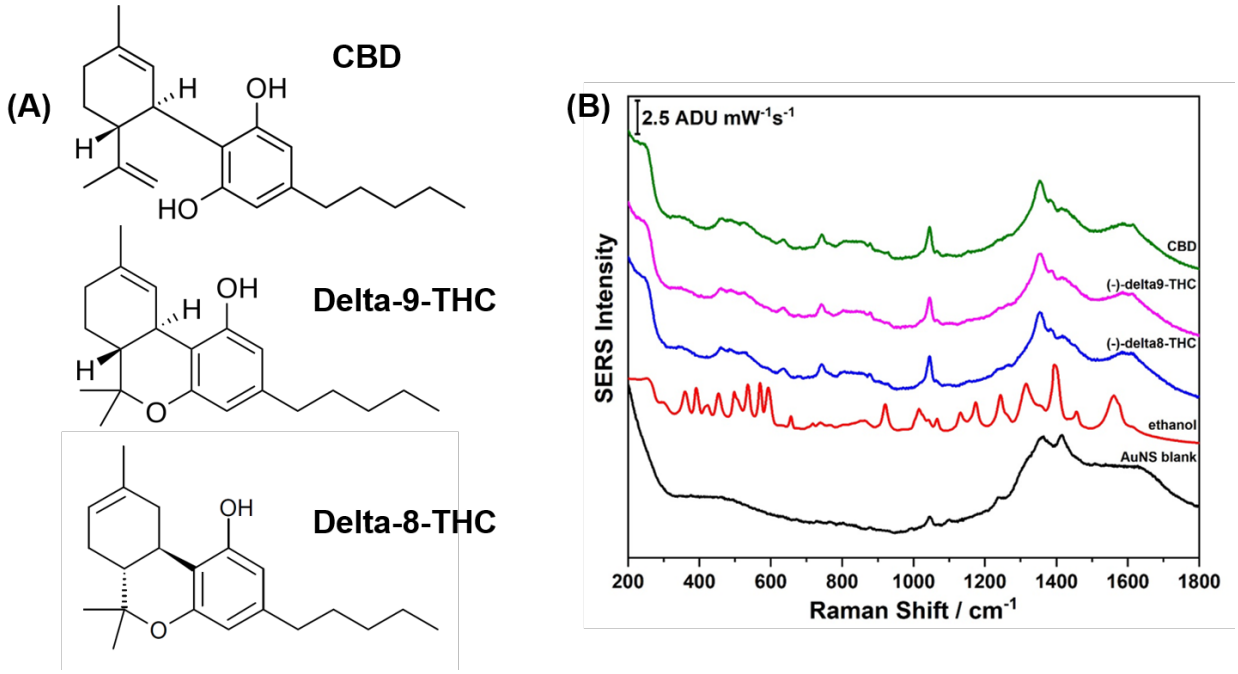

Figure 2-9. (A) Structures of cannabinoids used, and (B) Overlay of SERS spectra of various cannabinoids (indicated, 1 mg/mL in ethanol) with ethanol spectrum and AuNS blank spectrum obtained using solution-based SERS with AuNSs. SERS spectra were collected with an excitation wavelength of 785 nm using the InVia spectrometer.

The analyte that was the most successfully detected was β-pinene, with several well-defined bands in its SERS spectrum. An investigation was carried out to see if β-pinene could be

detected quantitatively using solution-based SERS with AuNSs based on the intensity of the 844 cm^{-1} band. The results of this study are shown in Figure 2-10 where A shows the increase of the SERS intensity of the 844 cm^{-1} band with increasing concentration, which corresponds to the linear relationship shown in the calibration curve in B. The large error bars for the higher concentrations is likely due to the effect that terpenes have on the aggregation of the AuNS substrate. It has been observed during these experiments that higher concentrations of terpenes contribute to the aggregation of the AuNS and cause more aggressive aggregation than what is observed at lower concentrations. This data demonstrates that solution-based SERS with AuNSs can be used for the qualitative and quantitative detection of β-pinene. Literature indicates that relevant concentrations for the detection of these terpenes would be around 0.1 - 7 mM, so the concentration range is comparable to other studies that have been reported.[26] The estimated limit of detection (LOD) from this calibration curve is 2.5 mM, which corresponds to approximately 0.3 ppm.

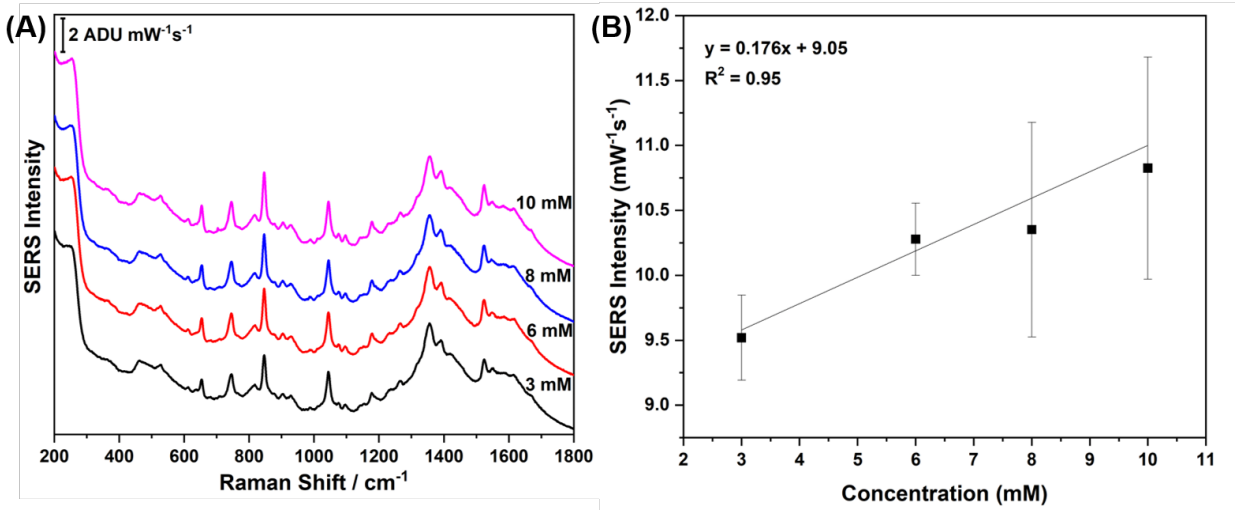

Figure 2-10. (A) Overlay of SERS spectra of various concentrations of β-pinene (indicated) using the solution-based SERS with AuNSs, and (B) calibration curve of intensity of 844 cm^{-1}, where the points represent the mean of three measurements and the error bars represent the standard deviation. SERS spectra were collected with an excitation wavelength of 785 nm using the InVia spectrometer.

2.3.5 Terpene and Cannabinoid Analysis using Solution-Based SERS with AuNPs

As a means of comparison to solution-based SERS with AuNSs, commercially available AuNPs were also evaluated for their ability to detect terpenes and cannabinoids. This would also allow for a broader statement to be made about the efficacy of solution-based SERS for terpene and cannabinoid detection. The main differences between the AuNSs and the commercial AuNPs are the shape (sphere vs star) and stabilization layer. Based shape difference, given that the AuNPs are isotropic and the AuNSs are anisotropic, the AuNSs should out-perform the AuNPs. However, the AuNSs are coated with a bilayer of buffer molecules, where the commercial AuNPs are coated with a more easily displaceable citrate layer. It is common for gold

nanospheres to be purposely aggregated to generate hot spots for solution-based SERS applications.[25] In this case, NaCl was added to induce aggregation. The commercial AuNPs for solution-based SERS were first optimized using MBN, where the aggregation time and AuNP size was investigated for its effect on the SERS performance. The results of these optimization studies are shown in Figure 2-11, where A shows the overlay of the spectra with 30 seconds of aggregation time and 2 minutes of aggregation time, where the 30 second aggregation time resulted in slightly higher SERS intensity. The aggregation time is defined as the time between salt addition and spectral acquisition. Figure 2-11 B shows the overlay of the spectra collected using 10 nm, 20 nm, and 30 nm AuNPs, all obtained with 30 seconds of aggregation time, where the strongest SERS signal was obtained from the 30 nm AuNPs. 30 nm AuNPs were used with 30 seconds of aggregation time for the detection of terpenes and cannabinoids in the following studies.

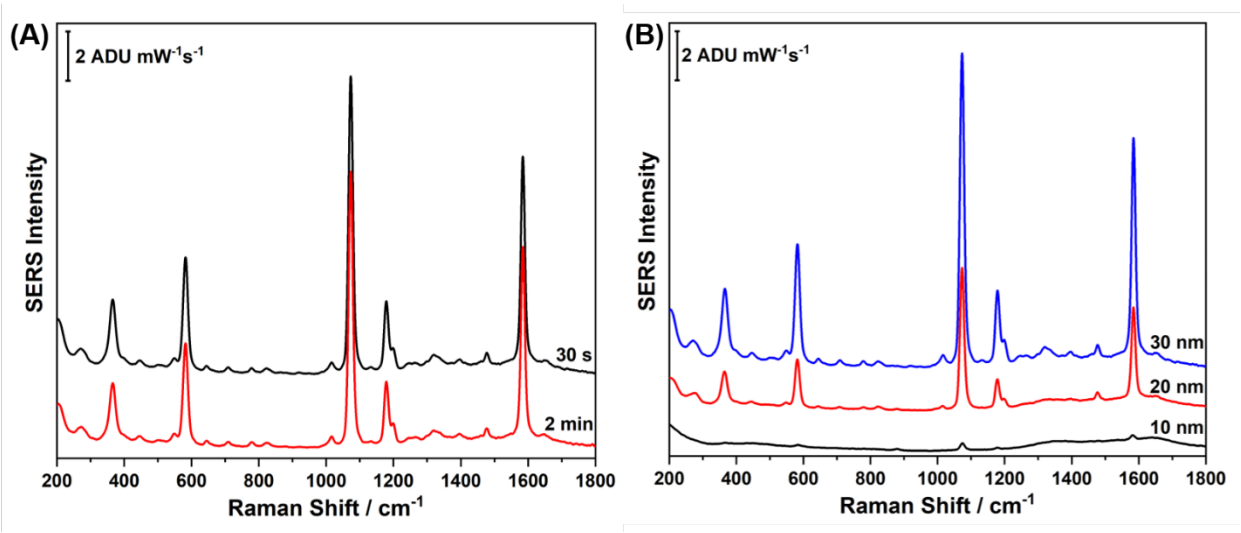

Figure 2-11. Overlay of SERS spectra of 1 μM 4-MBN obtained using (A) different aggregation times for AuNPs (30 seconds and 2 minutes after addition of 2 M NaCl), and (B) different AuNP diameter (10 nm, 20 nm, and 30 nm). SERS spectra were collected with an excitation wavelength of 785 nm using the NanoRam® spectrometer.

The optimized method for solution-based SERS with AuNPs was then used for terpene detection in the same way that they were with the AuNS substrate. The results of this study are shown in Figure 2-12, where the spectra for all of the terpenes are overlaid with the ethanol and black spectra. As can be seen in this figure, none of the terpenes produced bands aside from myrcene, which again were bands from ethanol, and a very small band at 844 cm^{-1} was visible for β-pinene. This study demonstrates that the AuNS method for solution-based SERS was actually more sensitive for the detection of terpenes, as AuNPs could only be used for the weak detection of one out of the five terpenes.

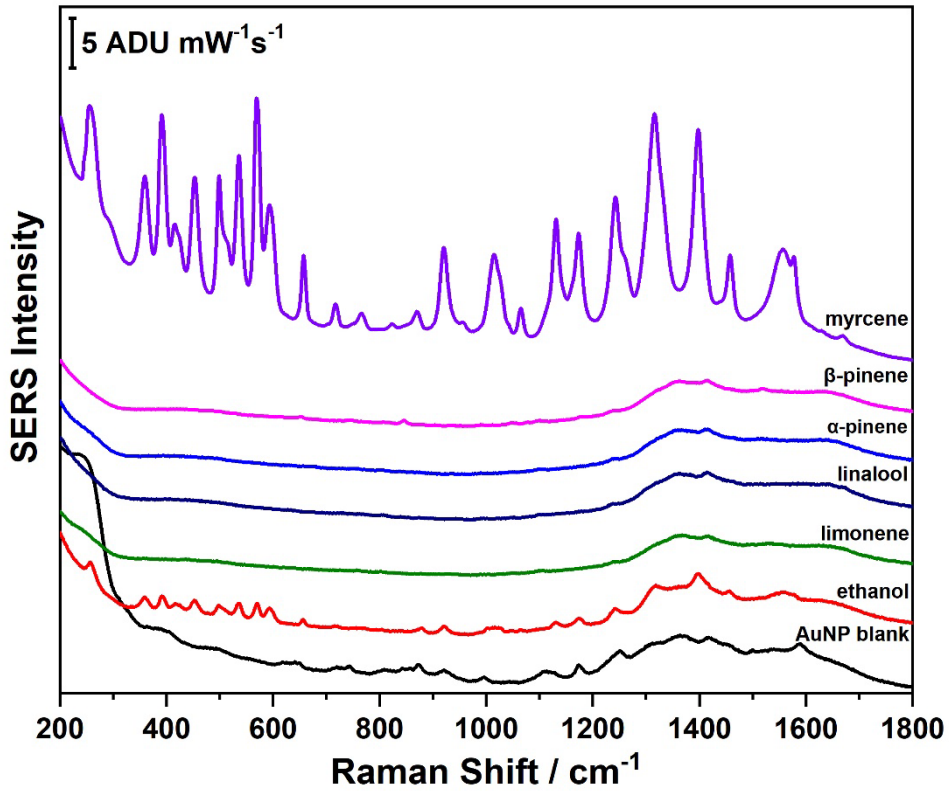

Figure 2-12. Overlay of SERS spectra of various terpenes (indicated) with ethanol spectrum and AuNP blank spectrum obtained using solution-based SERS with AuNPs. SERS spectra were collected with an excitation wavelength of 785 nm using the InVia spectrometer.

The optimized solution-based SERS method using AuNPs was again used for the detection of cannabinoids as a mode of comparison to the AuNS method. The results of this study are shown in Figure 2-13 with an overlay of the SERS spectra for all the cannabinoids as well as ethanol (the solvent) and the AuNP substrate blank. This method did not produce any bands from the cannabinoids, as all spectral features observed are from the ethanol and the substrate themselves. These data support that the AuNS method was more applicable for the detection of cannabinoids than commercial AuNPs.

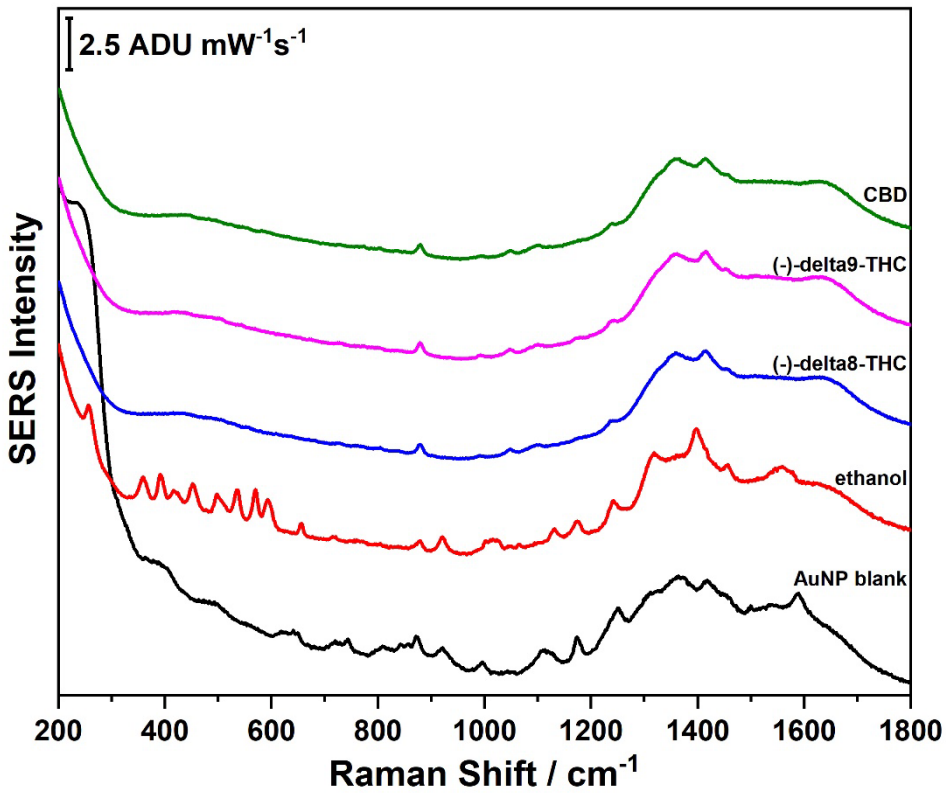

Figure 2-13. Overlay of SERS spectra of cannabinoids (indicated, 1 mg/mL in ethanol) with ethanol spectrum and AuNP blank spectrum obtained using solution-based SERS with AuNPs. SERS spectra were collected with an excitation wavelength of 785 nm using the InVia spectrometer.

2.3.6 Terpene Analysis in Beer using Solution-Based SERS with AuNSs

Any commercial cannabis beers would not be able to contain both alcohol and cannabis compounds thus, a method for removing ethanol from beer had to be established. Raman has been used in the past for the detection of ethanol in alcohol,[11] so it was able to be used to develop this method. Before beer was analyzed, a calibration curve was made with ethanol to have a reference when confirming that ethanol had been removed from the beer. The main band used for the calibration curve and determining if there was ethanol in the beer was chosen as the 883 cm^{-1}

band (C-O-O band). Once a reference was obtained for ethanol content (Figure 2-14A), a Raman spectrum for Alley Kat Scona Gold beer out of the bottle was recorded, as is shown in Figure 2-14B. Ethanol bands are present in this spectrum. A simple method of boiling the beer to remove the ethanol and filtering it was used. Both 30 and 60 minutes of boiling removed the ethanol from the beer, as is evident from the disappearance of the ethanol bands. The beer boiled for 30 minutes exhibited a lower background than the beer boiled for 60 minutes and was chosen as the method to remove alcohol from beer for spiking experiments. This study also shows that Raman spectroscopy can also be used for confirmation of the removal of ethanol from alcoholic beverages, which would be a vital step in the production process of cannabis-infused beers.

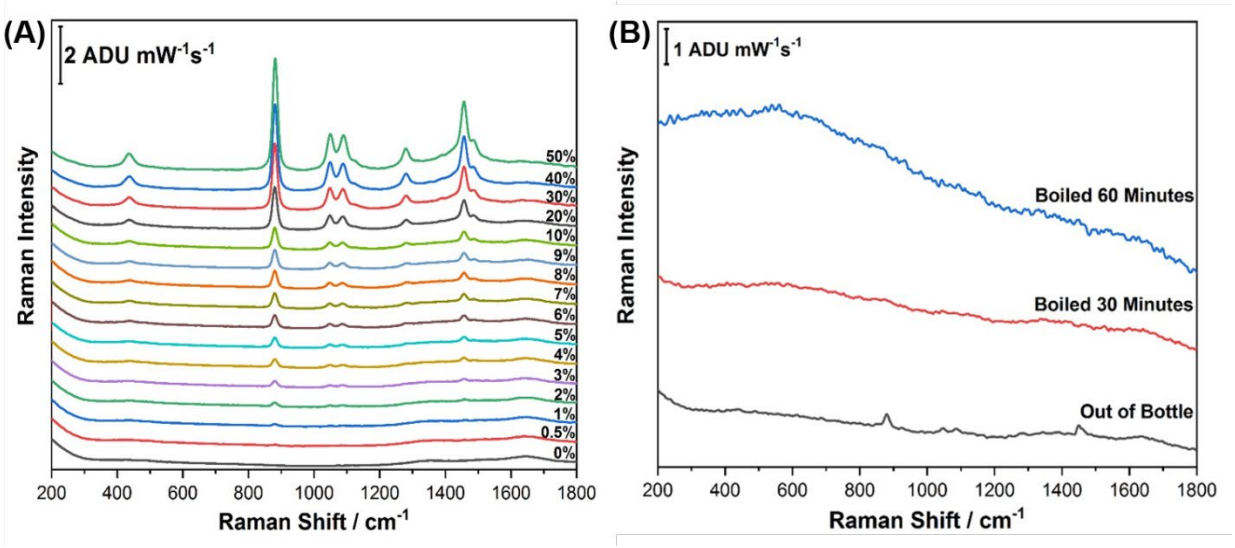

Figure 2-14. (A) Raman spectra of increasing concentration of ethanol and, (B) Overlay of Raman spectra of beer out of the bottle, and beer boiled for both 30 minutes and 60 minutes (indicated). Raman spectra were collected with an excitation wavelength of 785 nm using the TacticID® - GP Plus spectrometer.

As the AuNS method for terpene and cannabinoid detection proved to be the most successful solution-based SERS method evaluated, it was used for the detection of β-pinene in beer that had the alcohol removed by boiling for 30 minutes, followed by filtration through a 0.45 μm syringe to remove any sediment. Figure 2-15 shows the results of this study, where an overlay is presented of the SERS spectra for beer, beer with 0.03 M of β-pinene, and the spectrum for β-pinene alone. The characteristic 844 cm^{-1} band for β-pinene was not able to be detected in the beer using this method. It is likely that the beer matrix adsorbed to the surface of the AuNSs and prevented the adsorption of terpene to the surface to undergo signal enhancement. The peaks observed in beer are likely from sugars, and the peak at 737 cm^{-1} could be from coniferyl alcohol, which is found in many food products.[27] This study proves as a preliminary assessment and should be further explored with other terpenes and cannabinoids in future studies.

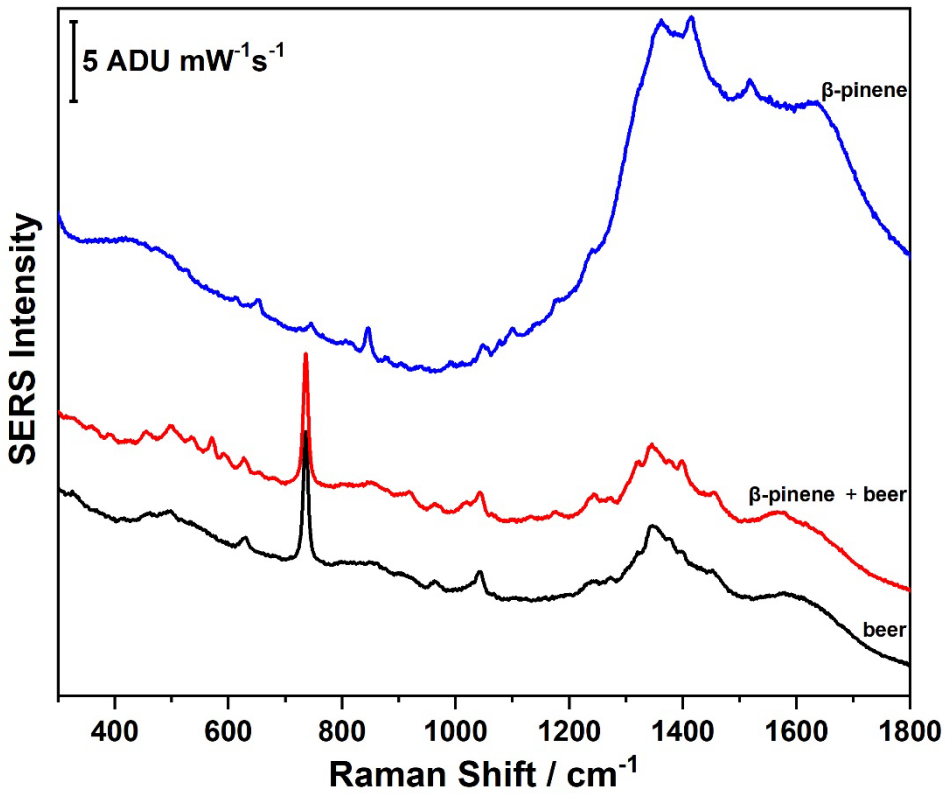

Figure 2-15. SERS overlay of the spectra collected using solution-based SERS with AuNSs of β-pinene (top/blue spectrum), 30 mM β-pinene spiked in beer (middle/red spectrum), and a blank of dealcolized beer (bottom/black spectrum). SERS spectra were collected with an excitation wavelength of 785 nm using the InVia spectrometer.

2.3.7 Terpene Analysis with Filter Paper Substrates

As the AuNSs showed promise for terpene and cannabinoid detection with solution-based SERS, solid substrates were also fabricated using AuNSs. The AuNSs were drop coated onto filter paper to create a 3D substrate. Solid substrates with filter paper have shown promise in past work for SERS detection of various analytes.[28,29] The first optimization that was done was

determining the appropriate number of layers of concentrated AuNS paste to use on the substrates. SERS measurements were performed using a handheld Raman spectrometer (TacticID® - GP Plus) using the TacPac attachment. Each spectrum is the average of three spectra taken from different spots on the same substrate. The results in Figure 2-16 show the SERS spectra of α-pinene from solid substrates with 1 layer and 3 layers of AuNS paste, as well as a blank of just the filter paper. All the bands visible in the α-pinene spectra are not from the substrate or ethanol. The peaks at 487 cm^{-1}, 1107 cm^{-1}, 1145 cm^{-1}, 1328 cm^{-1}, and 1406 cm^{-1} that are observed in the SERS spectra for α-pinene were also predicted in the DFT spectra, indicating that α-pinene was successfully detected using this method. Using three layers of AuNS paste produced less of a background signal, and so it was chosen as the conditions to use for subsequent studies.

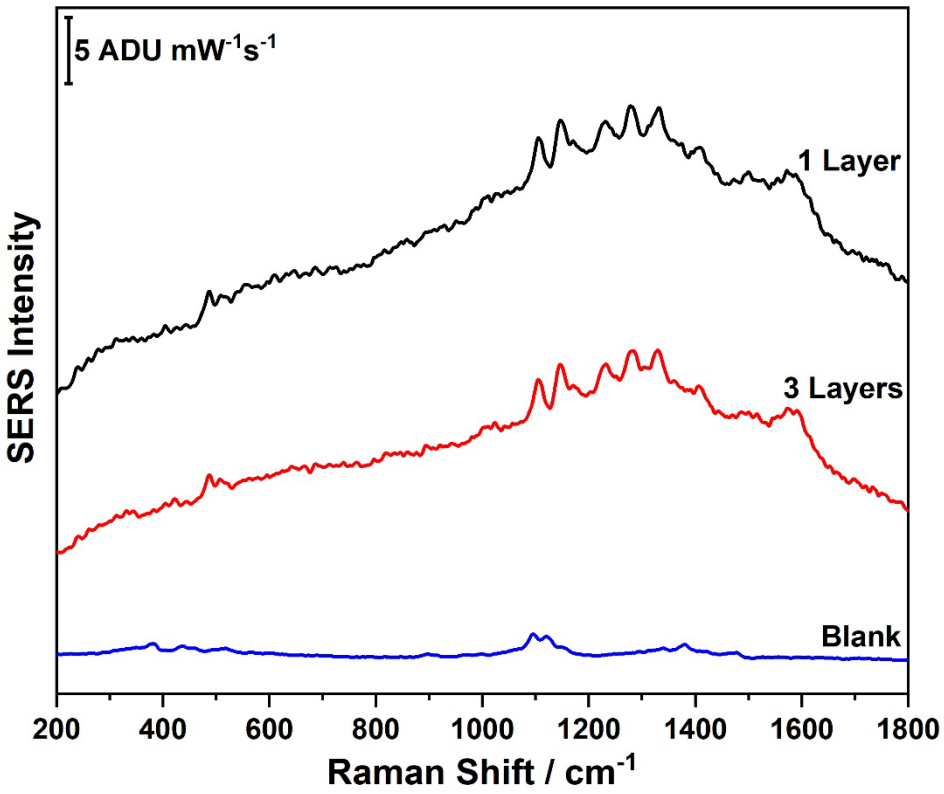

Figure 2-16. Overlay of SERS spectra of α-pinene drop coated on a solid filter paper substrate containing one and three layers (indicated) of R = 100 AuNSs and a blank spectrum with no α-pinene. SERS spectra were collected with an excitation wavelength of 785 nm using the TacticID® - GP Plus spectrometer.

Further optimization was done by collecting the SERS spectrum of α-pinene on a filter paper substrate with three layers of AuNSs of different R values. The R value dictates the length of the branches, where a larger R value indicates longer branches. R values of 100, 500, and 1000 were investigated in this study, for which the resulting spectra are shown in Figure 2-17. The spectra collected from the three R values of AuNSs investigated showed similar results, and again were all successful for the detection of α-pinene.

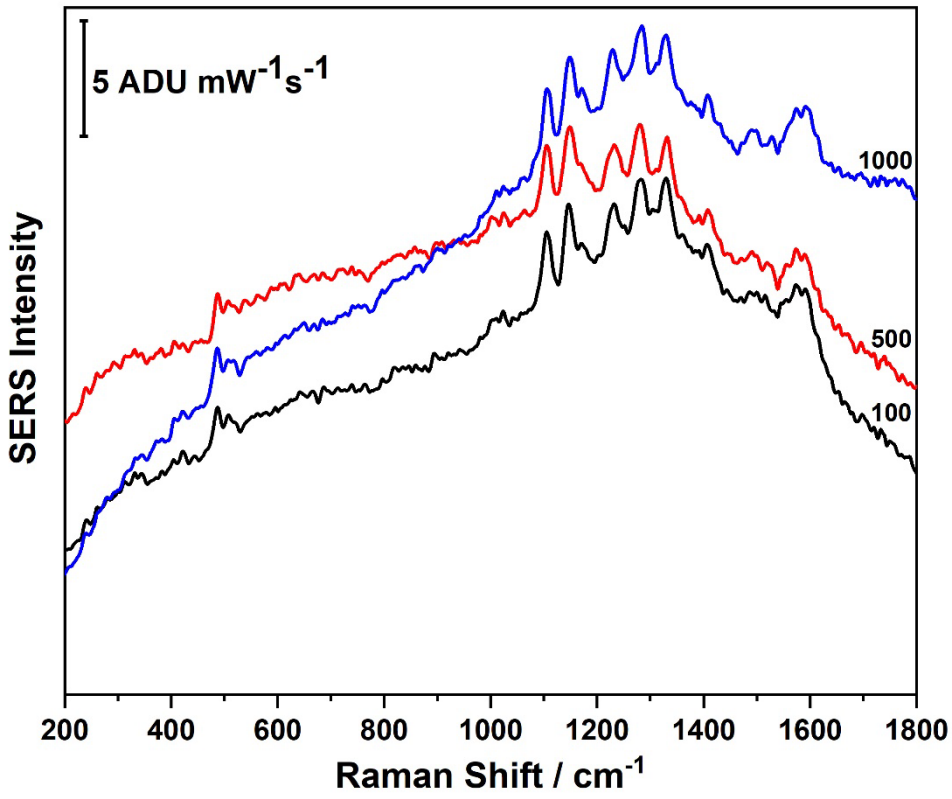

Figure 2-17. Overlay of SERS spectra of α-pinene drop coated on a solid filter paper with three layers of AuNSs of various R values (indicated). SERS spectra were collected with an excitation wavelength of 785 nm using the TacticID® - GP Plus spectrometer.

The results from the studies shown in Figures 2-16 and 2-17 show that AuNSs can be integrated into filter paper-based substrates for the detection of α-pinene. These substrates were able to be used for the detection of α-pinene whereas the solution-based SERS could not. This demonstrates the applicability of AuNSs in both solution-based and substrate SERS. The use of filter paper substrates fashioned using AuNSs should be further investigated for the detection of terpenes and cannabinoids.

2.4 Conclusion

This chapter demonstrates a preliminary investigation of Raman spectroscopy and surface-enhanced Raman spectroscopy for the detection of hemp and cannabis plants, terpenes, and cannabinoids. Raman spectroscopy was used for the analysis of growing hemp plants, as well as dried hemp and dried cannabis plant material. Some spectra were obtained from growing hemp plants, as well as from dried cannabis plant material when it was rehydrated with colloidal nanoparticles. Overall, Raman spectroscopy showed promise for analysis of growing and rehydrated plants, but not dried plants. Raman spectroscopy was also evaluated for the analysis of terpene standards, where the terpenes could only be detected at concentrations of 1 M, indicating the need for SERS.

Solution-based SERS using AuNSs was first optimized before being used for terpene and cannabinoid analysis. Some bands were observed for terpenes and cannabinoids using this solution-based SERS method, and β-pinene was detected quantitatively using this method. These results show great promise for this analytical methodology to be used for terpene and cannabinoid analysis. Commercial gold nanoparticles (AuNPs) were also evaluated for terpene and cannabinoid detection as a comparison to the AuNS method, where no cannabinoids and only β-pinene from the terpenes investigated could be detected with solution-based SERS using AuNPs. β-pinene was not able to be detected spiked into beer samples using AuNSs for solution-based SERS. Solid substrates fashioned from AuNSs were also evaluated for terpene analysis of α-pinene, where some bands were observed in the SERS spectrum, demonstrating the usefulness of AuNSs for both solid and solution phase SERS.

This work demonstrates a broad investigation of the applicability of Raman Spectroscopy and SERS for cannabis and hemp plant analysis and cannabinoid and terpene detection. Solution-based and filter paper SERS using AuNSs proved to be promising candidates for these applications and should be further investigated with other terpenes and cannabis samples.

2.5 References

1. Russo, E. B. The Case for the Entourage Effect and Conventional Breeding of Clinical Cannabis: No "Strain," No Gain. *Front Plant Sci.,* **2018**, 9, 1969.
2. Russo, E. B. Taming THC: Potential Cannabis Synergy and Phytocannabinoid-Terpenoid Entourage Effects. *Br J Pharmacol.*, **2011**, 163, 1344–1364.
3. Bill C-45, *An Act Respecting Cannabis and to Amend the Controlled Drugs and Substances Act, the Criminal Code and Other Acts*, 1st Sess, 42nd Parl, Canada, 2018 (assented to June 21, 2018), Section 139.
4. Mostowtt, T.; McCord, B. Surface Enhanced Raman spectroscopy (SERS) as a Method for the Toxicological Analysis of Synthetic Cannabinoids. *Talanta* **2017**, 164, 396.
5. Dies, H.; Raveendran, J.; Escobedo, C.; Docoslis. Rapid Identification and Quantification of Illicit Drugs on Nanodendritic Surface-Enhanced Raman Scattering Substrates. *Sens. Actuators B Chem.* **2018**, 257, 382.
6. Yüksel, S.; Schwenke, A. M.; Soliveri, G.; Arsizzone, S.; Weber, K.; Cialla-May, D.; Hoeppener, S.; Schubert, U. S.; Popp, J. Trace Detection of Tetrahydrocannabinol (THC) with a SERS-Based Capillary Platform Prepared by the In Situ Microwave Synthesis of AgNPs. *Anal. Chim. Acta* **2016**, 939, 93.
7. Milliken, S.; Fraser, J.; Poirier, S.; Hulse, J.; Tay, L. L. Self-Assembled Vertically Aligned Au Nanorod Arrays for Surface-Enhanced Raman Scattering (SERS) Detection of Cannabinol. *Spectrochim. Acta A* **2018**, 196, 222.
8. Islam, S. K.; Cheng, Y. P.; Birke, R. L.; Green, O.; Kubic, T.; Lombardi, J. R. Rapid and Sensitive Detection of Synthetic Cannabinoids AMB-FUBINACA and α-PVP Using Surface Enhanced Raman Scattering (SERS). *Chemical Physics* **2018**, 506, 31.

9. Sanchez, L.; Filter, C.; Dalensperger, D. ; Kurouski, D. Confirmatory Non-Invasive and Non-Destructive Differentiation Between Hemp and Cannabis Using a Hand-Held Raman Spectrometer. *RSC Adv.* **2020**, 10, 3212-3216.
10. Bindesri, S. D.; Jebailey, R.; Albarghouthi, N.; Pye, C. C.; Brosseau, C. L. Spectroelectrochemical and Computational Studies of Tetrahydrocannabinol (THC) and Carboxy-Tetrahydrocannabinol (THC-COOH). *Analyst* **2020**, 145, 1849-1857.
11. Sanford, C. L.; Mantooth, B. A.; Jones, B. T. Determination of Ethanol in Alcohol Samples Using a Modular Raman Spectrometer. *J. Chem. Educ.* **2001**, 78, 1221.
12. Rusin, C. J.; El Bakkari, M.; Du, R.; Boluk, Y.; McDermott, M. T. Plasmonic Cellulose Nanofibres as Water-Dispersible Surface-Enhanced Raman Scattering Substrates. *ACS Appl. Nano Mater.* **2020**, 3, 6584-6597.
13. Faulds, K.; Smith, W. E.; Graham, D.; Lacey, R. J. Assessment of Silver and Gold Substrates for the Detection of Amphetamine Sulfate by Surface Enhanced Raman Scattering (SERS). *Analyst* **2002**, 127, 282-286.
14. Saute, B. Premasiri, R.; Ziegler, L.; Narayanan, R. Gold Nanorods as Surface Enhanced Raman Spectroscopy Substrates for Sensitive and Selective Detection of Ultra-Low Levels of Dithiocarbamate Pesticides. *Analyst* **2012**, 137, 5082-5087.
15. Van der Ende, E.; Bourgeois, M. R.; Henry, A.- I.; Chavez, J. L.; Krabacher, R.; Schatz, G. C.; Van Duyne, R. P., Physicochemical Trapping of Neurotransmitters in Polymer Mediated Gold Nanoparticle Aggregates for Surface-Enhanced Raman Spectroscopy. *Anal. Chem.* **2019**, 91, 9554-9562.
16. Negru, B.; McAnally, M. O.; Mayhew, H. E.; Ueltschi, T. W.; Peng, L.; Sprague-Klein, E. A.; Schatz, G. C.; Van Duyne, R. P. Fabrication of Gold Nanosphere Oligomers for Surface-Enhanced Femtosecond Stimulated Raman Spectroscopy. *J. Phys. Chem. C.* **2017**, 121, 27004-27008.
17. Mahmoud, E. Y. F.; Rusin, C. J.; McDermott, M. T., Gold Nanostars as a Colloidal Substrate for In-Solution SERS Measurements Using a Handheld Raman Spectrometer. *Analyst* **2020**, 145, 1396-1407.
18. Harder, R. A.; Wijenayaka, L. A.; Phan, H. T.; Haes, A. J. Tuning Gold Nanostar Morphology for the SERS Detection of Uranyl. *J. Raman Spectrosc.* **2020**, 1-9.

19. Ortiz-Castillo, J. E.; Gallo-Villanueava, R. C.; Madou, M. J.; Perez-Gonzalez, V. H. Anisotropic Gold Nanoparticles: A Survey of Recent Synthetic Methodologies. *Coord. Chem. Rev.* **2020**, 425, 213489.
20. Khoury, C. G.; Vo-Dinh, T. Gold Nanostars for Surface-Enhanced Raman Scattering: Synthesis, Characterization and Optimization. *J. Phys. Chem. C.* **2008**, 112, 18849-18859.
21. Novak, J.; Zitterl-Eglsser, K.; Deans, S. G.; Franz, C. M. Essential Oils of Different Cultivars of *Cannabis Sativa* L. and Their Antimicrobial Activity. *Flavour Fragr. J.* **2001**, 16, 259-262.
22. Hanif, M. A.; Nawaz, H.; Naz, S.; Mukhtar, R.; Rashid, N.; Bhatti, I. A.; Saleem, M. Raman Spectroscopy for the Characterization of Different Fractions of Hemp Essential Oil Extracted at 130 °C Using Steam Distillation Method. *Spectrochim. Acta A* **2017**, 182, 168-174.
23. Salehi, B.; Upadhyay, S.; Orhan, I. E.; Jugran, A. K.; Jayaweera, S. L. D.; Dias, D. A.; Sharopov, F.; Teheri, Y.; Martins, N.; Baghalpour, N.; Cho, W. C.; Sharifi-Rad, J. Therapertic Potential of α- and β-Pinene: A Miracle Gift of Nature. *Biomolecules*, **2019**, 9, 738.
24. An, P.; Yuan, C. -Q.; Liu, X. -H.; Xiao, D. -B.; Luo, Z. -X. Vibrational Spectroscopic Identification of Isoprene, Pinenes and Their Mixture. *Chinese Chem. Lett.* **2016**, 27, 527-534.
25. Langer, J.; de Aberaturi, D. J.; Aizpurua, J.; Alvarez-Puebla, R. A.; Auguié, B.; Baumberg, J. J.; Bazan, G. C.; Bell, S. E. J.; Boisen, A.; Brolo, A. G.; Choo, J.; Cialla-May, D.; Deckert, V.; Fabris, L.; Faulds, K.; de Abajo, F. J. G.; Goodacre, R.; Graham, D.; Haes, A. J.; Haynes, C. L.; Huck, C.; Itoh, T.; Käll, M.; Kneipp, J.; Kotov, N. A.; Kuang, H.; Ru, E. C. L.; Lee, H. K.; Li, J. -F.; Ling, X. Y.; Maier, S. A.; Mayerhöfer, T.; Moskovits, M.; Murakoshi, K.; Nam, J. -M.; Nie, S.; Ozaki, Y.; Pastoriza-Santos, I.; Perez-Juste, J.; Popp, J.; Pucci, A.; Reich, S.; Ren, R.; Schatz, G. C.; Shegai, T.; Schlücker, S.; Tay, L. -L.; Thomas, K. G.; Tian, Z. -Q.; Van Duyne, R. P.; Vo-Dinh, T.; Wang, Y.; Willets, K. A.; Xu, C.; Xu, H.; Xu, Y.; Yamamoto, Y. S.; Zhao, B.; Liz-Marzán, L. M. Present and Future of Surface-Enhanced Raman Scattering. *ACS Nano* **2020**, 14, 28-117.

26. Giese, M. W.; Lewis, M. A.; Giese, L.; Smith, K. M. Development and Validation of a Reliable and Robust Method for the Analysis of Cannabinoids and Terpenes in Cannabis. *J. AOAC Int.* **2015**, 98, 1503-1522.
27. Bock, P.; Gierlinger, N. Infrared and Raman Spectra of Lignin Substructures: Coniferyl Alcohol, Abietin, and Coniferyl Aldehyde. *J. Raman Spectrosc.* **2019**, 50, 778-792.
28. Tay, L. -L.; Poirer, S.; Ghaemi, A.; Hulse, J.; Wang, S. Paper-Based Surface-Enhanced Raman Spectroscopy Sensors for Field Applications. *J. Raman Spectrosc.* **2020**, 1-10.
29. Xia, J.; Liu, Y.; Ran, M.; Lu, D.; Lao, X.; Wang, Y. SERS Platform Based on Bimetallic Au-Ag Nanowires-Decorated Filter Paper for Rapid Detection of miR-196a in Lung Cancer Patients Serum. **2020**, 2020.

Chapter 3: PVP-Mediated Controlled Aggregation of Gold Nanostars for Solution-Based Surface-Enhanced Raman Spectroscopy

3.1 Introduction

Solution-based analysis is an emerging technique in the field of surface-enhanced Raman spectroscopy (SERS).[1-8] Solution-based SERS can offer a shorter analysis time as it does not require solid substrates.[2-8] Anisotropic metal nanostructures have been identified as a very important type of material for SERS due to their remarkable SERS performance over isotropic metal nanoparticles.[6,9] Gold nanostars (AuNSs) have been employed in SERS substrates due to their anisotropic properties, showing great promise for providing significant SERS enhancement.[5,6,10] To benefit from the use of solution-based SERS methodology and the use of anisotropic nanomaterials, this thesis work is largely focused on employing AuNSs for solution-based SERS. One important consideration with solution-based SERS is that in order to generate a strong electromagnetic field, the nanoparticles in solution need to be aggregated to form hot-spots.[5,7,8] The simplest method to induce metal colloidal nanoparticle aggregation in solution is by the addition of salt. The solution composition to achieve optimal aggregation for in solution SERS can be challenging to define over a broad range of conditions.[7,8] This aggregation mechanism can also be affected by the presence of certain analytes or the analyte concentration.[5] Solution-based SERS is therefore not compatible for all analytes or concentration ranges, limiting its applicability.

One potential avenue for controlling the nanoparticle aggregation for solution-based SERS is the addition of polyvinylpyrrolidone (PVP). In one study, PVP was used to halt gold nanosphere aggregation for the detection of neurotransmitters.[7] PVP has also been used to halt gold nanosphere monomer aggregation.[8] PVP is able to immediately halt aggregation of nanoparticles and prevent sedimentation through the formation of a ~3 nm polymer layer on the surface of the nanoparticles.[7,8] By halting the aggregation mechanism, the plasmonic properties at the time of PVP addition are persevered indefinitely.[8] PVP addition provides unparalleled molecular control and can also entrap the target analyte within the sensing volume of the nanoparticles in solution.[7,8] PVP has also been used as a capping agent in nanoparticle synthesis.[10-12] It is thought to have selective interactions between various crystallographic planes of silver,[11] and shows discriminatory binding of select analytes at the adsorbed polymer layer.[12]

This chapter will explore the use for AuNSs for solution-based SERS with PVP-mediated aggregation control. While the AuNS substrate has been explored in Chapter 2, the method does suffer from a lack of applicability to a wide range of probes due to the lack of control of the aggregation mechanism. While using these AuNSs for SERS analysis of terpenes, it was found that the presence of terpenes themselves contributed to the aggregation of the AuNSs once the salt solution was added. Higher concentrations of some terpenes were observed to cause more aggressive aggregation in their presence than what would occur with the salt alone. PVP addition will be explored in order to have more consistent aggregation and have the aggregation occur before the addition of the probe molecule with the goal of making solution-based SERS with AuNSs more applicable for terpene analysis. This chapter presents the method development, optimization, and validation for PVP addition to AuNSs for SERS, as well as some preliminary terpene analysis using this method.

3.2 Experimental

3.2.1 Materials

Gold (III) chloride trihydrate (99.995%, HAuCl4), 4-(2-hydroxyethyl)-1-piperazineethanesulfonic acid buffer solution (1 M in H2O, HEPES), sodium chloride (≥ 99.5%, NaCl), (-)-β-pinene (99%), polyvinylpyrrolidone (average Mw ~1,300,000, PVP), polyvinylpyrrolidone (average Mw ~55,000, PVP), and polyvinylpyrrolidone (average Mw ~20,000, PVP) were purchased from Sigma-Aldrich Canada (Oakville, Ontario). 4-mercaptobenzonitrile (MBN) was purchased from Combi-Blocks, Inc. (San Diego, California, USA). Sodium hydroxide (NaOH) was purchased from Fisher Scientific Canada. 1-dram clear threaded vials, 4-dram glass vials, and 1 mL clear shell glass vials were purchased from Fisher Scientific Canada. Deionized (DI) water (18.2 MΩ·cm) was used for all syntheses and measurements in this work.

3.2.2 Gold Nanostar Synthesis

The pH of 1 M HEPES buffer solution was adjusted to 7.20 ± 0.01 using a solution of 1 M NaOH and a Fisher Scientific accumet research AR15 pH meter. A stock solution of $HAuCl_4$ (29.14 mM) was prepared in DI water. The ratio of buffer concentration to gold salt concentration, where the concentration of gold salt was held constant, was equal to 100 for this work. 20 mL of AuNSs were synthesized by adding DI water, HEPES buffer, and a small stir bar to a 4-dram glass vial. The gold salt was added to the solution which was then stirred at a rate of 400 rpm for 5 minutes. After stirring, the stir bar removed, and the solution left at room temperature overnight. After this time period, the AuNS solution was stored at 4°C for no more

than one week before use. Detailed synthetic details and characterization of these AuNSs can be found in a paper published by previous members of our research group.[5]

3.2.3 Characterization

UV-Vis spectroscopy experiments were done using a PerkinElmer Lambda 35 spectrometer. All experiments used a slit width of 1 nm and a scan rate of 960 nm/min. The samples were analyzed in 1.5 mL BRAND® polystyrene disposable cuvettes and scanned from 400 to 1100 nm.

Scanning electron microscopy (SEM) images were taken using a Hitachi S-4800 field emission SEM. Samples were prepared on Si wafers by drop-casting 10 µL of sample onto the wafer. Images were taken at 30 keV and 20 µA (SEM). The images were processed and analyzed using ImageJ (NIH, Maryland, USA).

Zeta potential measurements of AuNSs were determined using a Malvern Zetasizer Nano-ZS. The instrument is equipped with a 4 mW HeNe laser (633 nm) and 173 ° backscattering angle. The 1 mL aliquot samples were measured in 2.5 mL BRAND® polystyrene disposable cuvettes (pathlength=1cm) with each measurement consisting of 20 sub-runs.

3.2.4 Raman Instrumentation

Three different Raman spectrometers were used for this work, the instrument used is indicated in the figure caption. The first instrument used was a B&W Tek TacticID® -GP Plus handheld Raman spectrometer with a 785 nm laser. This instrument was standardized using a polystyrene standard and all samples were analyzed using a liquid cell adapter at 100% laser

power (~330 mW). Acquisition time is not user controlled for this instrument, so it varied from sample to sample.

The second instrument used was a B&W Tek NanoRam® handheld Raman spectrometer with a 785 nm laser. This instrument was standardized using a polystyrene standard and all samples were analyzed sing a liquid cell adapter at 100% laser power (~298 mW). Acquisition time is not user controlled for this instrument, so it varied from sample to sample.

The last instrument used was a Renishaw inVia confocal Raman microscope with a 785 nm laser. Samples were analyzed using a liquid cell adapter at 100% (~294 mW) for 10 seconds with 3 accumulations in extended mode. Data were acquired using Wire 3.4 software.

All spectra shown are corrected for power and time and are without baseline correction. All spectra shown are an average of 3 spectra to ensure accurate representation of results, unless indicated to be individual samples. All spectra were analyzed and prepared using Origin 2019 software (OriginLab Corporation, Northampton, MA, USA).

3.2.5 SERS Analysis with PVP-Mediated Aggregation Control

To a microcentrifuge tube containing a 795 µL aliquot of colloidal AuNSs, 100 µL of 2 M NaCl was added and vortex mixed for a length of time (indicated) followed by the addition of 100 µL of PVP and ~5 seconds of vortex mixing. During this process, the bright purple colour of the original colloid solution changes to a darker purple/blue. This solution is always used within one hour for SERS measurements, unless otherwise indicated. For SERS measurements, 5 µL of the probe solution is added to the microcentrifuge tube containing the pre-aggregated AuNS solution and vortex mixed for one minute before being transferred to a glass vial for SERS

measurement. SERS measurement is collected two minutes after the initial addition of probe. All samples contained the same concentration of AuNSs and a total sample volume of 1 mL.

3.3 Results and Discussion

3.3.1 Optimization of Controlled Aggregation of Gold Nanostars for Solution-Based SERS

As PVP controlled aggregation of AuNSs has not been explored, much of this work is focused on developing and optimizing this method. The order of addition of reagents was first investigated to ensure that the aggregation was sufficient, but that the solution did not aggregate too much as to allow sedimentation. As the goal of this controlled aggregation method is to ensure that the probe plays no role in the aggregation of the AuNSs, the probe would be added after the aggregation was stopped. As it was initially unclear how quickly the PVP acts, the order of addition of salt and PVP was investigated, as is shown in Figure 3-1. This study was done using ethanol as the Raman probe. First, PVP was added to the solution, followed by salt, which produced the black spectrum in Figure 3-1. Adding both salt and PVP together resulted in the red spectrum in Figure 3-1, which is an improvement over adding salt after PVP. Adding salt first followed by PVP produced the green spectrum in Figure 3-1, which exhibits the strongest SERS signal. These data confirm that the PVP acts rapidly, and it is therefore beneficial for the SERS performance of the AuNSs to allow some time after the addition of salt for aggregation to occur before adding the PVP to halt the aggregation process.

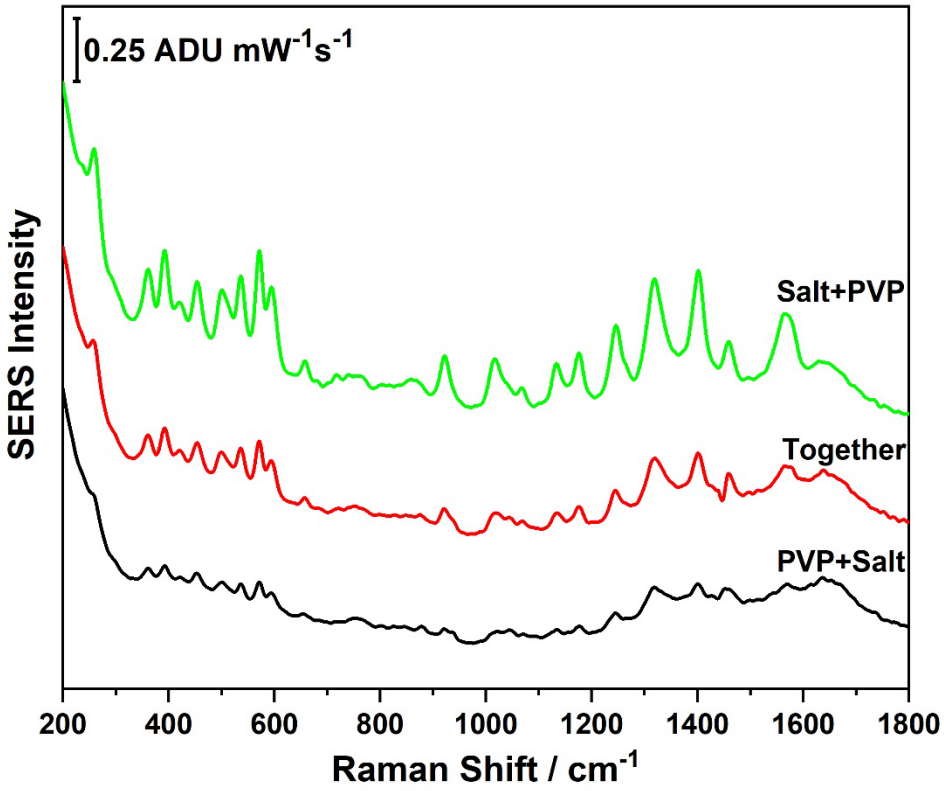

Figure 3-1. SERS spectra of ethanol with salt added before PVP (green), salt and PVP added together (red), and PVP added before salt (black). SERS spectra were collected with an excitation wavelength of 785 nm using the TacticID® - GP Plus spectrometer.

To compare the PVP addition method with the traditional method of SERS analysis using AuNSs, and to optimize the aggregation time before PVP addition, a spectral comparison is shown in Figure 3-2. In this case, the Raman reporter is 4-mercaptobenzonitrile (MBN), which adsorbs strongly to the AuNS and provides a larger signal than ethanol. PVP added immediately after salt addition (black spectrum) and PVP added after 1 minute of salt addition (red spectrum) produced the weakest spectra. PVP added after 2 minutes (blue spectrum) showed the strongest spectrum of the PVP method, and therefore was used going forward. The traditional method of

AuNS SERS analysis is shown in the pink spectrum, which produces a much stronger signal than the PVP method. While this may be the case, the PVP method is still valuable in studies where uncontrolled aggregation does not allow for SERS analysis at all, as is the case with some terpene analyses. The results of this study are also contradictory to the results in the paper that inspired this work, in which the authors found that the SERS results diminished once the AuNSs turned from purple to icy blue.[7] In our work, we have found it to be necessary for the AuNSs to aggregate to the point of turning from purple to blue (2 minutes of aggregation) to optimize the SERS signal.

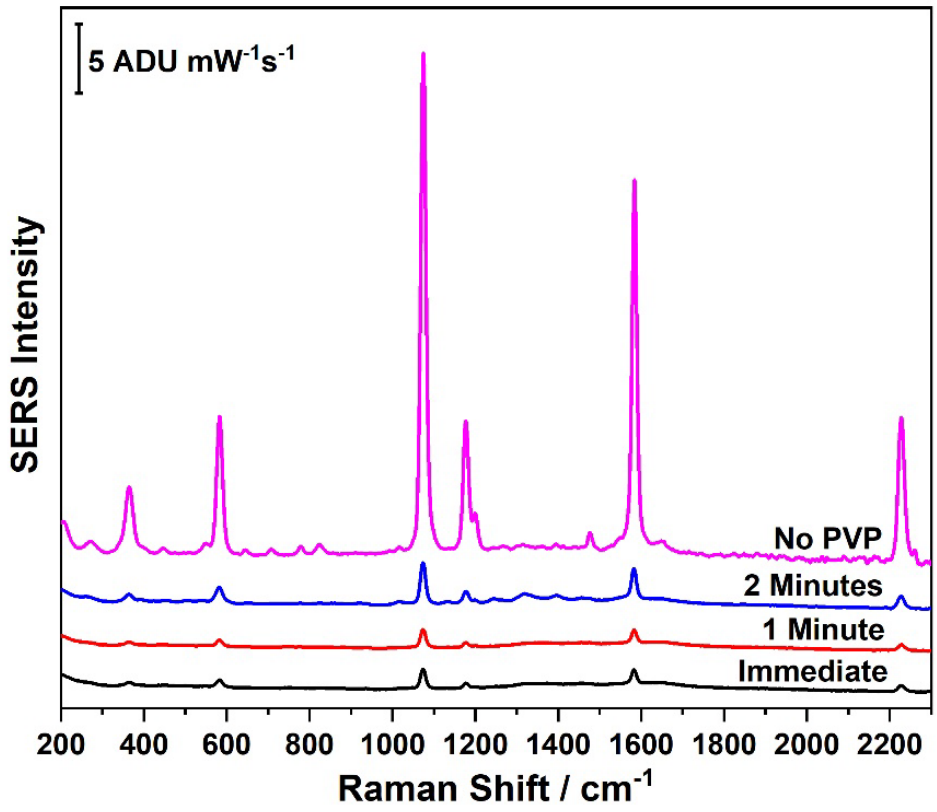

Figure 3-2. Overlay of SERS spectra of 5 nM MBN collected after various aggregation periods (indicated) followed by PVP addition and with no PVP addition at all. SERS spectra were collected with an excitation wavelength of 785 nm using the NanoRam® spectrometer.

Reproducibility was investigated by looking at the difference between using the AuNSs after aggregating and adding PVP as an individual sample versus combining several samples after PVP addition and redistributing the AuNSs to ensure equal aggregation across all samples. Figure 3-3A shows the comparison of the average of the individual samples and the redistributed samples. A slight improvement in band intensity is observed with the individual samples. Figure 3-3B is the overlay of 9 samples collected individually and 3-3C is the overlay of 9 samples collected after redistribution. Figure 3-3B and 3-3C clearly shows that the variation from sample to sample is much greater without redistributing the AuNSs before analysis. The coefficient of variance (CV) for each method can be compared as a measure of reproducibility to statistically represent these results. The CV value represents the variation in the SERS intensity, where the variability of the signal is an important experimental aspect to consider when considering a SERS platform for quantitative analysis. Using the 1076 cm^{-1} peak for MBN, the CV for the samples analyzed individually without redistribution is 28%, while the CV for the samples collected from redistributed AuNSs is 5.7%. This is an impressive display of reproducibility, as CV values for SERS can often be in excess of 20%.[13] This is also a further improvement upon the CV calculated for the same measurements when the PVP was added immediately after aggregation as opposed to waiting two minutes. In this study, which is shown in Figure A-1, the CV for the samples analyzed individually without redistribution is 47%, while the CV for the samples collected from redistributed AuNSs is 8.2%. This also supports that the most reproducible results are obtained with the PVP is added 2 minutes after aggregation is commenced. The redistribution step has shown to be useful and worth the additional step in the analysis process and was therefore employed in all subsequent experiments.

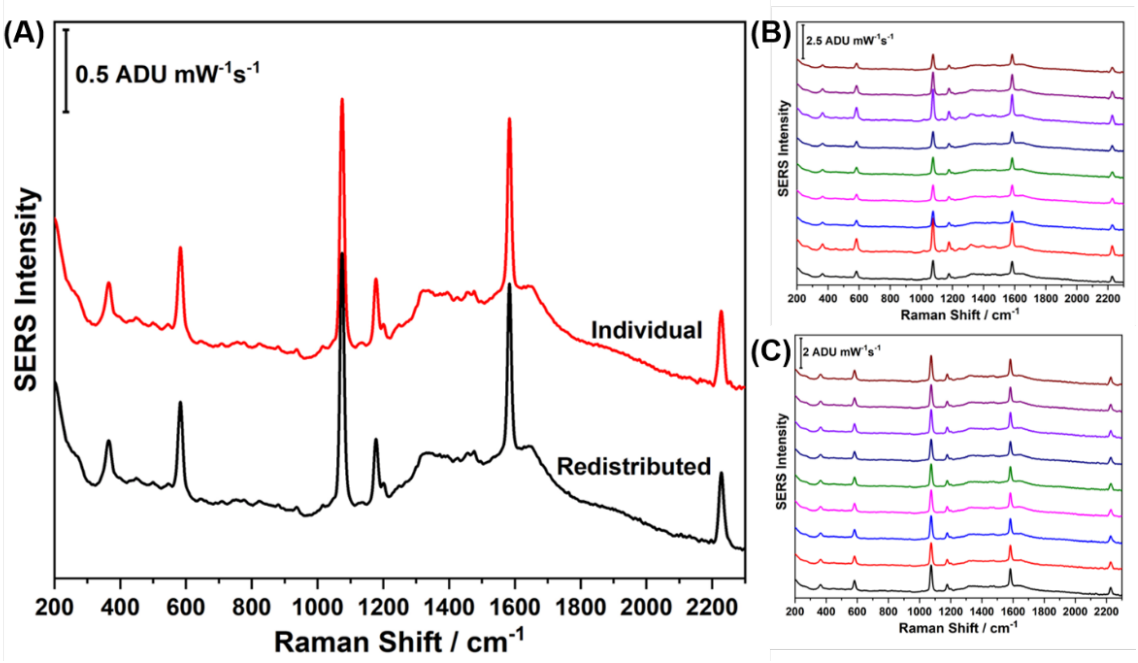

Figure 3-3. SERS spectra of 5 nM MBM (A) the average of 9 samples collected from individual samples without redistribution (red) overlaid with average SERS spectrum of 9 samples collected with redistributed AuNSs (black) and, (B) Overlay of SERS spectra from 9 different samples collected from each one individually and, (C) Overlay of SERS spectra from 9 different samples collected from redistributed samples. SERS spectra were collected with an excitation wavelength of 785 nm using the NanoRam® spectrometer.

The effect of molecular weight of the polymer was also investigated, as this was a factor that had not previously been explored for polymer control of nanoparticle aggregation. This experiment was done to see if the change in viscosity alone after polymer addition was able to halt aggregation, or if the effect of the polymer was unrelated to the viscosity of the solution. PVP of three molecular weights, 29,000 (13.0 wt%); 55,000 (10.8 wt%); and 1,300,000 (4.33 wt%) were explored, and each one was more viscous than the next. The 29,000 MW solution

was made to be 13.0 wt% based on the paper that inspired this work, and the other two polymers were made to the highest wt% that was soluble. Each of these polymers were used to halt the aggregation of AuNSs for the SERS analysis of 0.64 µM MBN, the results are shown in Figure 3-4, where the molecular weight of the PVP used is indicated on the corresponding spectrum. The molecular weight of the polymer used was found to have no affect on the SERS intensity, showing that the change in viscosity of the solution likely had little to do with the effect of PVP on aggregation.

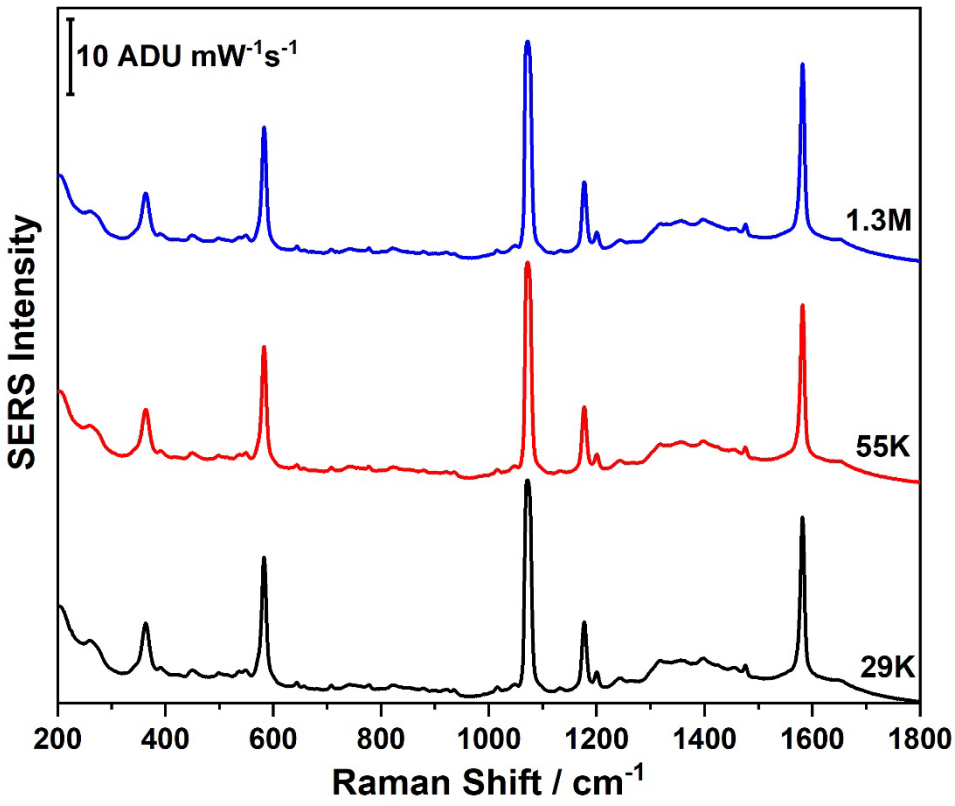

Figure 3-4. SERS spectra for 0.64 µM MBN with three different molecular weights of PVP added (indicated). SERS spectra were collected with an excitation wavelength of 785 nm using the InVia spectrometer.

The reproducibility study shown in Figure 3-4 above was done using the same batch of nanoparticles, it was important to ensure that the same reproducibility was observed from batch to batch of AuNSs used. Those results are shown in Figure 3-5, where the average spectrum obtained from three separate batches of AuNSs. The consistent peak intensity produced from all three batches indicates that this method demonstrates good batch-to-batch reproducibility, which is an important consideration for method consistency.

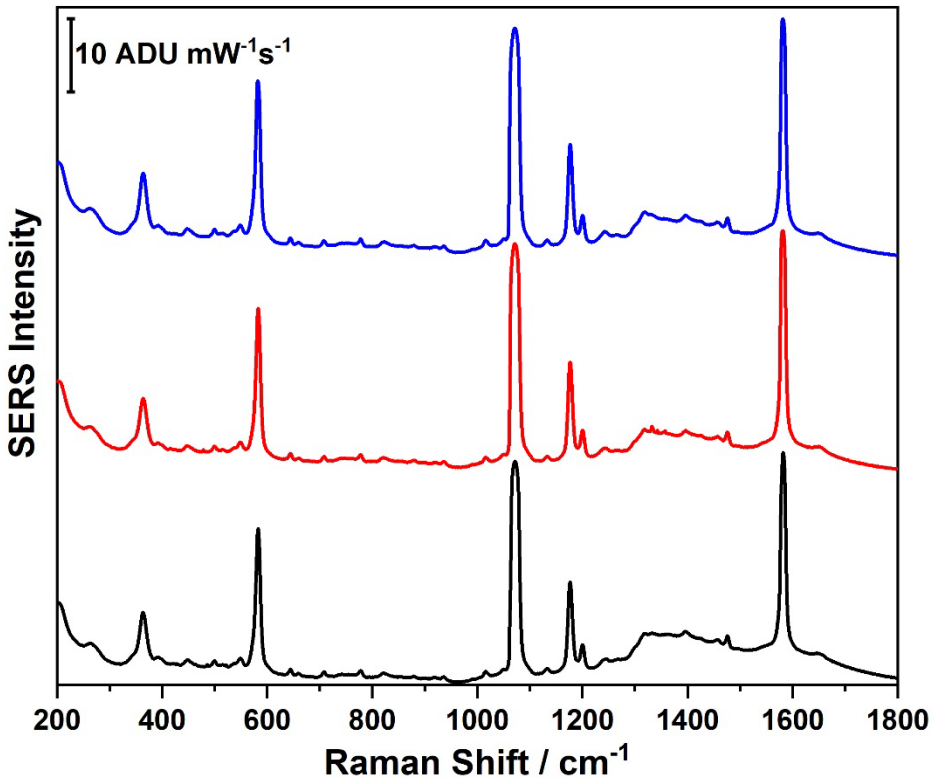

Figure 3-5. SERS spectra for 0.64 μM MBN with three different batches of AuNSs after PVP addition. SERS spectra were collected with an excitation wavelength of 785 nm using the InVia spectrometer.

An SEM image of various PVP-encapsulated AuNS aggregates is displayed in Figure 3-6A with an inset close-up SEM image of a single aggregate. Figure 3-6B is a size distribution ASH plot for the diameter of the aggregates as determined by the analysis of multiple SEM images with ImageJ software. The aggregate sizes are relatively polydisperse with an average diameter of 507 nm ± 148 nm (n=50), where for elliptical particles the horizontal and vertical cross sections were measured as the diameter.

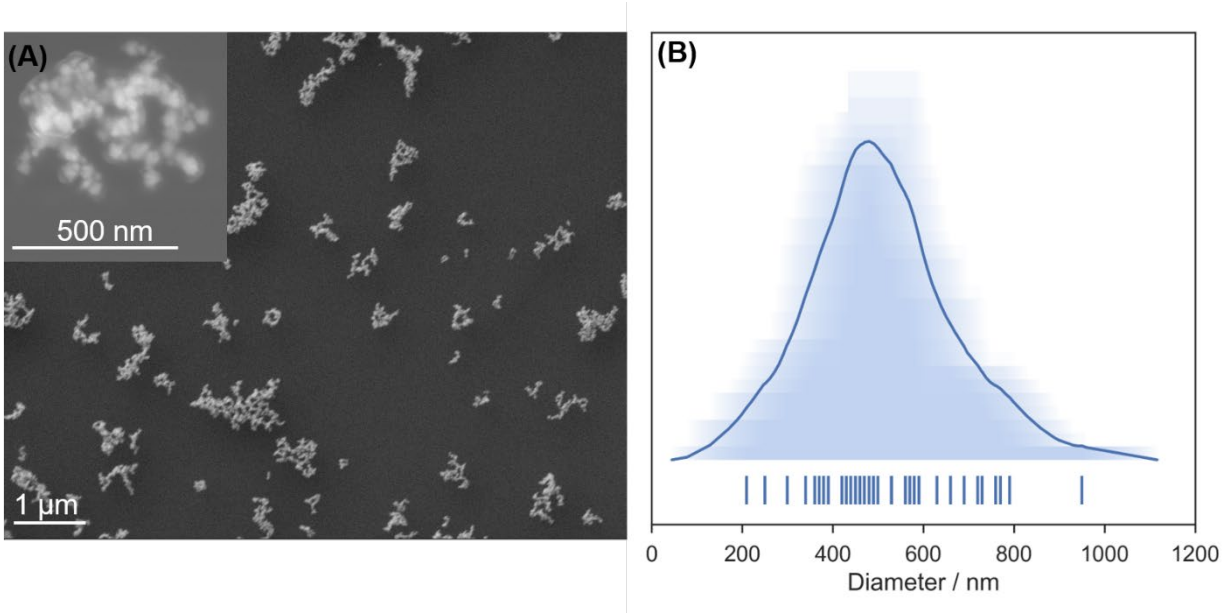

Figure 3-6. (A) SEM image of multiple PVP-encapsulated AuNS aggregates with inset SEM image of a single PVP-encapsulated AuNS aggregate, and (B) ASH plot of size distribution of PVP-encapsulated AuNS aggregates as determined from SEM images.

3.3.2 Quantitative Assessment of PVP Addition Method

A calibration curve with MBN was constructed in Figure 3-7 using the PVP-controlled aggregation method to assess this method for quantitative studies. Figure 3-7A shows the SERS

spectra of various concentrations of MBN, where the signal intensity is found to increase going from low to high concentration. Figure 3-7B shows the corresponding calibration curve, constructed using the intensity of the 1076 cm^{-1} peak of MBN. The quantitative ability of this method was found to have comparable, although slightly lower linearity to that of the non-PVP method. This is a promising observation as reliable and quantitative analysis can be difficult to obtain with some SERS substrates.[14]

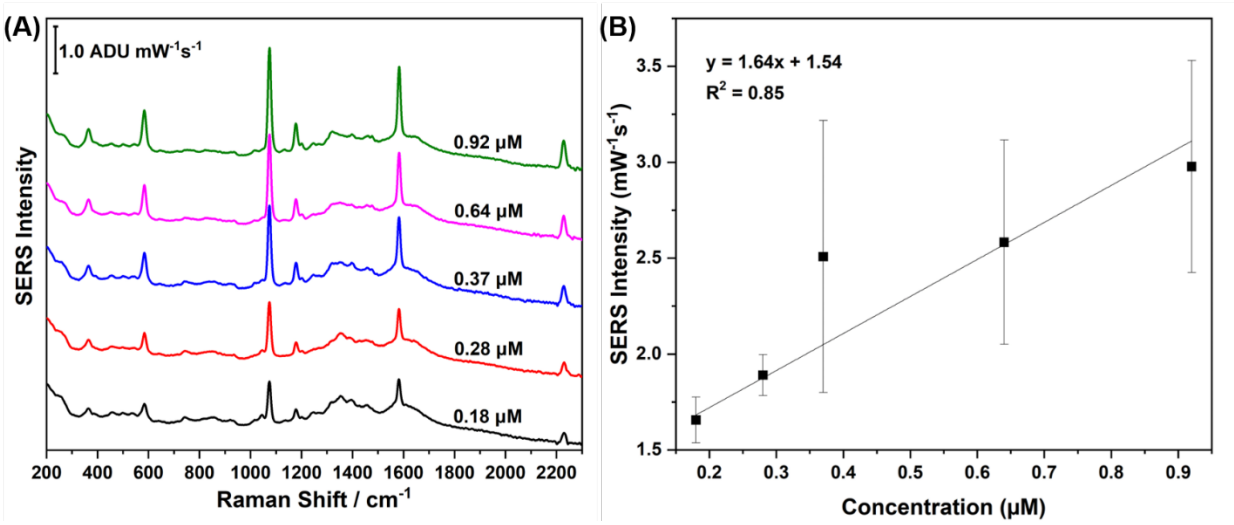

Figure 3-7. (A) Overlay of SERS spectra of various concentrations of MBN (indicated) using AuNSs with PVP addition, and (B) corresponding calibration curve of intensity of 1076 cm^{-1} band, where the points represent the mean of three measurements and the error bars represent the standard deviation SERS spectra were collected with an excitation wavelength of 785 nm using the InVia spectrometer.

3.3.3 Preliminary Assessment of Terpene Analysis

A preliminary assessment of the applicability of the PVP addition method for terpene analysis was done by measuring various concentrations of β-pinene. β-pinene was selected for

this preliminary study as it is a prominent terpene with medicinal benefits.[15] It was also found to produce the highest SERS signals in chapter 2 of this thesis work. The results of this SERS study are shown in Figure 3-8, where the characteristic 844 cm^{-1} band of β-pinene was indeed observed, showing that this method could be used to detect the presence of β-pinene. The signal intensity of this band, however, did not increase with increasing concentration of β-pinene. This likely means that further optimization of this method will be required for it to be used for quantitative detection of terpenes.

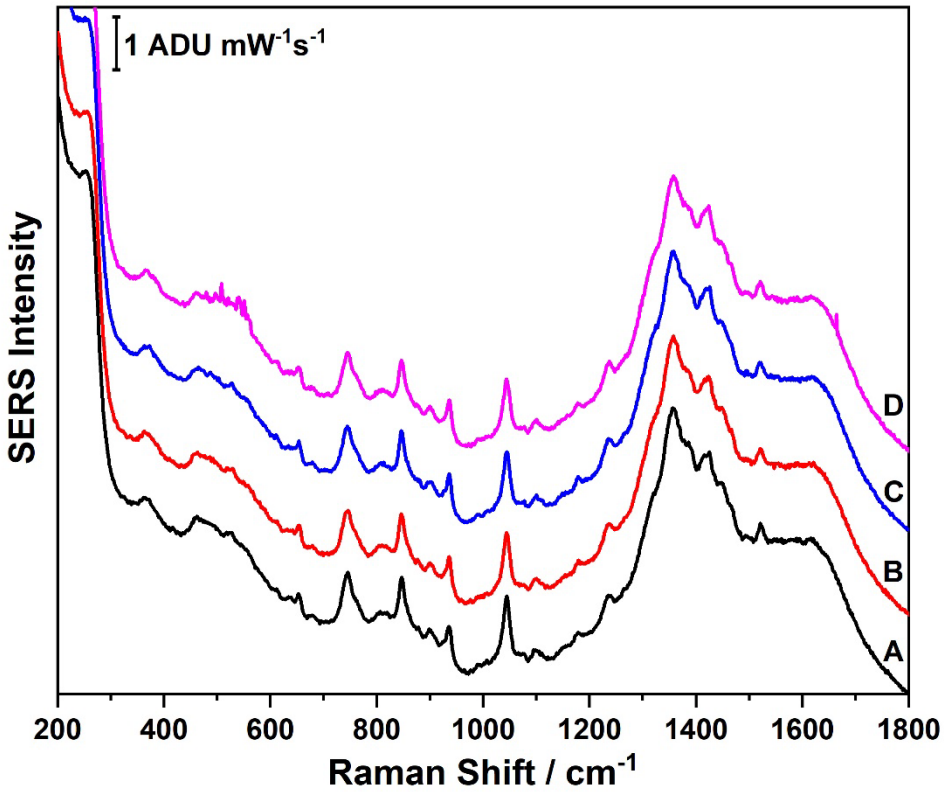

Figure 3-8. Overlay of SERS spectra for increasing concentrations of β-pinene, where spectrum A corresponds to 3 mM, spectrum B corresponds to 6 mM, spectrum C corresponds to 8 mM, and spectrum D corresponds to 10 mM. SERS spectra were collected with an excitation wavelength of 785 nm using the InVia spectrometer.

3.3.4 Investigating Other Effects of Controlled Aggregation with PVP

It was observed that the colour of the solutions of AuNSs with PVP added went back to their original purple colour approximately 24 hours after aggregation and PVP addition. This is a characteristic that has not been observed with AuNS solutions that contain no PVP, as those solutions turn clear several minutes after salt addition, as is a result of AuNS sedimentation. This prompted the idea that PVP addition after salt-induced aggregation of AuNSs could reverse the aggregation of the AuNSs. Visible extinction spectroscopy was used to explore the possibility of the aggregation reversing after some time with PVP in the AuNS solution. Figure 3-9A shows the extinction spectra taken before aggregation, immediately after PVP addition (2 minutes after aggregation was induced), and 24 hours after PVP addition. Figure 3-9A shows that the λmax and did return to that of the pre-aggregation solution of around 580 nm, which supports the visual observation that the solution colour returned to the pre-aggregation colour, although the OD is less intense 24 hours later than it was initially. The shape of the extinction spectrum after 24 hours also suggests that there were still some aggregates present.

Figure 3-9B shows that the SERS spectra of MBN immediately after PVP addition and 24 hours. These results show that the SERS intensity improves slightly using AuNSs that were aggregated 24 hours before use. These results support that the state of aggregation is somewhat changed after a day, although it is unclear if the shift in intensity suggests that the aggregation remained stable or reversed. The results in Figure 3-9 also indicates that the solutions can be aggregated and stored for at least one day prior to use without sacrificing SERS performance, which is an improvement in product applicability over the traditional (non-PVP) method of using AuNSs for in-solution SERS. With the traditional method, a SERS signal cannot be obtained longer than just several minutes after aggregation as the AuNSs crash out of solution entirely.

This demonstrates the robustness and stability of the PVP addition method and the advantages it has over the traditional method.

The zeta potential of pre-aggregated AuNSs was determined to be -32.32 mV ± 0.88 mV, and after aggregation and PVP addition it was -5.33 mV ± 1.46 mV. Zeta potential is a measure of the charge of the nanoparticles at the slipping plane and represents the colloidal stability. The more positive of the zeta potential after aggregation suggests that the aggregated solution was less colloidally stable than before aggregation. It is possible that this lack of stability stems from a dynamic state of aggregation, where the aggregation reversing would contribute to this observation. Due to time constraints, it was not possible to obtain a zeta potential reading for 24 hours after aggregation, however if it returned to a value close to -30 mV, that could also support the hypothesis of reversed aggregation. Overall, the ability of PVP to reverse the aggregation of AuNSs should be explored further, as both zeta potential and electron microscopy data of the AuNSs 24 hours after PVP addition could support or disprove this hypothesis.

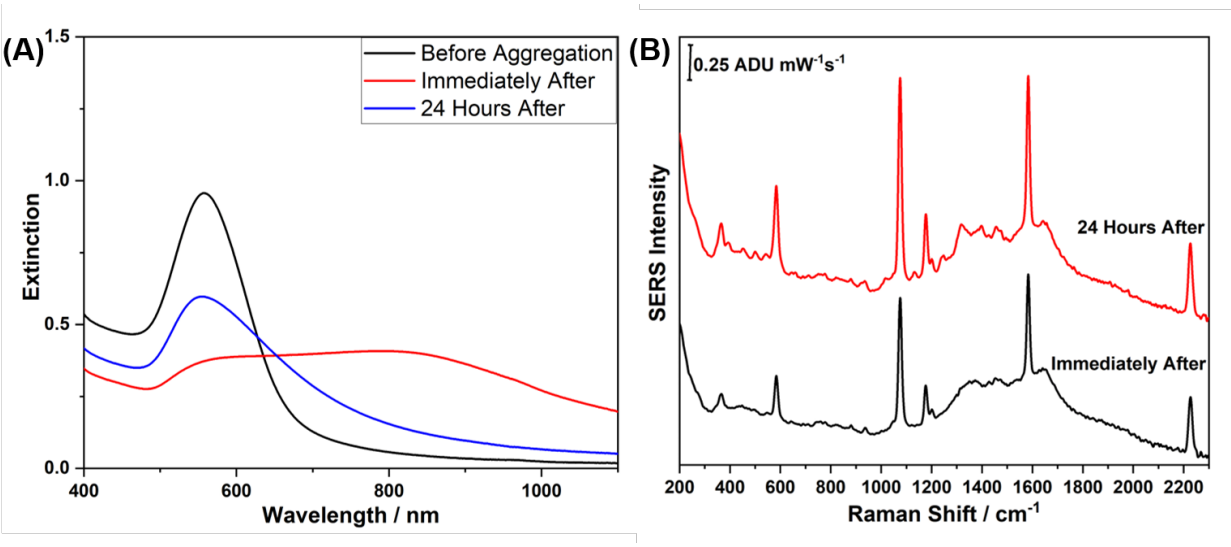

Figure 3-9. (A) Extinction spectra for AuNSs before aggregation (black spectrum), immediately after aggregation and PVP addition (red spectrum), and 24 hours after aggregations and PVP addition (blue spectrum), and (B) SERS spectra of 5 μM MBN using AuNSs immediately after aggregation and PVP addition (indicated), and 24 hours after aggregation and PVP addition (indicated). SERS spectra were collected with an excitation wavelength of 785 nm using the InVia spectrometer.

3.4 Conclusion

This research chapter shows the development, optimization, and validation of PVP-mediated aggregation control of AuNSs for solution-based SERS. The optimized coefficient of variance of the single intensity from sample to sample was determined to be 5.7%, which is indicative of impressive signal reproducibility. This method was found to be reproducible from batch to batch of AuNSs used. The molecular weight of PVP used was found to have no effect on the SERS performance of this method. The PVP-encapsulated AuNS

aggregates were determined to be 507 nm ± 148 nm in diameter based on size analysis of SEM images. This PVP-addition method was successfully used for the qualitative detection of a common terpene, β-pinene, as well as the quantitative detection of MBN. The addition of PVP to salt aggregated AuNSs also showed good SERS stability within 24 hours of PVP addition, which is an improvement over the non-PVP method. The addition of PVP to salt aggregated AuNSs possibly demonstrates the ability to partially reverse the aggregation of the AuNSs after 24 hours, as was observed using UV-Vis spectrophotometry. This effect should be further explored by collecting zeta potential data and SEM images for the aggregated AuNSs 24 hours after PVP addition. The applicability of this method should be further explored using other target analytes.

3.5 References

1. Zhao, Y.; Chang, X.; Malkani, A. S.; Yang, X.; Thompson, L.; Jiao, F.; Xu, B. Speciation of Cu Surfaces During the Electrochemical CO Reduction Reaction. *J. Am. Chem. Soc*. **2020**, 142, 9735-9743.
2. Rusin, C. J.; El Bakkari, M.; Du, R.; Boluk, Y.; McDermott, M. T. Plasmonic Cellulose Nanofibres as Water-Dispersible Surface-Enhanced Raman Scattering Substrates. *ACS Appl. Nano Mater.* **2020**, 3, 6584-6597.
3. Faulds, K.; Smith, W. E.; Graham, D.; Lacey, R. J. Assessment of Silver and Gold Substrates for the Detection of Amphetamine Sulfate by Surface Enhanced Raman Ccattering (SERS). *Analyst* **2002**, 127, 282-286.
4. Saute, B. Premasiri, R.; Ziegler, L.; Narayanan, R. Gold Nanorods as Surface Enhanced Raman Spectroscopy Substrates for Sensitive and Selective Detection of Ultra-Low Levels of Dithiocarbamate Pesticides. *Analyst* **2012**, 137, 5082-5087.
5. Mahmoud, E. Y. F.; Rusin, C. J.; McDermott, M. T., Gold Nanostars as a Colloidal Substrate for In-Solution SERS Measurements Using a Handheld Raman Spectrometer. *Analyst* **2020**, 145, 1396-1407.
6. Harder, R. A.; Wijenayaka, L. A.; Phan, H. T.; Haes, A. J. Tuning Gold Nanostar Morphology for the SERS Detection of Uranyl. *J. Raman Spectrosc.* **2020**, 1-9.

7. Van der Ende, E.; Bourgeois, M. R.; Henry, A.- I.; Chavez, J. L.; Krabacher, R.; Schatz, G. C.; Van Duyne, R. P., Physicochemical Trapping of Neurotransmitters in Polymer Mediated Gold Nanoparticle Aggregates for Surface-Enhanced Raman Spectroscopy. *Anal. Chem.* **2019**, 91, 9554-9562.
8. Negru, B.; McAnally, M. O.; Mayhew, H. E.; Ueltschi, T. W.; Peng, L.; Sprague-Klein, E. A.; Schatz, G. C.; Van Duyne, R. P. Fabrication of Gold Nanosphere Oligomers for Surface-Enhanced Femtosecond Stimulated Raman Spectroscopy. *J. Phys. Chem. C.* **2017**, 121, 27004-27008.
9. Ortiz-Castillo, J. E.; Gallo-Villanueava, R. C.; Madou, M. J.; Perez-Gonzalez, V. H. Anisotropic Gold Nanoparticles: A Survey of Recent Synthetic Methodologies. *Coord. Chem. Rev.* **2020**, 425, 213489.
10. Khoury, C. G.; Vo-Dinh, T. Gold Nanostars for Surface-Enhanced Raman Scattering: Synthesis, Characterization and Optimization. *J. Phys. Chem. C.* **2008**, 112, 18849-18859.
11. Sun, Y.; Xia, Y. Shape-Controlled Synthesis of Gold and Silver Nanoparticles. *Science* **2002**, 298, 2176-2179.
12. Moraes, B. R.; Campos, N. S.; Barra, A. C. C.; Izumi, C. M. S. Surface-Enhanced Raman Scattering of MEH-PPV on Gold and Silver Nanoparticles. *J. Spectrosc.* **2018**, 2018, 6924758.
13. Lynk, T. P.; Clarke, O. J. R.; Kesavan, N.; Brosseau, C. L. Development of a Sustainable Plasmon-Enhanced Spectroelectrochemical Sensor Using Avocado Pit (*Persea Americana*) extract. *Sens. Actuators, B.* **2018**, 257, 270-277.
14. Bell, S. E. J.; Charron, G.; Cortés, E.; Kneipp, J.; Chapelle, M. L.; Langer, J.; Procházka, M.; Tran, V.; Schlücker, S. Towards Reliable and Quantitative Surface-Enhanced Raman Scattering (SERS): From Key Parameters to Good Analytical Practice. *Agnew. Chem. Int. Ed.* **2020**, 59, 5454-5462.
15. Salehi, B.; Upadhyay, S.; Orhan, I. E.; Jugran, A. K.; Jayaweera, S. L. D.; Dias, D. A.; Sharopov, F.; Teheri, Y.; Martins, N.; Baghalpour, N.; Cho, W. C.; Sharifi-Rad, J. Therapertic Potential of α- and β-Pinene: A Miracle Gift of Nature. *Biomolecules*, **2019**, 9, 738.

Chapter 4: Conclusion and Future Directions

4.1 Conclusion

The motivation behind this thesis work was to assess the applicability of Raman and Surface-enhanced Raman spectroscopy (SERS) for quality control in the rapidly evolving Canadian cannabis industry. Raman and SERS have the potential to be used for both plant analysis, as well as the analysis of cannabis infused beverages. As the current literature lacks rapid solution-based assays for cannabinoid and terpene detection, SERS was shown to have the potential to fill an unmet need for this class of analysis.

In chapter 2, a preliminary investigation of Raman spectroscopy and SERS for living and dried plant analysis was investigated. Some spectra were obtained from growing hemp plants, as well as from dried cannabis plant material when it was rehydrated with colloidal nanoparticles. Overall, Raman spectroscopy showed promise for analysis of growing and rehydrated plants, but not dried plants. Raman spectroscopy was also evaluated for the analysis of terpene standards; however, it was not adequately sensitive without the use of SERS. Solution-based SERS using AuNSs was optimized for terpene and cannabinoid analysis. Some bands were observed for terpenes and cannabinoids using this solution-based SERS method, and β-pinene was detected quantitatively, although higher concentrations did present some signal reproducibility issues. Commercial gold nanoparticles (AuNPs) were also evaluated for terpene and cannabinoid detection as a comparison to the AuNS method, where they were shown to be less successful for these applications than AuNSs. Further investigation of cannabis-related analytes in real beverage matrices will be required. Solid substrates fashioned from AuNSs were also evaluated

for terpene analysis of α-pinene, demonstrating the versatility of AuNSs for both solid and solution phase SERS.

In chapter 3, the development, optimization, and validation of PVP-mediated aggregation control of AuNSs for solution-based SERS was presented, where the addition of PVP was used to halt the aggregation of AuNSs after salt addition. This method was developed in the hopes of making solution-based SERS more reproducible for high concentrations of terpenes. The PVP-encapsulated AuNS aggregates were determined to be 507 nm ± 148 nm in diameter based on size analysis of SEM images. This PVP-addition method was successfully used for the qualitative detection of a common terpene, β-pinene, as well as the quantitative detection of MBN. The addition of PVP to salt aggregated AuNSs showed low sample to sample and batch to batch variance, as well as good SERS stability within 24 hours of PVP addition. The addition of PVP to salt aggregated AuNSs possibly demonstrates the ability to partially reverse the aggregation of the AuNSs after 24 hours, which was a very uncommon and interesting observation. This method did show promise for terpene detection, although it will require further optimization and investigation.

4.2 Future Directions

This thesis work was a preliminary exploration of the applicability for Raman and SERS in the cannabis industry. The upcoming sections provide an opportunity for future research work to continue.

4.2.1 Raman and SERS in the Cannabis Industry

This thesis work has shown the potential of Raman spectroscopy to be used for the analysis of living hemp plants, as has a very recent study in literature.[1] The method of using

Raman spectroscopy for plant analysis should be further investigated in order to create a library for different cultivars of hemp and cannabis plants. Raman does have the potential to be used for discrimination between hemp and cannabis at the point of need,[1] however differentiation between cultivars of hemp or cannabis would be challenging without better amplification of the cannabinoid bands. Further studies to help strengthen this technique for possible cultivar differentiation could integrate SERS for plant analysis, which would require robust, reliable, and stable substrates. Certainly, the use of solution-based SERS with AuNSs could be investigated for plant analysis by introducing a sample of the plant into the substrate, however the amount of plant required would need to be adequately small, ideally on the mg scale, to minimize sample destruction.

Currently one of the main issues with SERS for cannabinoid and terpene detection is a lack of consistency and sensitivity. The target analytes in this case need to have a stronger affinity for the SERS substrate than other matrix components or the solution solvent. Future work is required to develop a method to measure these analytes that have a low affinity to the metal surface. While aptamer and antibodies would typically be a good choice for a SERS assay, they do not exist for analytes of this nature. It would perhaps be more helpful to treat the surface of the metal nanoparticles in some way to allow the analyte to get closer. One option would be a chloride displacement treatment which has the potential to clean the surface of the substrate being used to allow for terpene and cannabinoid molecules to come in closer proximity to the surface with minimal interference.[1] Another option would be to further explore the use of electrochemistry to draw the molecules closer to the surface, as has been shown to be a promising approach.[3] Another vital step in the future research of terpene and cannabinoid

detection with SERS is to establish a library of spectra for more molecules to help combat inconsistencies in the field.

4.2.2 Gold Nanostar Substrates for Headspace Analysis

This thesis work showed the preliminary success of filter paper substrates decorated with AuNSs to be used for terpene detection. This project requires further studies to optimize a substrate for terpene detection. In addition to substrate optimization, the exploration of incorporating these substrates in a headspace SERS assay would be an interesting avenue to explore. Headspace SERS has been explored with other analytes, such as bacteria,[4] however terpenes would make an excellent candidate for headspace SERS due to their volatile nature. In fact, terpenes have already been detected from the headspace of live cotton plants and dried tea, which does suggest that this method could also be extended to hemp or cannabis plants.[5] Future studies should explore terpene detection using AuNS decorated filter paper substrates for headspace SERS, which would be widely applicable for in-growth quality control of hemp and cannabis plant.

4.3 References

1. Sanchez, L.; Filter, C.; Dalensperger, D.; Kurouski, D. Confirmatory Non-Invasive and Non-Destructive Differentiation Between Hemp and Cannabis Using a Hand-Held Raman Spectrometer. *RSC Adv.* **2020**, 10, 3212-3216.
2. Lynk, T. P.; Clarke, O. J. R.; Kesavan, N.; Brosseau, C. L. Development of a Sustainable Plasmon-Enhanced Spectroelectrochemical Sensor Using Avocado Pit (*Persea Americana*) Extract. *Sens. Actuators, B.* **2018**, 257, 270-277.
3. Bindesri, S. D.; Jebailey, R.; Albarghouthi, N.; Pye, C. C.; Brosseau, C. L. Spectroelectrochemical and Computational Studies of Tetrahydrocannabinol (THC) and Carboxy-Tetrahydrocannabinol (THC-COOH). *Analyst* **2020**, 145, 1849-1857.

4. Kelly, J.; Patrick, R.; Patrick, S.; Bell, S. E. J. Surface-Enhanced Raman Spectroscopy for the Detection of a Metabolic Product in the Headspace Above Live Bacterial Cultures. *Angew. Chem. Int. Ed.* **2018**, 57, 15686-15690.
5. Park, J.; Thomasson, J. A.; Gale, C. C.; Sword, G. A.; Lee, K. -M.; Herrman, T. J.; Suh, C. P. -C. Adsorbent-SERS Technique for Determination of Plant VOCs from Live Cotton Plants and Dried Teas. *ACS Omega* **2020**, 5, 2779-2790.

Complete List of References

Albrecht, M. G.; Creighton, J. A. Anomalously Intense Raman Spectra of Pyridine at a Silver Electrode. *J. Am. Chem. Soc.* **1977**, 99, 5215-5217.

An, P.; Yuan, C. -Q.; Liu, X. -H.; Xiao, D. -B.; Luo, Z. -X. Vibrational Spectroscopic Identification of Isoprene, Pinenes and Their Mixture. *Chin. Chem. Lett.* **2016**, 27, 527-534.

Bell, S. E. J.; Charron, G.; Cortés, E.; Kneipp, J.; Chapelle, M. L.; Langer, J.; Procházka, M.; Tran, V.; Schlücker, S. Towards Reliable and Quantitative Surface-Enhanced Raman Scattering (SERS): From Key Parameters to Good Analytical Practice. *Agnew. Chem. Int. Ed.* **2020**, 59, 5454-5462.

Bill C-45, *An Act Respecting Cannabis and to Amend the Controlled Drugs and Substances Act, the Criminal Code and Other Acts*, 1st Sess, 42nd Parl, Canada, 2018 (assented to June 21, 2018), Section 139.

Bindesri, S. D.; Jebailey, R.; Albarghouthi, N.; Pye, C. C.; Brosseau, C. L. Spectroelectrochemical and Computational Studies of Tetrahydrocannabinol (THC) and Carboxy-Tetrahydrocannabinol (THC-COOH). *Analyst* **2020**, 145, 1849-1857.

Bock, P.; Gierlinger, N. Infrared and Raman Spectra of Lignin Substructures: Coniferyl Alcohol, Abietin, and Coniferyl Aldehyde. *J. Raman Spectrosc.* **2019**, 50, 778-792.

Bumbrah, G. S.; Sharma, R. M. Raman Spectroscopy – Basic Principle, Instrumentation and Selected Applications for the Characterization of Drugs and Abuse. *Egypt. J. Forensic Sci.* **2016**, 6, 209-215.

Chen, W. -L.; Huang, Y. -H. Cheng, H. -Y. Kuo, T. -R. Chang, Y. -M. Statistical Analysis of Cuboctahedral Silver Nanocrystals Langmuir–Blodgett Film SERS Substrate. *J. Raman Spectrosc.* **2018**, 49, 792-799.

Dégardin, K.; Guillemain, A.; Roggo, Y. Comprehensive Study of a Handheld Raman Spectrometer for the Analysis of Counterfeits of Solid-Dosage Form Medicines. *J. Spectrosc.* **2017**, 2017.

Dies, H.; Raveendran, J.; Escobedo, C.; Docoslis. Rapid Identification and Quantification of Illicit Drugs on Nanodendritic Surface-Enhanced Raman Scattering Substrates. *Sens. Actuators B Chem.* **2018**, 257, 382.

Dreaden, E. C.; Austin, L. A.; Mackey, M. A.; El-Sayed, M. A. Size Matters: Gold Nanoparticles in Targeted Cancer Drug Delivery. *Ther. Deliv.* **2012**, 3, 457-478.

Eberhardt, K.; Stiebing, C.; Matthaus, C.; Schmitt, M.; Popp, J. Advantages and Limitations of Raman Spectroscopy for Molecular Diagnostics: an Update. *Expert Rev. Mol. Diagn.* **2015**, 15, 773-787.

Ebersbach, P.; Stehle, F.; Kayser, O.; Freier, E. Chemical Fingerprinting of Single Glandular Trichomes of Cannabis Sativa by Coherent Anti-Stokes Raman Scattering (CARS) Microscopy. *BMC Plant Biol.* **2018**, 18, 275.

Fan, M.; Andrade, G. F. S.; Brolo, A. G. A Review on the Fabrication of Substrates for Surface Enhanced Raman Spectroscopy and Their Applications in Analytical Chemistry. *Anal. Chim. Acta* **2011**, 693, 7-25.

Faulds, K.; Smith, W. E.; Graham, D.; Lacey, R. J. Assessment of Silver and Gold Substrates for the Detection of Amphetamine Sulfate by Surface Enhanced Raman Scattering (SERS). *Analyst* **2002**, 127, 282-286.

Fleischmann, M.; Hendra, P. J.; McQuillan, A. J. Raman Spectra of Pyridine Adsorbed at a Silver Electrode. *Chem. Phys. Lett.* **1974**, 26, 163-166.

Giese, M. W.; Lewis, M. A.; Giese, L.; Smith, K. M. Development and Validation of a Reliable and Robust Method for the Analysis of Cannabinoids and Terpenes in Cannabis. *J. AOAC Int.* **2015**, 98, 1503-1522.

Hanif, M. A.; Nawaz, H.; Naz, S.; Mukhtar, R.; Rashid, N.; Bhatti, I. A.; Saleem, M. Raman Spectroscopy for the Characterization of Different Fractions of Hemp Essential Oil Extracted at 130 °C Using Steam Distillation Method. *Spectrochim. Acta A* **2017**, 182, 168-174.

Harder, R. A.; Wijenayaka, L. A.; Phan, H. T.; Haes, A. J. Tuning Gold Nanostar Morphology for the SERS Detection of Uranyl. *J. Raman Spectrosc.* **2020**, 1-9.

Haynes, C. L.; McFarland, A. D.; Van Duyne, R. P. Surface-Enhanced Raman Spectroscopy. *Anal. Chem*. **2005**, 77, 338A-346A.
Huang, C. -C. Applications of Raman Spectroscopy in Herbal Medicine. *Appl. Spectrosc. Rev.* **2016**, 51, 1-11.

Islam, S. K.; Cheng, Y. P.; Birke, R. L.; Green, O.; Kubic, T.; Lombardi, J. R. Rapid and Sensitive Detection of Synthetic Cannabinoids AMB-FUBINACA and α-PVP Using Surface Enhanced Raman Scattering (SERS). *Chemical Physics* **2018**, 506, 31.

Izake, E. L. Forensic and Homeland Security Applications of Modern Portable Raman Spectroscopy. *Forensic Sci. Int.* **2010**, 202, 1-8.

Jagielski, D. Why Aurora Cannabis May Have Made a Big Mistake by Not Partnering With a Beverage Company. *The Motley Fool* [Online], Aug 22, 2019 https://www.fool.com/investing/2019/08/22/why-aurora-cannabis-may-have-made-a-big-mistake-by.aspx (accessed Apr 3, 2020).

Jardine, J. The Four Terpenes Every Stoner Should Know. *The Stranger* [Online], Nov 8, 2018, https://www.thestranger.com/weed/2018/11/08/35236014/the-four-terpenes-every-stoner-should-know (accessed Jan 2, 2021).

Jeanmarie, D. L.; Van Duyne, R. P. Surface Raman Spectroelectrochemistry: Part I. Heterocyclic, Aromatic, And Aliphatic Amines Adsorbed on the Anodized Silver Electrode. *J. Electroanal. Chem. Interfacial Electrochem.* **1977**, 84, 1-20.

Kauffman, T. H.; Kokanyan, N.; Fontana, M. D. Use of Stokes and Anti-Stokes Raman Scattering for New Applications. *J. Raman Spectrosc.* **2019**, 50, 418-424.
Kelly, J.; Patrick, R.; Patrick, S.; Bell, S. E. J. Surface-Enhanced Raman Spectroscopy for the Detection of a Metabolic Product in the Headspace Above Live Bacterial Cultures. *Angew. Chem. Int. Ed.* **2018**, 57, 15686-15690.

Khoury, C. G.; Vo-Dinh, T. Gold Nanostars for Surface-Enhanced Raman Scattering: Synthesis, Characterization and Optimization. *J. Phys. Chem. C.* **2008**, 112, 18849-18859.

Kohout, C.; Santi, C.; Polito, L. Anisotropic Gold Nanoparticles in Biomedical Applications. *Int. J. Mol. Sci.* **2018**, 19, 3385.

Kudelski, A. Analytical applications of Raman spectroscopy. Talanta **2008**, 76, 1-8.
Lagerquist, J. Aurora CEO Says 'The Market is Just Not There' for Cannabis Drinks. *Yahoo Finance Canada* [Online], May 15, 2019 https://ca.finance.yahoo.com/news/aurora-ceo-says-the-market-is-just-not-there-for-cannabis-drinks-190208438.html (accessed Apr 3, 2020).

Langer, J.; de Aberaturi, D. J.; Aizpurua, J.; Alvarez-Puebla, R. A.; Auguié, B.; Baumberg, J. J.; Bazan, G. C.; Bell, S. E. J.; Boisen, A.; Brolo, A. G.; Choo, J.; Cialla-May, D.; Deckert, V.; Fabris, L.; Faulds, K.; de Abajo, F. J. G.; Goodacre, R.; Graham, D.; Haes, A. J.; Haynes, C. L.; Huck, C.; Itoh, T.; Käll, M.; Kneipp, J.; Kotov, N. A.; Kuang, H.; Ru, E. C. L.; Lee, H. K.; Li, J. -F.; Ling, X. Y.; Maier, S. A.; Mayerhöfer, T.; Moskovits, M.; Murakoshi, K.; Nam, J. -M.; Nie, S.; Ozaki, Y.; Pastoriza-Santos, I.; Perez-Juste, J.; Popp, J.; Pucci, A.; Reich, S.; Ren, R.; Schatz, G. C.; Shegai, T.; Schlücker, S.; Tay, L. -L.; Thomas, K. G.; Tian, Z. -Q.; Van Duyne, R. P.; Vo-Dinh, T.; Wang, Y.; Willets, K. A.; Xu, C.; Xu, H.; Xu, Y.; Yamamoto, Y. S.; Zhao, B.; Liz-Marzán, L. M. Present and Future of Surface-Enhanced Raman Scattering. *ACS Nano* **2020**, 14, 28-117.

Lauwers, D.; Hutado, A. G.; Tanevska, V.; Moens, L; Bersani, S.; Vandenabeele, P. Characterization of a Portable Raman Spectrometer for *In Situ* Analysis of Art Objects. *Spectrochm. Acta A* **2014**, 118, 294-301.

Le Ru, E. C.; Blackie, E.; Meyer, M.; Etchegoin, P. G. Surface Enhanced Raman Scattering Enhancement Factors: A Comprehensive Study. *J. Phys. Chem. C* **2007**, 111, 13794-13803.

Lee, M.; Oh, K.; Choi, H. -K.; Lee, S. G.; Youn, H. J.; Le, H. L.; Jeong, D. H. Subnanomolar Sensitivity of Filter Paper-Based SERS Sensor for Pesticide Detection by Hydrophobicity Change of Paper Substrate. *ACS Sens.* **2018**, 3, 151-159.

Leonard, J.; Haddad, A.; Green, O.; Birke, R.; Kubic, T.; Lombardi, J. R. SERS, Raman and DFT Analyses of Fentanyl and Carfentanil: Toward Detection of Trace Samples. *J. Raman Spectrosc*. **2017**, 48, 1323-1329.

Li, Y.; Zhu, J.; Weng, G.; Li, J.; Xiang, T. Zhao, J. “Magic mitt”: Morphologically Controllable AuAg@AuAg Yolk-Shell Nanostars with Better Plasmonic Optical Properties. *J. Alloys Compd.* **2020**, 844, 156134.

Li, Z. Self-Assembly Ag Nanoparticle Monolayer Film as SERS Substrate for Pesticide Detection. *Appl. Surf. Sci.* **2013**, 270, 292-294.

Liu, G.; Young, K. L.; Liao, X.; Personick, M. L.; Mirkin, C. A. Anisotropic Nanoparticles as Shape Directing Catalysis for the Chemical Etching of Silicon. *J. Am. Chem. Soc.* **2013**, 135, 12196-12199.

Lombardi, J. R.; Birke, R. L. A Unified Approach to Surface-Enhanced Raman Spectroscopy. *J. Phys. Chem. C* **2008**, 112, 5605-5617.

Lynk, T. P.; Clarke, O. J. R.; Kesavan, N.; Brosseau, C. L. Development of a Sustainable Plasmon-Enhanced Spectroelectrochemical Sensor Using Avocado Pit (*Persea Americana*) Extract. *Sens. Actuators, B*. **2018**, 257, 270-277.

Mahmoud, E. Y. F.; Rusin, C. J. ; McDermott, M. T., Gold Nanostars as a Colloidal Substrate for In-Solution SERS Measurements Using a Handheld Raman Spectrometer. *Analyst* **2020**, 145, 1396-1407.

Mazur, A. Ontario Government Gives $300,000 to Fund Research for World’s First Cannabis Beer. *Global News* [Online], May 4, 2018 https://globalnews.ca/news/4187677/ontario-government-gives-300000-to-fund-research-for-worlds-first-cannabis-beer/ (accessed Mar 30, 2020).

Meng, X. Dyer, J.; Huo, Y.; Jiang, X. Greater SERS Activity of Ligand-Stabilized Gold Nanostars with Sharp Branches. *Langmuir* **2020**, 36, 3558-3564.

Milliken, S.; Fraser, J.; Poirier, S.; Hulse, J.; Tay, L. L. Self-Assembled Vertically Aligned Au Nanorod Arrays for Surface-Enhanced Raman Scattering (SERS) Detection of Cannabinol. *Spectrochim. Acta A* **2018**, 196, 222.

Moraes, B. R.; Campos, N. S.; Barra, A. C. C.; Izumi, C. M. S. Surface-Enhanced Raman Scattering of MEH-PPV on Gold and Silver Nanoparticles. *J. Spectrosc.* **2018**, 2018, 6924758.

Mostowtt, T.; McCord, B. Surface Enhanced Raman Spectroscopy (SERS) as a Method for the Toxicological Analysis of Synthetic Cannabinoids. *Talanta* **2017**, 164, 396.

Moye, D. This Non-Alcoholic, Cannabis-Infused White Wine Might Be A Harbinger. *Huffington Post* [Online], July 24, 2018 https://www.huffingtonpost.ca/entry/molson-coors-marijuana-beer_n_5b3145e8e4b0b745f176fab1 (accessed Apr 1, 2020).

Negru, B.; McAnally, M. O.; Mayhew, H. E.; Ueltschi, T. W.; Peng, L.; Sprague-Klein, E. A.; Schatz, G. C.; Van Duyne, R. P. Fabrication of Gold Nanosphere Oligomers for Surface-Enhanced Femtosecond Stimulated Raman Spectroscopy. *J. Phys. Chem. C.* **2017**, 121, 27004-27008.

Novak, J.; Zitterl-Eglsser, K.; Deans, S. G.; Franz, C. M. Essential Oils of Different Cultivars of *Cannabis Sativa* L. and Their Antimicrobial Activity. *Flavour Fragr. J.* **2001**, 16, 259-262.

Nurturing New Growth: Canada Gets Ready for Cannabis 2.0. *Deloitte*. https://www2.deloitte.com/content/dam/Deloitte/ca/Documents/c-and-ip/ca-en-consumer-nurturing-new-growth-en-aoda-may31.pdf (accessed Apr 6, 2020).

Ortiz-Castillo, J. E.; Gallo-Villanueava, R. C.; Madou, M. J.; Perez-Gonzalez, V. H. Anisotropic Gold Nanoparticles: A Survey of Recent Synthetic Methodologies. *Coord. Chem. Rev.* **2020**, 425, 213489.

Park, J.; Thomasson, J. A.; Gale, C. C.; Sword, G. A.; Lee, K. -M.; Herrman, T. J.; Suh, C. P. -C. Adsorbent-SERS Technique for Determination of Plant VOCs from Live Cotton Plants and Dried Teas. *ACS Omega* **2020**, 5, 2779-2790.

Pazos-Perez, N.; Guerrini, L.; Alvarez-Puebla, R. A. Fabrication of Hybrid Silver Microstructures from Vermiculite Templates as SERS Substrates. *Nanomaterials* **2020**, 10, 481.

Raman, C. V.; Krishnan, K. S. A New Type of Secondary Radiation. *Nature* **1928**, *121*, 501.

Reuters, T. Coca-Cola, Aurora Exploring Potential for Cannabis-Infused Drinks. *CBC News* [Online], Sept 17, 2018 https://www.cbc.ca/news/business/coke-aurora-cannabis-drinks-1.4826474 (accessed Apr 1, 2020).

Rusin, C. J.; El Bakkari, M.; Du, R.; Boluk, Y.; McDermott, M. T. Plasmonic Cellulose Nanofibres as Water-Dispersible Surface-Enhanced Raman Scattering Substrates. *ACS Appl. Nano Mater.* **2020**, 3, 6584-6597.

Russo, E. B. Taming THC: Potential Cannabis Synergy and Phytocannabinoid-Terpenoid Entourage Effects. *Br J Pharmacol.*, **2011**, 163, 1344–1364.

Russo, E. B. The Case for the Entourage Effect and Conventional Breeding of Clinical Cannabis: No "Strain," No Gain. *Front Plant Sci.,* **2018**, 9, 1969.

Rycenga, M.; Cobley, C. M.; Zeng, J.; Li, W.; Moran, C. H.; Zhang, Q.; Qin, D.; Xia, Y. Controlling the Synthesis and Assembly of Silver Nanostructures for Plasmonic Applications. *Chem. Rev*. **2011**, 111, 3669-3712.

Salehi, B.; Upadhyay, S.; Orhan, I. E.; Jugran, A. K.; Jayaweera, S. L. D.; Dias, D. A.; Sharopov, F.; Teheri, Y.; Martins, N.; Baghalpour, N.; Cho, W. C.; Sharifi-Rad, J. Therapertic Potential of α- and β-Pinene: A Miracle Gift of Nature. *Biomolecules*, **2019**, 9, 738.

Sanchez, L.; Filter, C.; Dalensperger, D.; Kurouski, D. Confirmatory Non-Invasive and Non-Destructive Differentiation Between Hemp and Cannabis Using a Hand-Held Raman Spectrometer. *RSC Adv.* **2020**, 10, 3212-3216.

Sanford, C. L.; Mantooth, B. A.; Jones, B. T. Determination of Ethanol in Alcohol Samples Using a Modular Raman Spectrometer. *J. Chem. Educ.* **2001**, 78, 1221.

Saute, B. Premasiri, R.; Ziegler, L.; Narayanan, R. Gold Nanorods as Surface Enhanced Raman Spectroscopy Substrates for Sensitive and Selective Detection of Ultra-Low Levels of Dithiocarbamate Pesticides. *Analyst* **2012**, 137, 5082-5087.

Saverot, S.; Geng, X.; Leng, W.; Vikesland, P. J.; Grove, T. Z.; Bickford, L. R. Facile, Tunable, and SERS-Enhanced HEPES Gold Nanostars. *RSC Adv.* **2016**, 6, 29669-29673.

Schulz, H.; Baranska, M.; Belz, H. -H.; Rösch, P.; Strehle, M. A.; Popp, J. Chemotaxonomic Characterization of Essential Oil Plants by Vibrational Spectroscopy Measurements. *Vib. Spectrosc.* **2004**, 35, 81-86.

Schulz, H.; Schrader, B.; Quilitzsch, R.; Steuer, B. Quantitative Analysis of Various Citrus Oils by ATR/FT-IR -and NIR-FT Raman Spectroscopy. *Appl. Spectrosc.* **2002**, 56, 117-124.

Sharma, B.; Frontiera, R. R.; Henry, A. I.; Ringe, E.; Van Duyne, R. P. SERS: Materials, Applications, and the Future. *Mater. Today* **2012**, 15, 16-25.

Sivashanmugan, K.; Zhao, Y.; Wang, A. X. Tetrahydrocannabinol Sensing in Complex Biofluid with Portable Raman Spectrometer Using Diatomaceous SERS Substrates. *Biosensors* **2019**, 9, 125.

Song, C.; Li, F.; Guo, X.; Chen, W.; Dong, C.; Zhang, J.; Zhang, J.; Wang, L. Gold Nanostars for Cancer Cell-Targeted SERS-Imaging and NIR Light-Triggered Plasmonic Photothermal Therapy (PPTT) in the First and Second Biological Windows. *J. Mater. Chem. B* **2019**, 7, 2001-2008.

Su, Q.; Ma, X.; Dong, J. ; Jiang, X. ; Qian, W. A Reproducible SERS Substrate Based on Electrostatically Assisted APTES-Functionalized Surface-Assembly of Gold Nanostars. *ACS. Appl. Mater. Interfaces* **2011**, 3, 1873-1879.

Sun, Y.; Xia, Y. Shape-Controlled Synthesis of Gold and Silver Nanoparticles. *Science* **2002**, 298, 2176-2179.

Suresh, V.; Ding, L.; Chew, A. B.; Yap, F. L. Fabrication of Large-Area Flexible SERS Substrates by Nanoimprint Lithography. *ACS Appl. Nano Mater.* **2018**, 1, 886-893.

Tay, L. -L.; Poirer, S.; Ghaemi, A.; Hulse, J.; Wang, S. Paper-Based Surface-Enhanced Raman Spectroscopy Sensors for Field Applications. *J. Raman Spectrosc.* **2020**, 1-10.

Toronto-Based Startup in Race to Develop Cannabis 'Beer'. *CityNews Toronto* [Online], June 26, 2018 https://toronto.citynews.ca/video/2018/06/26/toronto-based-startup-in-race-to-develop-cannabis-beer/ (accessed Mar 30, 2020).

Vagnini, M.; Gabrieli, F.; Daverni, A.; Saili, D. Handheld New Technology Raman and Portable FT-IR Spectrometers as Complementary Tools for the In Situ Identification of Organic Materials in Modern Art. *Spectrochim. Acta A* **2017**, 176, 174-182.

Van der Ende, E.; Bourgeois, M. R.; Henry, A.- I.; Chavez, J. L.; Krabacher, R.; Schatz, G. C.; Van Duyne, R. P., Physicochemical Trapping of Neurotransmitters in Polymer Mediated Gold Nanoparticle Aggregates for Surface-Enhanced Raman Spectroscopy. *Anal. Chem.* **2019**, 91, 9554-9562.

Visser, B. J.; de Vreies, S. G.; Bache, E. B.; Meerveld-Gerrits, J.; Kroon, D.; Boersma, J.; Agnandji, S. T.; van Vugt, M.; Grobusch, M. P. *Malar. J.* **2016**, 15.

Wu, L. New Beer Standards In Canada Could Lead To Big Profit With Marijuana-Infused Brews. *Forbes* [Online], Jun 28, 2018 https://www.forbes.com/sites/lesliewu/2018/06/28/new-beer-standards-in-canada-could-lead-to-big-profit-with-marijuana-infused-brews/#49e1197a7d1d (accessed Mar 30, 2020).

Xia, J.; Liu, Y.; Ran, M.; Lu, D.; Lao, X.; Wang, Y. SERS Platform Based on Bimetallic Au-Ag Nanowires-Decorated Filter Paper for Rapid Detection of miR-196a in Lung Cancer Patients Serum. **2020**, 2020.

Yüksel, S.; Schwenke, A. M.; Soliveri, G.; Arsizzone, S.; Weber, K.; Cialla-May, D.; Hoeppener, S.; Schubert, U. S.; Popp, J. Trace Detection of Tetrahydrocannabinol (THC) with a SERS-Based Capillary Platform Prepared by the In Situ Microwave Synthesis of AgNPs. *Anal. Chim. Acta* **2016**, 939, 93.

Zenabis Provides Cannabis 2.0 Product and Strategy Update. Feb 19, 2020 https://www.zenabis.com/zenabis-provides-cannabis-2-0-product-and-strategy-update/ (accessed Apr 2, 2020).

Zhao, Y.; Chang, X.; Malkani, A. S.; Yang, X.; Thompson, L.; Jiao, F.; Xu, B. Speciation of Cu Surfaces During the Electrochemical CO Reduction Reaction. *J. Am. Chem. Soc*. **2020**, 142, 9735-9743.

Zheng, J.; Pang, S.; Labuza, T. P.; He, L. Evaluation of Surface-Enhanced Raman Scattering Detection Using a Handheld and a Bench-Top Raman Spectrometer: A Comparative Study. *Tantala* **2014**, 129, 79-85.

Appendix

Figure A-1 shows the results of the signal reproducibility study conducted using AuNSs after immediate PVP addition.

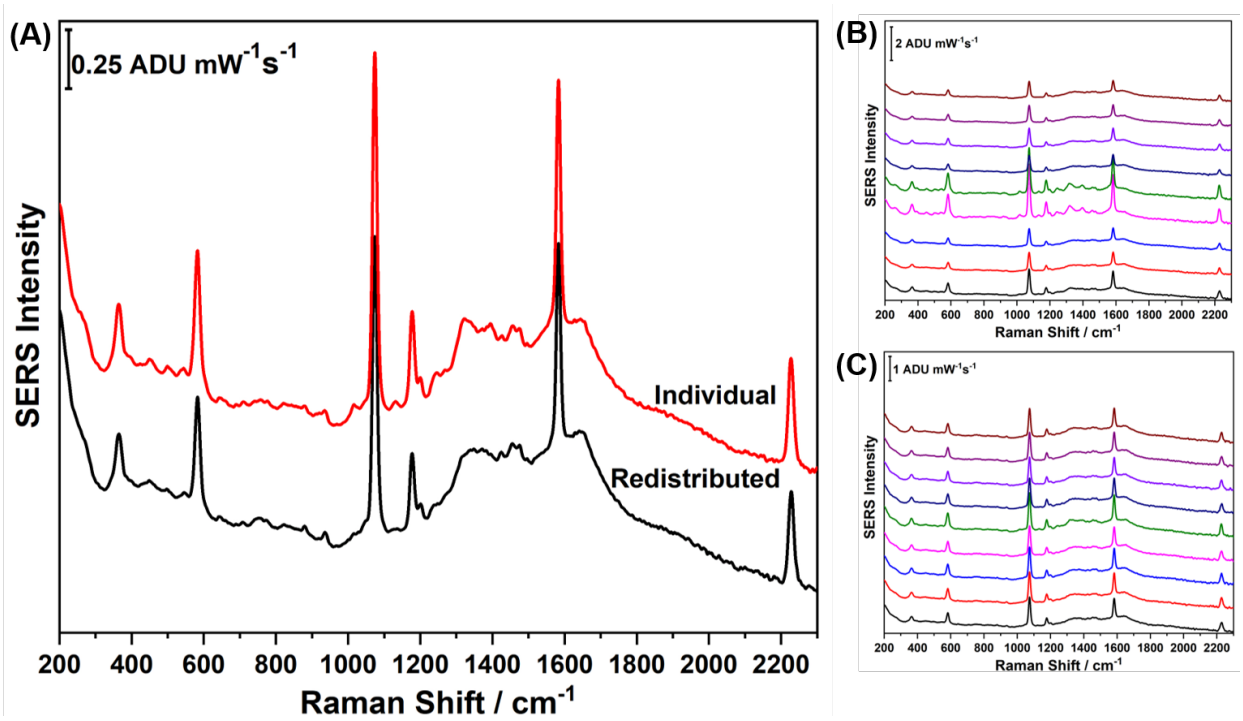

Figure A-1. SERS spectra of 5 nM MBM (A) the average of 9 samples collected from individual samples without redistribution (red) overlaid with average spectrum of 9 samples collected from redistributed AuNS (black) and, (B) Overlay of spectra from 9 different samples collected from individual samples and, (C) Overlay of spectra from 9 different samples collected from redistributed samples. Spectra collected with an excitation wavelength of 785 mn using the NanoRam spectrometer.